Toward a Personal Quantum Computer

by

Henry H. W. Chong
Physics and Media Group
MIT Media Laboratory

Submitted to the Department of Electrical Engineering and Computer Science
in Partial Fulfillment of the Requirements for the Degree of
Master of Engineering in Electrical Engineering and Computer Science
at the Massachusetts Institute of Technology

July 29, 1997

Author_____

Henry H. W. Chong
Physics and Media Group, MIT Media Laboratory
Department of Electrical Engineering and Computer Science
July 29, 1997

Certified by_____

Neil A. Gershenfeld
Director, Physics and Media Group, MIT Media Laboratory
Thesis Supervisor

Accepted by_____

Arthur C. Smith
Chairman, Department Committee on Graduate Thesis

Toward a Personal Quantum Computer

by

Henry H. W. Chong
Physics and Media Group
MIT Media Laboratory

Submitted to the
Department of Electrical Engineering and Computer Science

July 29, 1997

In Partial Fulfillment of the Requirements for the Degree of
Master of Engineering in Electrical Engineering and Computer Science.

ABSTRACT

The realization of nuclear magnetic resonance (NMR) as a means to perform useful quantum computations has warranted a detailed discussion regarding the physics and instrumentation underlying the construction of a NMR quantum computer to facilitate the design of a desktop quantum computer.

A brief overview of classical mechanics, quantum mechanics, and statistical mechanics is presented with Newton's first law as a starting point. A correspondence between an initially postulated classical magnetic moment model and first principles will be made, and methods for the measurement and interpretation of macroscopically manifest observables are discussed.

An introduction to quantum computation will delineate the elements required for computation in analogy to those required for conventional digital computation. The advantages afforded through the use of quantum computational algorithms are discussed, and the employment of NMR to perform quantum computations is presented.

Design considerations for the instrumentation necessary to observe NMR with the cost and physical constraints of a desktop apparatus are reviewed. Low-noise and radio-frequency (RF) instrumentation design needs and constraints are explained in the context of refining sensitivity and frequency resolution requirements of an NMR spectrometer. Experimental considerations for the use of physical processes to enhance sensitivity and spectral resolution are also described.

Results from a desktop NMR spectrometer is presented with a prescription for future progress.

Thesis Supervisor: Neil A. Gershenfeld
Title: Director, Physics and Media Group, MIT Media Laboratory

ACKNOWLEDGMENTS

The completion of this thesis represents the culmination of partnerships and friendships which have spanned a lifetime. My respect and deepest gratitude to all my family, friends, teachers and mentors.

Specifically, I would like to thank the men and women who have supported me through my exhausting sojourn through college. Thanks to Claude for being the candle of inspiration in my darkest hours; to Danika for love and patience; to the Leducs for a second home; to Tito for dedication and temperance; to Dave for a second decade as my baby-sitter; to Craig for being in Spain; to Mike for the Eatery and Indian buffet; to Grace for teaching me civility; to Sharon for indulgence; to Chris for keeping me awake in class; to Neil for wisdom, guidance and the opportunity to learn and contribute; to Joe for late nights and music; to Susan for being the best; to Josh for maturity and cool; to Matt for insight; to Rich for honesty; to Melinda, Tobie, Anne, Joann, Debbie and Debra for laughter and perseverance; to 5W for accepting absence; to 3W for celebrating presence; and to 2W for big chickens and HA—LL FE—EDs.

I would also like to thank Fred, Melissa, Liz, Mary Lynne, 03A wing and the rest of those crazy kids from high school for sharing adolescence. I thank the folks in Carbondale for keeping me real.

And, to Dad, Mom and Aimee: all the love and thanks I can muster for unwaivering and unconditional love, patience, and support.

TABLE OF CONTENTS

1 AN INTRODUCTION, MOTIVATION AND CONTEXT

The detection and identification of natural resonance is an old problem that has re-emerged with new applications. Advances in technology have paved the way for resonant structures to be detected remotely, and allowed information to be encoded in their resonant signatures. Through careful use of materials, resonant structures have been demonstrated to be practical remote temperature and moisture sensors; through careful construction, they promise to bear many bits worth of identification information. Resonant structure have slowly woven themselves into the fabric of our lives as anti-theft tags in libraries and stores. In the near future, they promise to offer a means by which to remotely locate, identify, and provide information regarding themselves, an entity bearing them, or their environment.

Systems which are naturally resonant possess a common property: they all absorb and sometimes re-emit energy at a given natural frequency. Figure 1.1 is an absorption spectrum of a resonant object. Examples of naturally resonant objects include inductive-capacitive tank circuits, electromagnetic wave cavities, spring-mass systems, mechanical swings, magnetostrictive materials, and bridges over the Tacoma Narrows. For simple resonant systems, if energy is used to drive resonant object, the object will absorb energy at its natural frequency. If the object does not dissipate the energy, it will re-emit the energy absorbed at its resonant frequency. More complex resonant systems may possess many resonant frequencies, or *modes*, all of which behave similarly.

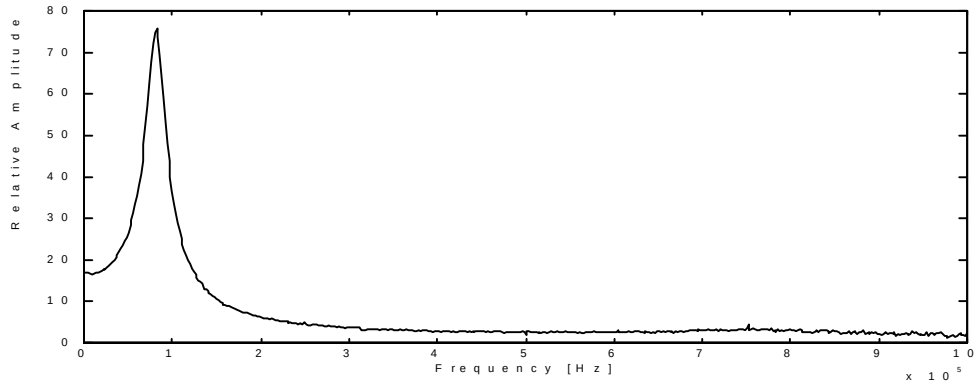

Figure 1.1: Spectrum of a resonant structure.

The most fundamental of naturally resonant structures is the quantum mechanical spin of an atomic nucleon or electron. Chemist and physicists have developed techniques by which to manipulate and interrogate spins in a fashion similar to methods which are used for anti-theft tags. These mature techniques fall under the study of nuclear magnetic resonance (NMR) and electron paramagnetic (or spin) resonance (EPR or ESR). These techniques have enabled scientists to learn about the immediate (chemical) environment of proton and electron spins, leading to developments such a the determination of protein structures and dynamics.

The observable states of a spin are binary, either spin-up or spin-down. Such a description is highly suggestive of a digital bit, which takes either a logical value of one or zero. David DiVinchenzo noted that a NMR experiment named electro-nuclear double resonance (ENDOR) resembles the logical operation XOR. Seth Lloyd outlined a proposal for how spins maybe used as bits for a classical single-instruction multiple data cellular automata (SIMD-CA) computer.

The ultimate goal of his proposal is the creation of a quantum computer—a computer whose bits behave quantum mechanically (referred to as *qubits*)—to perform computations at rates unapproachable by present-day classical computers.

There are a couple reasons to consider practical quantum computation. Attempts to perform faster and faster computations have demanded the fabrication of denser microprocessors, use of faster clock speeds, and the use of many processors in parallel. The progressive use of these methods to achieve faster computation rates will soon meet economical and physical limitations.

The facilities to support further scaling reductions to fabricate denser processors currently cost roughly $5 billion to build. For the past three decades, the rate for the cost for building micro-fabrication facilities has been growing exponentially. At the present rate of increase, the construction of fabrication facilitates required to support continued advances will eventually cost the equivalent of the Earth's GNP.

Physically, semiconductor pitch sizes can only decrease until linewidths are a single atom in size. The use of faster microprocessor clocks also finds physical limitations. Clocks running at near gigahertz frequencies expend great amounts of energy and raise issues regarding clock distribution due propagation delays and transmission line effects. The clock can deliver its signal only as fast as light will travel. The use of parallel processors is limited by physical space and heat dissipation. Current massively parallel computers require a large racks of processors and memory and a room full of cryogens to prevent meltdown. Any hope to realize computations beyond silicon implementations requires a dramatically different paradigm.

Quantum computation finds its speed in exploring an exponentially large Hilbert space, as opposed to physical space. It is not constrain by the same limitations as silicon-based computers, but rather those of quantum mechanics. Quantum computation has been a topic of theoretical rhetoric for decades. Much has been said about its potential for ultra-fast computations, most notably for polynomial time prime factorization of large numbers, but not until recently has work been undertaken to demonstrate its practicality. Early attempts used quantum cavities and atom traps to isolate individual quantum entities to perform simple two-bit operations. These experiments required unwieldy instrumentation, years of development, and were limited to computation with a couple of bits.

A recent experimental breakthrough in the field involved the use of thermal ensembles in bulk materials to perform quantum computations. Neil Gershenfeld and Isaac Chuang realized that NMR techniques provide a means by which to effect a quantum coherent computation using spins as qubits. NMR techniques can be adapted to set initial conditions, apply an algorithm, and read out results on spin systems—operations required of a computer. This development presently promises ten-bit computations in liquids, allowing for the development and testing of quantum computational algorithms.

1.1 Aperitif

A natural place to form intuition for magnetic resonance is the classical magnetic moment model described analytically by the Bloch equations and pictorially by the Purcell vector model. A spin in a time-invariant (DC) bias magnetic field can be thought of as a charge revolving abut an axis. It generates a magnetic field equivalent to that of bar magnet and possesses an angular momentum. This spinning bar magnet can be represented as a vector called a *magnetic moment*.

The magnetic moment points in the direction of the north pole of the magnet, as in Figure 1.2. The direction of the magnetic moment μ can be described in the Cartesian coordinate system in terms of the components μ_x, μ_y and μ_z, in the *x*, *y*, and *z* bases; the magnitude never changes, since the size of magnet never increases.

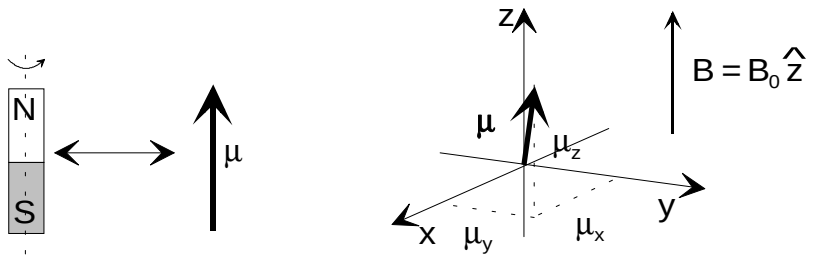

Figure 1.2: The Purcell vector model.

The nature of the magnetic moment is to align itself with the bias magnetic field, much as bar magnets on a table re-orient themselves so that opposite poles attract to maintain the lowest energy configuration possible. The magnetic moment is in its lowest energy configuration when aligned with the bias magnet field. When the magnet is anti-aligned with the field, its possesses the most energy it can acquired.

In equilibrium, the magnetic moment is completely aligned with the bias field and noted as μ_0. By convention, the bias field is designated to be in the *z*-direction, so the equilibrium magnetic moment, μ_0, is also in the *z*-direction. If the moment is tipped away from the bias field axis, energy has been imparted to the it. Something did work on it to tip it away from the lowest energy configuration. However, when an magnetic moment is tipped away from alignment with the bias magnetic field, classical electromagnetism requires that the bias field to apply a torque to the magnetic moment due to its intrinsic angular momentum. Since the applied torque is also the time-derivative of the angular momentum,

$$\vec{\tau} = \frac{d\vec{\mu}}{dt} = \vec{\mu} \times \gamma \vec{B},$$

the magnetic moment will *precess* about the bias field like a gyroscope in a gravitational field. The coefficient on the magnetic flux, γ, is the *gyromagnetic ratio* of the magnetic moment. The rate at which the magnetic moment precesses about the bias field is set by the strength and direction of the bias field, and is called the *Larmor precession frequency*,

$$\vec{\omega} = \gamma \vec{B}.$$

As the magnetic moment precesses, it accelerates. As it accelerates it radiates. As the magnetic moment radiates, it loses energy and slowly returns to its equilibrium position. Hence, the *z*-component of the magnetic moment has a decay term in its evolution, characterized by a decay constant T_1,

$$\frac{d\mu_z}{dt} = -\frac{\mu_z - \mu_0}{T_1}.$$

In a bulk sample with many, many magnetic moments, the net *bulk magnetization* of the sample is simply the vector sum of the individual magnetic moments,

$$\vec{M} = \sum_i \vec{\mu}_i \ .$$

The corresponding equation of motion for the bulk magnetization is,

$$\frac{d\vec{M}}{dt} = \vec{M} \times \gamma \vec{B} \ ,$$

with the decay of the *z*-component of magnetization as

$$\frac{dM_z}{dt} = -\frac{M_z - M_0}{T_1} \ .$$

If energy is introduced to the sample to tip the magnetic moments, then all the individual magnetic moments precess together. The *x*- and *y*-components of the bulk magnetization are a reflection of this group precession. However, in a bulk sample, each magnetic moment will interact with its neighboring magnetic moments. By virtue of being a small bar magnet, each individual magnetic moment alters the field immediately around it. What results is each magnetic moment will perceive a different local bias field and have a different Larmor precession frequency. Within the sample, some magnetic moments will precess slower than others. As the individual magnetic moments fan out, the *x*- and *y*-components of magnetization cancel. The effect is accounted for by the decay of the *x*- and *y*-components of the bulk magnetization characterized by a second time constant, T_2,

$$\frac{dM_x}{dt} = -\frac{M_x}{T_2} \qquad\qquad \frac{dM_y}{dt} = -\frac{M_y}{T_2} \ .$$

The combined expressions for torque and decay of bulk magnetization due to individual spin magnetic moments yield

$$\begin{aligned}
\frac{dM_z}{dt} &= \left[M_y B_z - M_z B_y \right] - \frac{\left(M_z - M_0 \right)}{T_1} \\
\frac{dM_y}{dt} &= \left[M_z B_x - M_x B_z \right] - \frac{M_y}{T_2} \\
\frac{dM_x}{dt} &= \left[M_z B_y - M_y B_z \right] - \frac{M_x}{T_2} \ .
\end{aligned}$$

These are the *Bloch equations*.

It is important to note the difference in the bulk magnetization decay mechanisms. The mechanism for T_2 decay is different from that of T_1. T_1 decay is irreversible; it is due to energy

exchange with the environment, and only effects the *z*-component, or the *longitudinal* component, of magnetization. T_2 decay is reversible, and is simply due to the individual magnetic moments precessing out of phase with each other. By its nature, it only effects the *x*- and *y*-, or the *transverse*, components of the bulk magnetization.

Though the Bloch equations and Purcell vector model accurately explain the macroscopic manifestations of spin, they neglect the quantum mechanical nature of spins. The pre-requisite for a candidate quantum computer is a physical system which allows for the manipulation of quantum mechanical entities without unnecessarily disturbing them. A quantum mechanical system must assume a quantum states when it is disturbed; a disturbance consists of any attempt to observe or manipulate the system. When a quantum mechanical system is disturbed, it loses any quantum mechanical complexity it may possess to assume a single state. It is this complexity which allows quantum computations to be completed faster than traditional computations.

To understand how NMR systems allow for a quantum computer to be initialized, manipulated, and read without the loss of quantum mechanical complexity requires an understanding of the quantum mechanics and statistical mechanics which underlie the Purcell vector model and the Bloch equations. To this end, those descriptions of physics will be introduced beginning with the most fundamental of physical laws, Newton's first law. Once the foundation has been laid, the formalisms of quantum mechanics and statistical mechanics will be used to illustrate in full detail the phenomena of magnetic resonance. The Bloch equations will be re-derived from first principles, and the connection between NMR and quantum computation will be made.

1.2 Overview

Section 1: An Introduction, Motivation and Context
The problem addressed in this thesis, the design and construction of a desktop quantum computer is introduced and motivated. An intuitive picture is provided for the physical system used to implement quantum computation.

Section 2: Background
Underlying quantum computation are very fundamental physical processes. The background required to understand NMR quantum computation requires preparation in quantum mechanics and statistical mechanics, which both use Hamiltonian dynamics to describe physical systems. A natural introduction to these studies is made beginning with classical mechanics and Newton's first law. The eventual derivation of the Hamiltonian formulation for the study dynamical systems is followed with introductions to the mathematical formalisms of quantum mechanics and statistical mechanics.

Section 3: The Problem of Magnetic Resonance
Magnetic resonance is formally introduced from first principles. The connections between quantum mechanical effects and physically observable processes are drawn. The relations stated in the *Aperitif* are reconciled with expressions derived from quantum mechanics and statistical mechanics.

Section 4: NMR Quantum Computation
The premise of quantum computation is outlined. The use of NMR as a means to perform quantum computations is introduced.

Section 5: Instrumentation Design Considerations
A model for a general NMR spectrometer is offered, and design considerations are provided in the context of available technologies. Physical noise sources and sources of external interference are introduced with techniques to manage their influence on measurement electronics.

Section 6: Experimental Considerations
An overview of possible experimental techniques to enhance signal-to-noise is presented. Averaging techniques, physical preparation of the spin system, and polarization transfer techniques are discussed.

Section 7: Instrumentation Design and Construction and Experimental Methods
The instrumentation and experimental methods used to observe magnetic resonance signals is detailed.

Section 8: Results
The results obtained from the experiments are objectively displayed in time-series plots and spectra.

Section 9: Reflections
A short discussion regarding the results is offered. A general direction for continued research is outlined, and a specific proposal is made.

2 BACKGROUND

The physics of magnetic resonance covers a broad range of physical ideas and offers a simple, yet broad introduction for a beginning student interested in physics. The basis of NMR is the manipulation and interrogation of quantum mechanical spins. Spins are purely quantum mechanical entities which can be described classically as magnetic dipoles. Though these classical analogs are helpful to develop intuition, their validity is limited. Quantum mechanics offers a description for the true behavior of spin systems, and shows how classical models relate to quantum mechanical behavior. In practice, spins are rarely isolated. More often, they are dealt with in ensembles. Statistical mechanics provides a description of the *macroscopic* properties of a material due to the aggregate behavior of individual constituents. It is these properties which are observed in NMR experiments.

2.1 Classical Mechanics

Classical mechanics describes the world with which people are familiar: the macroscopic, the physics of our intuitive reality—big things moving slowly. The most basic formulation of classical mechanics is Newtonian mechanics, which is embodied in Equation (2.1.1),

$$\sum \vec{F} = m\ddot{\vec{r}} \qquad (2.1.1).$$

The vector sum of the forces felt by a system is equal to the acceleration of the system scaled by its total mass. Described by this equation, a system can be fully characterized at any moment in time.

2.1.1 The Lagrangian Formulation

Though the expression for the force acting on a system may indicate that it has a given number of degrees of freedom, the system may actually be constrained to move in only a few of those degrees of freedom. The classical example of a constraint problem is a bead threaded on a loop of wire. The loop is two-dimensional, so the equation of motion for the trajectory of the bead can be described in terms of two degrees of freedom. But, the bead is constrained to travel along the wire, it can only move in one-dimension—forward or backward. It only possesses a single degree of freedom. Though a problem can be initially described in a conventional coordinate system, r_i (e.g., Cartesian, spherical), underlying those coordinates is a set of *generalized coordinate*s, q_i, which succinctly describes the system in its true, independent degrees of freedom,

$$\vec{r}_i = \vec{r}_i(q_1, q_2, \ldots q_{n-1}, q_n) .$$

To understand how forces are altered under the transformation from a standard coordinate system to a generalized coordinate system, the principle of virtual work is employed. Equation (2.1.2) defines a virtual displacement.

$$\delta\vec{r}_i = \sum_m \frac{\partial \vec{r}_i}{\partial q_m}\delta q_m \qquad (2.1.2).$$

To visualize the dynamics of systems, *configuration space* is used. Configuration space is constructed using the position and the rate of change of the position as its axes. For a one-dimensional system, configuration space is a graph with the position on the horizontal axis and

the position's first derivative in time on the vertical axis. Additional degrees of freedom require additional pairs of axes per degree of freedom. A virtual displacement is an infinitesimal change in the configuration space. Virtual work is then defined as the dot product of the forces acting on the system and the virtual displacement, as in Equation (2.1.3).

$$W_{virtual} = \sum_i \vec{F}_i \cdot \delta\vec{r}_i \tag{2.1.3}$$

Associated with generalized coordinates are a *generalized forces*. The substitution of Equation (2.1.2) into Equation (2.1.3) yields an the expression for virtual work in terms of generalized coordinates and generalized forces.

$$W_{virtual} = \sum_i \vec{F}_i \cdot \sum_m \frac{\partial r_i}{\partial q_m}\delta q_m = \sum_m Q_m \delta q_m \tag{2.1.4}$$

where,

$$Q_m = \sum_i F_i \cdot \frac{\partial r_i}{\partial q_m}$$

is the generalized force in the *m*th direction. As with the Newtonian formulation of classical mechanics, the purpose of this analysis to determine the equations of motion for a system. To continue, the following relation is established,

$$\vec{F} = \dot{\vec{p}},$$

where

$$\vec{p}_i = m_i \vec{v}_i$$

is the momentum of the system, and

$$\vec{v}_i = \sum_j \frac{\partial \vec{r}_i}{\partial q_j}\frac{\partial q_j}{\partial t} + \frac{\partial \vec{r}_i}{\partial t}$$

is the velocity. Thus,

$$\frac{d}{dt}\left(\frac{\partial r_i}{\partial q_j}\right) = \frac{\partial v_i}{\partial q_j} \tag{2.1.5}$$

by exchanging the order of differentiation. From the velocity expression

$$\frac{\partial v_i}{\partial \dot{q}_j} = \frac{\partial r_i}{\partial q_j} \tag{2.1.6},$$

where

$$\dot{q} \equiv \frac{\partial q}{\partial t}.$$

Returning to the expression for virtual work,

$$\begin{aligned}
\sum_i \vec{F}_i \cdot \delta\vec{r}_i &= \sum_i \dot{\vec{p}}_i \cdot \delta r_i \\
&= \sum_i m_i \dot{\vec{v}}_i \cdot \delta r_i \\
&= \sum_i m_i \dot{v}_i \cdot \sum_j \frac{\partial r_i}{\partial q_j} \delta q_j \\
&= \sum_i \sum_j m_i \ddot{\vec{r}}_i \cdot \frac{\partial r_i}{\partial q_j} \delta q_j \\
&= \sum_i \sum_j \left\{ \frac{d}{dt}\left(m_i \dot{\vec{r}}_i \cdot \frac{\partial \vec{r}_i}{\partial q_j} \right) - m_i \dot{\vec{r}}_i \cdot \frac{d}{dt}\left(\frac{\partial \vec{r}_i}{\partial q_j} \right) \right\} \delta q_j ,
\end{aligned}$$

where the right-hand side of the final expression can be deduced using the product rule of differentiation. Making the appropriate substitutions from Equation (2.1.5) and Equation (2.1.6),

$$\sum_i \vec{F}_i \cdot \delta\vec{r}_i = \sum_i \sum_j \left\{ \frac{d}{dt}\left(m_i \dot{\vec{r}}_i \cdot \frac{\partial \vec{v}_i}{\partial \dot{q}_j} \right) - m_i \dot{\vec{r}}_i \cdot \left(\frac{\partial \vec{v}_i}{\partial q_j} \right) \right\} \delta q_j .$$

Rewriting the two terms within the brackets to explicitly show the various differentiation operations,

$$\sum_i \vec{F}_i \cdot \delta\vec{r}_i = \sum_i \sum_j \left\{ \frac{d}{dt}\left(\frac{\partial}{\partial \dot{q}_j}\left(\frac{1}{2} m_i v_i^2 \right) \right) - \frac{\partial}{\partial q_j}\left(\frac{1}{2} m_i v_i^2 \right) \right\} \delta q_j .$$

The kinetic energy of the system is $T = \sum_i \frac{1}{2} m_i v_i^2$, so the expression for virtual work reduces to

$$\sum_i \vec{F}_i \cdot \delta\vec{r}_i = \sum_j \left\{ \frac{d}{dt}\left(\frac{\partial T}{\partial \dot{q}_j} \right) - \frac{\partial T}{\partial q_j} \right\} \delta q_j .$$

By expressing virtual work in terms of generalized coordinates and generalized forces,

$$\sum_j \left[\left\{ \frac{d}{dt}\left(\frac{\partial T}{\partial \dot{q}_j} \right) - \frac{\partial T}{\partial q_j} \right\} - Q_j \right] \delta q_j = 0 .$$

Since generalized coordinates are independent,

$$\frac{d}{dt}\left(\frac{\partial T}{\partial \dot{q}_j}\right) - \frac{\partial T}{\partial q_j} = Q_j \qquad (2.1.7),$$

where j indexes the set of N independent equations, and N is the number of degrees of freedom accessible to the system. If the forces applied to the system are derived from a scalar potential V which depends solely on position, i.e.,

$$Q_j = \frac{\partial V(\boldsymbol{q})}{\partial q_j},$$

where $\boldsymbol{q}$ implies all the generalized coordinates, Equation (2.1.7) can be expressed as the *Lagrange-Euler equations*,

$$\frac{d}{dt}\left(\frac{\partial L}{\partial \dot{q}_j}\right) - \frac{\partial L}{\partial q_j} = 0,$$

where

$$L(\boldsymbol{q}, \dot{\boldsymbol{q}}, t) = T - V$$

is the *Lagrangian*.

Now, rather than performing a vector sum of all the forces acting on a system, reducing the number of degrees of freedom through constraints, and then solving for the equations of motion using Newton's first law, the Lagrangian formulation takes into account the various constraints, and allows for the generation of the equations of motion using a scalar expression involving kinetic energy and potential energy. The application of the Lagrange-Euler equations yield a set of second-order equations to describe the dynamics of a system, like the application of Newton's equation yields second-order equations,.

This derivation of Lagrange-Euler equations employed D'Alembert's principle, a differential principle. The derivation of Lagrange-Euler equations is usually performed using Hamilton's principle, an integral principle which produces equations of motion for systems which have scalar potentials which describe conservative forces (i.e., not dissipative forces like friction). Mathematically, Hamilton's principle is an application of the calculus of variation, where

$$S = \int_{t_2}^{t_1} L(\boldsymbol{q}(\alpha, t), \dot{\boldsymbol{q}}(\alpha, t), t)dt$$

is the path integral between two fixed point in configuration space called the *action integral*. The action integral is minimized in the parameter α. The Langragian is postulated to be the difference between the kinetic energy and the potential energy, and the Lagrange-Euler equations result as a condition for the minimization of the action integral.

2.1.2 The Hamiltonian Formulation

The Hamiltonian formulation of classical mechanics builds upon the Lagrangian formulation to provide more powerful tools to analyze dynamical systems (i.e., systems which evolve with time). Rather than using configuration space and second-order equations to analyze systems, the Hamiltonian formulation uses *phase space* and a system of first-order equations.

To facilitate this change from configuration space to phase space and from second-order systems to first-order systems, a new variable is introduced to describe systems. In the Lagrangian formulation, generalized forces and generalized coordinates describe a system in its true degrees of freedom. Related to each component of the generalized force is a momentum, which specifies the momentum of the system in the direction of its associated generalized coordinate. The momentum is conjugate to its generalized coordinate. Each generalized coordinate and its associated momentum constitute a *conjugate pair*, and are denoted as (q_i, p_i). As a coordinate and its time derivative define the axes for configuration space for the Largrangian formulation, a conjugate pair defines a set of axes for phase space: for a one-dimensional system, the coordinate is the horizontal axis and its conjugate momentum is vertical axis.

At the heart of the Lagrangian formulation was the Lagrangian—once the Lagrangian was determined, the system could be fully characterized for all time. Similarly, the Hamiltonian formulation of classical mechanics revolves around a expression called *the Hamiltonian*. The Hamiltonian and the Lagrangian are related through a Legendre transformation. To perform the Legendre transformation simply subtract the function to be transformed from the product of the variables to be exchanged, i.e.,

$$L(\boldsymbol{q},\dot{\boldsymbol{q}},t) \Rightarrow H(\boldsymbol{q},\boldsymbol{p},t) \qquad \Rightarrow \qquad H(\boldsymbol{q},\boldsymbol{p},t) = \sum_i \dot{q}_i p_i - L(\boldsymbol{q},\dot{\boldsymbol{q}},t)\,,$$

where H is the Hamiltonian. To extract useful information from the Hamiltonian take its differential,

$$dH = \frac{\partial H}{\partial q_i} dq_i + \frac{\partial H}{\partial p_i} dp_i + \frac{\partial H}{\partial t} dt\,.$$

The Legendre transformation expression produces an equivalent expression,

$$dH = p_i d\dot{q}_i + \dot{q}_i dp_i - \frac{\partial L}{\partial \dot{q}_i} d\dot{q}_i - \frac{\partial L}{\partial p_i} dp_i - \frac{\partial L}{\partial t} dt\,.$$

Matching terms from the two expressions yields the definition for the conjugate momentum and Hamilton's equations. Thus,

$$p_i = \frac{\partial L}{\partial \dot{q}_i} \qquad\qquad \dot{p}_i = \frac{\partial L}{\partial q_i}\,,$$

and

$$\dot{q}_i = \frac{\partial H}{\partial p_i} \tag{2.1.8a}$$

$$\dot{p}_i = -\frac{\partial H}{\partial q_i} \tag{2.1.8b}$$

$$\frac{\partial L}{\partial t} = -\frac{\partial H}{\partial t} \tag{2.1.8c}.$$

Equations (2.1.8) are Hamilton's equations, which can be used to derive the equations which govern the time-evolution of the system.

The physical interpretation for the Hamiltonian is apparent after massaging the Legendre transformation equation,

$$\begin{aligned} H(\boldsymbol{q},\boldsymbol{p},t) &= \sum_i \dot{q}_i p_i - L(\boldsymbol{q},\dot{\boldsymbol{q}},t) \\ &= \sum_i \dot{q}_i p_i - T + V(\boldsymbol{q}) \\ &= \sum_i \dot{q}_i m_i \dot{q}_i - \frac{1}{2} m \dot{q}_i^2 + V(\boldsymbol{q}) \\ &= \sum_i \frac{1}{2} m_i \dot{q}_i^2 + V(\boldsymbol{q}) \\ &= T + V(\boldsymbol{q}) . \end{aligned}$$

Alas, the Hamiltonian is an expression for the total energy for a system with conservative potentials. For most systems of interest, this is the case. Essentially, the Hamiltonian is the energy function.

A final note regarding the Hamiltonian formulation of classical mechanics regards the evolution of any measurable quantity. The change of a quantity in time is expressed by its complete derivative in time. So, starting with a quantity $A(\boldsymbol{q},\boldsymbol{p},t)$, consider its time derivative. Using the chain rule,

$$\frac{dA}{dt} = \sum_i \frac{\partial A}{\partial q_i}\dot{q}_i + \frac{\partial A}{\partial p_i}\dot{p}_i + \frac{\partial A}{\partial t}$$

Recognizing the recently derived expressions from Hamilton's equations, appropriate substitutions yield

$$\frac{dA}{dt} = \sum_i \frac{\partial A}{\partial q_i}\frac{\partial H}{\partial p_i} - \frac{\partial A}{\partial p_i}\frac{\partial H}{\partial q_i} + \frac{\partial A}{\partial t} .$$

By defining the *Poisson brackets*,

$$\{A,H\} \equiv \sum_i \frac{\partial A}{\partial q_i}\frac{\partial H}{\partial p_i} - \frac{\partial A}{\partial p_i}\frac{\partial H}{\partial q_i}$$

which have the mathematical properties of anti-symmetry, linearity, and satisfy the Jacobi identity under cyclic permutation, the time derivative of *A* can be expressed as Equation (2.1.9),

$$\frac{dA}{dt} = \{A,H\} + \frac{\partial A}{\partial t} \qquad (2.1.9).$$

From Equation (2.1.9), it is apparent that encoded in the Hamiltonian is the dynamical evolution of a quantity. Also of note is that if a quantity has no explicit time dependence and produces a zero when taken in a poisson bracket with the Hamiltonian, the quantity is a constant of motion. The poisson bracket reveals underlying symmetries in a system. In fact if any two quantities taken in a poisson bracket yield a zero, the two quantities are completely independent of each other.

However, in dealing with entities on a small scale, which in aggregate compose of the reality which can be sensed and for which there is intuition, classical mechanics fails. To deal with small scale entities, quantum mechanics was developed. Though quantum mechanics seems magical, and produces results which seem physically impossible, the mathematical machinery by which quantum mechanics operates is extremely similar to that of classical mechanics.

2.2 Quantum Mechanics

Quantum mechanics is phrased in terms of operators, spaces, and states. These ideas are represented in Dirac notation, and are introduced with the means to mathematically manipulate them. Though the notation may appear obscure initially, simple explanations and analogies will reveal its beauty and generality.

The basis of understanding a quantum mechanical system is the consideration of its *state*. The state is of system contains all the information regarding the system. If the system of interest is a point-like particle, then the state of the system includes the particle's position and momentum. More complex systems, like a volume of gas, may have more properties to describe its state, such as pressure and temperature. To mathematically represent the state of quantum mechanical system, a *state vector* is used, and from it is generated a *wave function*. A state vector is analogous to a vector in linear algebra, and contains all the information and all the properties which describe the system; this state vector resides in *Hilbert space*, like a three component vector resides in a three-dimensional space.

To extract information from and manipulate states requires the use of *operators*. Operators are conceptually easy to understand. They can be thought of as machines which take an input and spit out an output. A negative sign can be thought of as operator—it takes a value and returns the opposite of the value. Differentiation and integration are calculus operators—they take a function and return the derivative and integral of the function respectively. Operators in linear algebra take the form of matrices, which act as maps between vector spaces; this map interpretation of an operator is valid and useful for all operators.

2.2.1 Dirac Notation

Dirac notation is a general and concise mathematical description of quantum mechanics. It serves to define notions of states, spaces, and operators in a form which can be manipulated to prescribe the physical behavior of a system.

The notion of a state and a space are intimately intertwined—a state exists in a space. Operators are used to map a given state in its initial space to a second space. To represent a state vector, Dirac uses *bras* and *kets*. A bra and a ket are duals of each other. In linear algebra, a column vector is a dual of its transpose, the associated row vector. They are not equivalent since they exist in different spaces (if the column vector exists in a *Nx1* space, then its transpose exists in a *1xN* space). In a similar way bras and kets are related; however, rather than being transposes of each other, they are *Hermitian adjoints* of each other. The crucial difference is that *the ket is the transposed complex conjugate of the bra and vice-versa*. The expressions in Equation (2.2.1) illustrate this notion and explain the origin for the names bra and ket,

$$\langle a| \quad \Rightarrow \quad \begin{bmatrix} a_1 & a_2 \end{bmatrix} \qquad \text{a bra, left-side of a bracket} \qquad (2.2.1a)$$

$$|a\rangle \quad \Rightarrow \quad \begin{bmatrix} a_1 * \\ a_2 * \end{bmatrix} \qquad \text{a ket, the right-side of a bracket} \qquad (2.2.1b)$$

$$\langle a|^{\dagger} = |a\rangle \qquad \dagger \text{ is the adjoint operation: } a^{\dagger} = (a^T) * \qquad (2.2.1c).$$

The a is simply a label for the state vector in question; the elements of $|a\rangle$ are complex numbers. To add bras or kets, simply sum the corresponding components. An inner product is taken by multiplying a bra with a ket, in that order. To form an outer product between the two, simply reverse the order. Equation (2.2.2) demonstrates mathematical manipulations in Dirac notation,

$$|a_i\rangle + |a_j\rangle \quad \Rightarrow \quad \begin{bmatrix} a_{i1} \\ a_{i2} \end{bmatrix} + \begin{bmatrix} a_{j1} \\ a_{j2} \end{bmatrix} = \begin{bmatrix} a_{i1} + a_{j1} \\ a_{i2} + a_{j2} \end{bmatrix} \qquad \text{addition} \qquad (2.2.2a)$$

$$\langle a_i | a_j \rangle \quad \Rightarrow \quad \begin{bmatrix} a_{j1} & a_{j2} \end{bmatrix} \begin{bmatrix} a_{i1} \\ a_{i2} \end{bmatrix} = (a_{i1} a_{j1} + a_{i2} a_{j2}) \qquad \text{inner product} \qquad (2.2.2b)$$

$$|a_i >< a_j| \quad \Rightarrow \quad \begin{bmatrix} a_{i1} \\ a_{i2} \end{bmatrix} \begin{bmatrix} a_{j1} & a_{j2} \end{bmatrix} = \begin{bmatrix} a_{i1} a_{j1} & a_{i1} a_{j2} \\ a_{i2} a_{j1} & a_{i1} a_{j2} \end{bmatrix} \qquad \text{outer product} \qquad (2.2.2c).$$

In the matrix formalism of quantum mechanics, linear algebra is used to perform calculations. The correlation is apparently simple.

2.2.2 Properties of State Vectors

A state vector can be decomposed into a complete basis set, much as function can be decomposed into Fourier components or a vector can be decomposed into its basis vectors. In quantum mechanics, the basis set is conveniently the set of eigenvectors. An arbitrary state, $|\Psi\rangle$, can be described by the weighted some of its eigenvectors, a_i's,

$$|\Psi\rangle = \sum_i c_i \left| a_i \right\rangle \qquad (2.2.3).$$

By virtue of being bases, these eigenvectors are orthogonal, so the inner product of an eigenvector with second eigenvector is zero, unless the inner product is with itself, as in Equations (2.2.4),

$$\left\langle a_i \middle| a_j \right\rangle = \delta_{i,j} \quad \text{for denumerable eigenvectors} \qquad (2.2.4a)$$

$$\langle x | x' \rangle = \delta(x - x') \quad \text{for non-denumerable eigenvectors} \qquad (2.2.4b).$$

Wave functions, the inner product of state vectors, are normalized, so that the sum of the weighting coefficients, the c_i's, sum to unity. So, when constructing a general wave function solution, normalization must be satisfied,

$$\frac{|\Psi\rangle}{\left|\langle \Psi | \Psi \rangle\right|^2} = |\Psi\rangle \qquad \Rightarrow \qquad \left|\langle \Psi | \Psi \rangle\right|^2 = 1.$$

These are the orthonormal properties of state vectors and wave functions. Eigenstates form a basis which must be orthogonal; wave functions are probability amplitudes which must be normalized.

2.3.3 Operators

Operators are applied to states to manipulate or obtain information from them. Using the orthonormal properties of bras and kets, an identity operator can be constructed. The application of a bra to a general wave function extracts the coefficient of that particular eigenstate,

$$c_i = \langle a_i | \Psi \rangle .$$

Substitution into Equation (2.2.3) yields

$$|\Psi\rangle = \sum_i \langle a_i | \Psi \rangle \cdot \left| a_i \right\rangle = \sum_i \left| a_i \right\rangle \left\langle a_i \right| \cdot |\Psi\rangle ,$$

which suggests the operator

$$\sum_i \left| a_i \right\rangle \left\langle a_i \right| = 1.$$

This is the *identity operator*, which is often used to change bases in the course of derivations. This progression has also suggested an interesting possibility—the possibility of *projecting* out a chosen component of a state. Again, by employing the orthonormal properties of state vectors,

$$\hat{A}_i = \left| a_i \right\rangle \left\langle a_i \right| ,$$

which is the *projection operator*. When applied to a state vector, it yields the eigenstate scaled by the weight of that eigenstate in the general state vector. This operator *collapses* the wave function into the chosen state.

Wave functions are generally not in a single eigenstate. They are usually in a *coherent superposition* of states. To determine the expectation value of the operator,

$$\langle A\rangle = \langle \Psi | \hat{A} | \Psi \rangle = \int \Psi^* \hat{A} \Psi dx \qquad \text{for non-denumerable quantities}$$

$$\langle A\rangle = \sum \langle a_i | \hat{A} | a_i \rangle = \sum a_i |c_i|^2 \qquad \text{for denumerable quantities}$$

which is the same manner an expectation value of a variable is taken in probability. The nature of the wave function as a probability distribution is revealed. If the wave function is, however, in an eigenstate, then the expected value will simply yield the eigenvalue; the adjoint of the of the operator will produce the complex conjugate of the eigenvalue,

$$\langle A\rangle = \langle a_i | \hat{A} | a_i \rangle = a_i \qquad\qquad \langle A^\dagger \rangle = \langle a_i | \hat{A}^\dagger | a_i \rangle = a_i^* .$$

The implication for Hermitian operators, operators which are equal to their adjoint,

$$\hat{A} = \hat{A}^\dagger ,$$

is that their eigenvalues are real.

2.2.4 Dynamics

All quantum mechanical systems are Hamiltonian, and described by Hamiltonian evolution. In quantum mechanics, the dynamics of a system can be considered in two different, but equivalent perspectives. The first, is termed the Heisenberg picture. Under this interpretation, quantum dynamics is embodied in the operators. The operators are explicit functions of time, and the wave functions are static. In the second interpretation, the Schrodinger picture, it is the wave functions which evolve in time and the operators which remain static. Mathematically, the two interpretations are completely identical prior to evolution:

$$|\Psi_S(t=0)\rangle = |\Psi_H(t)\rangle \qquad\qquad \hat{A}_H(t=0) = \hat{A}_S(t) .$$

In the Schrodinger picture, the parallel between quantum mechanics and classical mechanics becomes apparent. The dynamics of a wave function is again encoded in the system's Hamiltonian, and is described by the *Schrodinger's equation*

$$i\hbar \frac{d|\Psi(t)\rangle}{dt} = \hat{H}|\Psi(t)\rangle .$$

The application of the Hamiltonian operator yields the time derivative of the state vector scaled by a constant. The actual time evolution of a wave function can be interpreted as the application of a time-evolution operator to a state vector, which produces a state vector at a later time, i.e.,

$$\left|\Psi(t_1)\right\rangle = \hat{U}\left|\Psi(t_0)\right\rangle \qquad \text{or} \qquad \left\langle\Psi(t_1)\right| = \hat{U}^{\dagger}\left\langle\Psi(t_0)\right|.$$

As a condition for the wave function to be properly normalized at each moment in time,

$$\hat{U}\hat{U}^{\dagger} = 1,$$

which is the property of *unitarity*. Wave functions must evolve unitarily to conserve probability. Massaging the expression for the unitary evolution of a state vector, employing Schrodinger's equation, and solving a first-order differential equation yields the time evolution operator

$$\hat{U} = e^{-i\frac{\hat{H}}{\hbar}t}.$$

The form of this operator confirms the intuitive assertion of a normalized wave function at every moment in time. It describes the evolution of a wave function as rotations in Hilbert space.

Associated with every quantum mechanical observable *D* is a Hermitian operator $\hat{D}$. The measurement of quantum mechanical observable determines the expected value of the associated operator applied to the wave function. As in classical mechanics, the time evolution of an operator is

$$\frac{d\langle D\rangle}{dt} \equiv \frac{d}{dt}\left(\langle\Psi|\hat{D}|\Psi\rangle\right).$$

Under the Heisenberg interpretation, the derivation is trivial since only the operator changes with time. The evolution of the observable, then, also relies solely on the time-derivative of its associated operator. In the Schrodinger picture of quantum mechanics, however, it is the wave function which evolves,

$$\begin{aligned}\frac{d\langle D\rangle}{dt} &= \frac{d}{dt}\langle\Psi|\cdot\hat{D}|\Psi\rangle + \langle\Psi|\cdot\hat{D}\frac{d}{dt}|\Psi\rangle \\ &= -\frac{1}{i\hbar}\langle\Psi|\hat{H}^{\dagger}\cdot\hat{D}|\Psi\rangle + \langle\Psi|\cdot\hat{D}\frac{1}{i\hbar}\hat{H}|\Psi\rangle \\ &= \frac{1}{i\hbar}\langle\Psi|\left(\hat{D}\hat{H} - \hat{H}\hat{D}\right)|\Psi\rangle\end{aligned}$$

where the Hermitian property of the Hamiltonian is used.

As in classical mechanics, a mathematical entity can be extracted from the derivation for the dynamics of a measured quantity. The quantum mechanical equivalent of the poisson bracket is the quantum mechanical *commutator*, defined generically as

$$\left[\hat{F},\hat{G}\right] = \left(\hat{F}\hat{G} - \hat{G}\hat{F}\right),$$

which allows the derivation to be completed efficiently as

$$\frac{d\langle D\rangle}{dt} = \frac{1}{i\hbar}\langle\Psi|\left[\hat{D},\hat{H}\right]|\Psi\rangle = \frac{1}{i\hbar}\left\langle\left[\hat{D},\hat{H}\right]\right\rangle.$$

As with the poisson brackets, the commutator reveals the constants of motions of the system, and speaks to the independence of measurable quantities of the system.

2.3.5 Measurement and Uncertainty

Two commonly used operators in quantum mechanics are the position and momentum operators. These two operators are useful to introduce the notion of measurement. Quantum measurement is, in itself, a field of research, which deals with the limits of measurement precision imposed by quantum mechanics on the simultaneous measurement of *conjugate quantities* and the extraction of information from physical systems. As in classical mechanics, in quantum mechanics, linear momentum and position constitute a conjugate pair. If a simultaneous measurement is made on the linear momentum and position of a system, quantum mechanics limits the precision to which each quantity can be measured. Mathematically, this is stated in the Heisenberg uncertainty relation,

$$\Delta x \Delta p \geq \frac{\hbar}{2}.$$

More generally, a state possesses different eigenstates for different operators, denoted as, $\left|a_i, b_i\right\rangle$, where a_i is an eigenvalue for the operator *A*, and b_i is the corresponding eigenvalue for the operator *B*. If the operators *A* and *B* commute, applying either operator first and then the other produces the same results. Mathematically, this is embodied in the commutator,

$$\hat{A}\hat{B}\left|a_i, b_i\right\rangle = \hat{B}\hat{A}\left|a_i, b_i\right\rangle \qquad \Rightarrow \qquad \left[\hat{A},\hat{B}\right] = 0.$$

However, in a general wave function, two observables may not commute; the measurement of one interferes with the simultaneous measurement of the other. The Heisenberg uncertainty principle speaks to the variance of measured quantities. From operators of two non-commuting observables, operators can be constructed,

$$\Delta\hat{X} = \hat{X} - \langle X\rangle \qquad\qquad \Delta\hat{Y} = \hat{Y} - \langle Y\rangle.$$

A similarity to mathematical variances becomes apparent upon squaring the new operators,

$$\left\langle\left(\Delta\hat{X}\right)^2\right\rangle = \left\langle\hat{X}^2\right\rangle - \langle X\rangle^2.$$

Beginning with the Schwarz inequality,

$$\left\langle\left(\Delta\hat{X}\right)^2\right\rangle\left\langle\left(\Delta\hat{Y}\right)^2\right\rangle \geq \left|\left\langle\Delta\hat{X}\Delta\hat{Y}\right\rangle\right|^2$$

and manipulating the right-hand side terms yields,

$$\left\langle \left(\Delta\hat{X}\right)^2 \right\rangle \left\langle \left(\Delta\hat{Y}\right)^2 \right\rangle \geq \frac{1}{4}\left|\left\langle \left[\hat{X},\hat{Y}\right] \right\rangle\right|^2,$$

which is a general form of Heisenberg's uncertainty relationship. Again, the appearance of the commutator on the right-hand side confirms the notion that non-commuting observables interfere with the measurement of each other. Commuting observables have no quantum mechanically imposed limit of measurement precision when measured simulateously.

Uncertainty is fundamental to quantum mechanics. In Hamiltonian dynamics, phase space is used to completely characterize a system. Since the axes of phase space are conjugate quantities, uncertainty imposes strong limitations on the complete characterization of a quantum mechanical system. For quantum mechanical systems, phase space must, itself, be quantized into elemental volumes to account for this imprecision.

To measure a quantum observable, measurements are either made on an ensemble of equivalent systems or many measurements are made repeatedly on the same system. The equivalence of the two measurement philosophies and the study of large, aggregate systems constitute the study of statistical mechanics, which ties macroscopic, thermodynamic properties to the microscopic dynamics of the underlying constituent systems. The formalisms of statistical mechanics also provide a means to reconcile quantum physics with classical intuition. It addresses the shortcomings of Dirac notation when dealing with measurements made on equivalent systems prepared in different states and the degeneracy of configurations which underlie the manifest state of a system composed of many constituent systems.

2.3 Statistical Mechanics

Statistical mechanics is a method to describe aggregate physical processes, and is applicable to ensembles of quantum or classical systems. Its beauty lies in its ability to predict the behavior of systems composed of a large number of constituent systems without considering each constituent system individually. Particularly interesting is the manner in which statistical mechanics bridges quantum mechanics and classical mechanics in the thermodynamic limit. By considering an ensemble of quantum mechanical systems, classical, macroscopic properties—properties which can be measured and observed—can be predicted.

2.3.1 Ensembles in Phase Space

The pillars of statistical mechanics rest on the analysis of systems in phase (or state) space. Classical mechanics introduced the notion of phase space through the Hamiltonian dynamics, where, for example, a coordinate and its canonically conjugate momentum form the axes of a two-dimensional phase space for a single degree-of-freedom point-particle. A point in phase space fully characterizes the position and momentum of the particle—the complete state of the system—at each moment in time. As the system evolves, the point will traverse the regions of phase space to which it has access.

Statistical mechanics considers systems composed of N equivalent constituents, where N is on the order of 10^{23}. Examples of such systems are gases, where the constituents are molecules, or solids, where the constituents are atoms in a lattice. If these atoms or molecules have three-degrees of freedom, then phase space become $6N$-dimensional to account for a coordinate and momentum for each degree of freedom for each particle. If the exact location of the point in phase space is known, then the *microstate* of the system is specified. However, many

microstates underlie the same *macrostate*—the manifestly observable physical state of the system.

Take for example the simple case of a harmonic oscillator in one-dimension. Given the system has a certain energy *E*, the Hamiltonian is a constant for all time. The phase space trajectory for this system, pictured in Figure 2.1, is an ellipse. At any moment in time, the harmonic oscillator is macroscopically characterized as occupying the same volume, containing the same number of particles, and having the same energy, even though its exact location in phase space—the microstate—may be different.

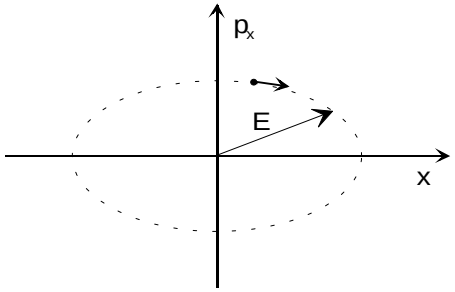

Figure 2.1: The phase space trajectory of a system is the portion of phase space to which the system has access. In the case of a simple harmonic oscillator, the phase space trajectory is an ellipse.

In large systems with *3N* degrees of freedom, such degeneracy also exists. To address this issue, the notion of a *phase density function* and *ensemble* are introduced. Rather than considering a single point which traverses all accessible microstates of phase space, consider an ensemble of systems—infinitely many of them—each occupying a microstate of the system as in Figure 2.2. Rather than having a single point which traverses phase space in time, this phase density function, $\rho(\boldsymbol{p},\boldsymbol{q},t)$, now represents a distribution of microstates in phase space. The expression $\rho(\boldsymbol{p},\boldsymbol{q},t)d\boldsymbol{p}d\boldsymbol{q}$ is the number of microstates in a volume $d\boldsymbol{p}d\boldsymbol{q}$ at $(\boldsymbol{p},\boldsymbol{q},t)$. Ultimately, there is an elemental phase space volume size set by quantum mechanical uncertainty; intuitively, this volume is roughly $d\boldsymbol{q}d\boldsymbol{p} \approx \hbar$.

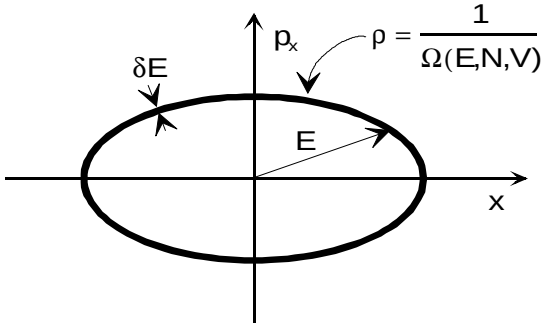

Figure 2.2: The statistical mechanical approach is to use the phase density function to describe the phase space properties of a system rather than phase space trajectories. In the case of the simple harmonic oscillator, the phase density function is uniform through the portion of phase space to which the oscillator has access, an ellipse.

Since a representative point in phase space evolves under Hamiltonian dynamics, so must the phase density,

$$\frac{d\rho}{dt} = \{\rho, H\} + \frac{\partial \rho}{\partial t}.$$

Since members of the ensemble cannot be arbitrarily destroyed or created, the number of representative points in phase space is conserved, i.e.,

$$\frac{d\rho}{dt} = 0,$$

which is *Liouville's Theorem*. In the vernacular, Liouville's Theorem states that the phase density behaves like an incompressible fluid or a bulging suitcase: if it is squeezed in one place, it will spurt in another place.

Ensembles are specified in a myriad of ways by constraining certain macroscopic properties and relaxing others. The properties which macroscopically characterize a system are energy, physical volume, and the number of particles in the system. Fixing or allowing fluctuations in these quantities produces different ensembles and provides a means to make contact with empirically derived thermodynamic relations.

2.3.2 The Microcanonical Ensemble

The microcanonical ensemble is the most restrictive and pedagogical ensemble formulation. Though its use is limited in physical systems, its formalisms have taken root in fields such as information theory. In the microcanonical ensemble, the physical volume and particle number of the system are fixed, and the energy of the system to be constrained to a small band about a fixed energy. Mathematically, the macroscopic state and hence ensemble, is specified by the parameters $(\delta E, E, V, N)$, where $\delta E << E$. This small δE band about E is usually assumed, and is negligible in calculations given its infinitesimal weight relative to other values.

The previously discussed harmonic oscillator is an example of such a system. In phase space, the harmonic oscillator was constrain to exist in only one-dimension of a two-dimensional phase space—an ellipse in a plane. To generalize, the phase space picture of an N-particle ensemble with three-degrees of freedom is a $6N-1$ shell in a $6N$-dimensional space. On this shell in phase space, the phase density is postulated to be evenly distributed and constant. This postulate of *equal a priori probabilities* is the fundamental assumption of statistical mechanics. It states that given a macrostate, a system is equally likely to be in any microstate consistent with that macrostate. Mathematically, the phase density is

$$\rho(\boldsymbol{p}, \boldsymbol{q}) = \frac{1}{\int \delta(H(\boldsymbol{p}, \boldsymbol{q}) - E) d\boldsymbol{p} d\boldsymbol{q}}.$$

With a probability distribution in hand, calculations for the *ensemble average* can easily be calculated as

$$< D >= \frac{\int D(\boldsymbol{p}, \boldsymbol{q}) \rho(\boldsymbol{p}, \boldsymbol{q}) d\boldsymbol{p} d\boldsymbol{q}}{\int \rho(\boldsymbol{p}, \boldsymbol{q}) d\boldsymbol{p} d\boldsymbol{q}},$$

much as any expected value is calculated given a probability distribution. Systems which are *ergodic* are system for which the ensemble average and time-average properties of the system are the same. This is the case for almost all conceivable physical systems.

2.3.3 Enumeration of States and Entropy

Given a fixed energy, volume, and particle number of the system, the number of microstates which are consistent with a specified macrostate can be counted—an enumeration of microstates. The number of microstates can be counted in different ways. Since $\rho(\boldsymbol{p},\boldsymbol{q},t)d\boldsymbol{p}d\boldsymbol{q}$ is simply the number of microstates per incremental volume, then its sum over all relevant phase space yields the total number of microstates. So, most generally,

$$\Omega(E,V,N) = \int \rho(\boldsymbol{p},\boldsymbol{q})d\boldsymbol{p}d\boldsymbol{q} = \delta E \cdot \Pi(E,V,N) .$$

where $\Omega(E,V,N)$, is the number of microstates consistent with a specified macrostate, and $\Pi(E,V,N)$ is the number of microstates per incremental energy—the density of microstates as a function energy.

The number of microstates underlying a specified macrostate determines a degeneracy in the system. An example which best illustrates this is a quantized system. The definition of the ensemble provides constraints,

$$N = \sum_i n_i \qquad\qquad E = \sum_i n_i \varepsilon_i$$

where the $\varepsilon_i's$ are the different quantized energy levels, and the n_i's are the number of particles in *ith* energy level. With these constraints, the enumeration of microstates becomes a chore in combinatorics. The many combinations which provide the same microstate imply the existence of a statistical or mixing entropy. Statistical entropy and thermodynamic entropy differ by the factor of a Boltzmann constant. The thermodynamic entropy calculated from Hamiltonian dynamics is

$$S = k_B \ln \Omega(E,V,N) .$$

In terms of the phase density, the entropy can be re-expressed as,

$$S = -k_B \int \rho(\boldsymbol{p},\boldsymbol{q}) \ln\left[\rho(\boldsymbol{p},\boldsymbol{q})\right] d\boldsymbol{p}d\boldsymbol{q} .$$

Notice that on any constant energy surface in phase space, entropy is maximized.

Empirically, thermodynamics requires entropy maximization for a system in equilibrium. With a normalization constraint placed on the phase density,

$$\int \rho(\boldsymbol{p},\boldsymbol{q})d\boldsymbol{p}d\boldsymbol{q} = 1 \qquad (2.3.1)$$

entropy can be maximized by the method of *Lagrange multipliers*: the normalization condition constrains the maximization of entropy. The result is a phase density function for the ensemble that confirms the postulate of *equal a priori probability*.

2.3.4 The Canonical Ensemble and The Method of Lagrange Multipliers

The microcanonical ensemble corresponds to a physically isolated and closed system—isolated in the sense that no energy exchange is allowed, and closed in the sense that no particle flux in or out of the system is allowed. Though analysis is made simple by these provisions, the physical situation seldom occurs. Realistically, physical systems under experimental consideration are at thermal equilibrium with a heat bath or reservoir—an infinite sink and source of energy—like its environment. Rather than possessing a fixed energy, such systems possess a fixed temperature, an experimentally accessible observable. Exchanges with the heat bath to maintain a constant temperature cause the energy of the system to fluctuate, making all possible values of energy accessible to the system.

To compensate for this relaxed condition in the construction of an ensemble, the addition of a second constraint to the Lagrange multiplier maximization of entropy is made. Though the system energy fluctuates, it makes sense that a system in equilibrium possesses a mean energy, the phase average of the Hamiltonian,

$$< H >= \int H(\boldsymbol{p},\boldsymbol{q})\rho(\boldsymbol{p},\boldsymbol{q})d\boldsymbol{p}d\boldsymbol{q}\,, \qquad (2.3.2)$$

$<H>$ is a constant. Combined with Equation (2.3.2), the method of Lagrange multipliers can be employed to maximize entropy and yield a phase density for the ensemble,

$$\delta\left[\int \alpha_0\rho(\boldsymbol{p},\boldsymbol{q}) + \alpha_E H(\boldsymbol{p},\boldsymbol{q})\rho(\boldsymbol{p},\boldsymbol{q}) - k_B\rho(\boldsymbol{p},\boldsymbol{q})\ln\left(\rho(\boldsymbol{p},\boldsymbol{q})\right)d\boldsymbol{p}d\boldsymbol{q}\right] = 0\,.$$

By taking the variation under the integral,

$$\int\left(\alpha_0 + \alpha_E H(\boldsymbol{p},\boldsymbol{q}) - k_B\ln\left(\rho(\boldsymbol{p},\boldsymbol{q})\right) - k_B\right)\delta\rho(\boldsymbol{p},\boldsymbol{q})d\boldsymbol{q}d\boldsymbol{p} = 0\,.$$

To satisfy the equation generally, the integrand can be chosen to be zero. Since the variation of $\rho(\boldsymbol{p},\boldsymbol{q})$ is arbitrary,

$$\alpha_0 + \alpha_E H(\boldsymbol{p},\boldsymbol{q}) - k_B\ln\left(\rho(\boldsymbol{p},\boldsymbol{q})\right) - k_B = 0 \qquad (2.3.3)$$

is chosen to satisfy the maximization condition. The phase density takes the form

$$\rho(\boldsymbol{p},\boldsymbol{q}) = \exp\left[\frac{\alpha_0}{k_B} + \frac{\alpha_E}{k_B}H(\boldsymbol{p},\boldsymbol{q}) - 1\right],$$

To determine the Lagrange multipliers, a_0 and a_E, the constraint equations are used to first find a relation between the two. En route, a means to sum over the microstates is encountered. The substitution of the normalization condition produces the intermediate expression,

$$e^{\left(\frac{\alpha_0}{k_B}-1\right)}\int e^{\frac{\alpha_E}{k_B}H(\boldsymbol{p},\boldsymbol{q})}d\boldsymbol{p}d\boldsymbol{q}=1.$$

The canonical partition function is defined to be

$$Z(\alpha_E,V,N)\equiv\int e^{\frac{\alpha_E}{k_B}H(\boldsymbol{p},\boldsymbol{q})}d\boldsymbol{p}d\boldsymbol{q}=e^{\left(1-\frac{\alpha_0}{k_B}\right)}.$$

As a sum over microstates, the partition function serves as a normalization factor for calculations such as those used to determine expected values for macroscopic properties, since energy, in the canonical ensemble, fluctuates.

The use of the energy constraint is made convenient by multiplying Equation (2.3.3) by the phase density and integrating over phase space. By using the energy constraint, the definition of entropy and the newly defined partition function, Equation (2.3.3) becomes,

$$<H>+\frac{S}{\alpha_E}-\frac{k_B}{\alpha_E}\ln[Z(\alpha_E,V,N)]=0,$$

which has an uncanny resemblance to the thermodynamic relation for *Helmholtz free-energy*,

$$F=U-ST,$$

a thermodynamic expression which describes closed systems in thermal contact with their environment.

Since both expressions must agree with each other, a correspondence is made:

$$F=-k_BT\ln[Z(T,V,N)]\qquad <H>=U\qquad \frac{1}{\alpha_E}=-T.$$

The phase space averaged energy is actually the internal energy of the system. The minimal free-energy corresponds to the most likely state. Again, contact is made between the microscopic dynamics which underlie macroscopic properties.

A return to the phase space representation finds the canonical distribution function or *Boltzmann distribution*,

$$\rho(\boldsymbol{p},\boldsymbol{q})=\rho(E)=\frac{e^{-\beta H(\boldsymbol{p},\boldsymbol{q})}}{Z(T,V,N)},\qquad \text{where } \beta=\frac{1}{k_BT},$$

as conventionally noted in thermodynamics. The appearance of the partition function is comforting: the probability distribution is properly normalized. As the construction of the microcanonical ensemble yielded a uniform distribution of accessible microstates in an energy shell, the construction of the canonical ensemble produces a very peaked phase space probability distribution which falls off exponentially as the energy of the system deviates from the mean.

2.3.5 Generalized Ensembles

General ensembles can be characterized in a fashion similar to that used to characterize the canonical ensemble. With each ensemble, connections to thermodynamics require the construction of a partition function and contact with a generalized potential.

The canonical ensemble eased the restriction of fixed energy required by the microcanonical ensemble. Physically, this meant the system went from being thermally isolated to being in contact with a thermal environment. The corresponding change in the characterization of ensembles replaced fixed energy with a fixed temperature, a physical property which resulted from a Lagrange multiplier. The phase space distribution could now be characterized as function of energy. The system, however, remained closed; the system could not change particle number. The construction of the *grand canonical ensemble* loosens this constraint.

The macrostate of a grand canonical ensemble allows the particle number, *N*, to fluctuate—particles can now flow in and out of the volume. Physically, such a system might be one separated from its environment by a diffusive membrane. With the fluctuation of particle number, the conception of phase space changes dramatically. In the canonical ensemble, when the constraint on fixed energy was relaxed, the range of accessible state spanned all of a *6N*-dimensional phase space. Now, with fluctuations in particle number, phase space becomes a collection of phase spaces; as *N* fluctuates, so does the dimensionality of the corresponding phase space. A photo album of phase spaces with a snapshot for each dimensional phase space comes to mind. The existence of each snapshot is weighted by some distribution. Again, in equilibrium, an average particle number must exist over the collection of phase spaces,

$$< N >= \sum_{N=0}^{\infty} \int N \rho(\boldsymbol{p},\boldsymbol{q}) d\boldsymbol{q} d\boldsymbol{p} \,,$$

where the summation indexes each phase space snapshot.

The normalization condition and the mean energy condition are equivalently altered,

$$\sum_{N=0}^{\infty} \int \rho(\boldsymbol{p},\boldsymbol{q}) d\boldsymbol{q} d\boldsymbol{p} = 1$$

$$< H >= \sum_{N=0}^{\infty} \int H(\boldsymbol{p},\boldsymbol{q}) \rho(\boldsymbol{p},\boldsymbol{q}) d\boldsymbol{q} d\boldsymbol{p} \,.$$

Again, the boldface coordinate and momentum are defined to represent all dimensions of phase space. In this case, they change as dimension of phase space changes. The maximization of entropy using these constraints yields the *grand canonical partition function*,

$$Z_G(T,V,\mu) \equiv \sum_{N=0}^{\infty} e^{\beta\mu N} \int e^{-\beta H(\boldsymbol{p},\boldsymbol{q})} d\boldsymbol{p} d\boldsymbol{q} = \sum_{N=0}^{\infty} e^{\beta\mu N} Z(T,V,N) \qquad (2.3.4).$$

Identification with the thermodynamic expression for open, non-isolated systems, the *grand potential*,

$$\mathcal{G} = U - TS - \mu N ,$$

produces the microscopic-macroscopic correspondence,

$$\mathcal{G}(T,V,\mu) = -k_B T \ln\left[Z_G(T,V,\mu)\right].$$

The associated phase density is

$$\rho(\boldsymbol{p},\boldsymbol{q}) = \rho(E,N) = \frac{e^{-\beta H(\boldsymbol{p},\boldsymbol{q})+\beta\mu N}}{Z_G(T,V,\mu)},$$

where, again, the correct partition function appears as normalization.

A mathematical note of interest: the grand canonical partition function is a discrete Fourier transform of the canonical partition function, Equation (2.3.4). The sum is over the denumerable quantity of particle number and associated quanta of chemical potential. The canonical partition function is, itself, a Fourier transform of the microcanonical partition function, which is constant by postulate. The variables of exchange are the non-denumerable quantities of energy and temperature. If the Lagrange multiplier method is applied to construct an ensemble where energy and volume are allowed to fluctuate, the so-called *T-p* ensemble (the allowance of mechanical variation at constant pressure), the associated partition function, $Z_p(T,p,N)$, would be the Fourier transform of the canonical partition function, where the variables of exchange are the non-denumerable quantities of pressure and volume.

These ensemble formulations form the foundation of equilibrium statistical mechanics. Applied appropriately, physical processes of aggregate systems can be described with exquisite precision in the thermodynamic limit, where

$$N \to \infty \text{ , } V \to \infty \text{ , and } \frac{N}{V} \to \text{constant} .$$

3 THE PROBLEM OF MAGNETIC RESONANCE

Magnetic resonance is a powerful tool which has found a home in disciplines as divergent as medicine and geology, and now includes electrical engineering and computer science. The problem of magnetic resonance originated in the attempt to understand the quantum mechanical nature of the universe, and led to the discovery of the *quantum mechanical spin.* Practically, magnetic resonance has been used by chemists to determine complex chemical structures, like proteins; by geologists to determine the chemical composition of unknown substances; and by physicians to provide images for clinical diagnosis and treatment.

Pedagogically, the problem of magnetic resonance is rich with physics. Magnetic resonance provides a means to teach quantum, statistical, and classical mechanics, and to forge connections between the three. It also serves as an interesting, yet rudimentary introduction to experiment, incorporating knowledge of introductory electromagnetism and fundamental circuit design to observe behavior predicted by theory.

3.1 Spin

Early in the development of quantum mechanics, physicists used atoms as model quantum mechanical systems. In their analysis of atomic spectra, physicists were pleased to find quantum energy states, but were dismayed by the presence of multiplet structures (splitting of energy levels) which arose due to the presence of magnetic fields—what is termed the *Zeeman effect*. Physicists had observed similar spectral structures caused by the orbital angular momentum of electrons about the nucleus. To account for Zeeman effect, Uhlenbeck and Goudsmit postulated a second source of angular momentum—*spin angular momentum*—attributed to the electron spinning about its axis. Experiments performed by Stern and Gerlach confirmed the existence of spin as postulated by Uhlenbeck and Goudsmit. In time, the confluence of quantum mechanics and special relatively would yield the theoretical rationale for the existence of spin.

Spin exists in a reduced physical dimensional space and takes on quantized states when measured. Particles may possess half-integer spin (fermions) or integer spin (bosons); both can be observed in magnetic resonance spectra.

NMR specifically refers to the interrogation and manipulation of proton spins. Protons are spin-½ particles, which is to say they are two-state systems in which the spin can only be observed either aligned or anti-aligned with the reference static magnetic field. These form the basis of any possible wave function which describes a two-state system,

$$|\Psi\rangle = c_{\downarrow}|\downarrow\rangle + c_{\uparrow}|\uparrow\rangle,$$

where $c_{\downarrow}, c_{\uparrow}$ are complex numbers. The normalization condition required of wave functions further simplifies analysis by reducing the Hilbert space of the two-state system to the surface of a sphere. Associated with this basis is the spin projection operator,

$$\hat{S} = \frac{1}{2}\hbar\left[\vec{x}\hat{\sigma}_x + \vec{y}\hat{\sigma}_y + \vec{z}\hat{\sigma}_z\right].$$

By convention, the positive *z*-direction is that of the static magnetic field. The spin operator is composed of operators in each Cartesian direction called *Pauli matrices*,

$$\hat{\sigma}_x \equiv \begin{bmatrix} 0 & 1 \\ 1 & 0 \end{bmatrix} \qquad \hat{\sigma}_y \equiv \begin{bmatrix} 0 & -i \\ i & 0 \end{bmatrix} \qquad \hat{\sigma}_z \equiv \begin{bmatrix} 1 & 0 \\ 0 & -1 \end{bmatrix},$$

and has a coefficient corresponding to a quanta of spin angular momentum. Though the Pauli matrices appear arbitrary, their construction follows quite simply from the discussion of quantum mechanical projection operators.

Generically, the spin operator is

$$\hat{S} = \vec{\boldsymbol{x}}\hat{S}_x + \vec{\boldsymbol{y}}\hat{S}_y + \vec{\boldsymbol{z}}\hat{S}_z .$$

The eigenstates of a spin-½ system can be physically described as the spin being aligned or anti-aligned with a static magnetic field. Thus, the projection operator in the *z*-direction must yield the appropriate eigenvalue for either spin state; the eigenvalue should possess the correct units and reflect the binary nature of the state, hence

$$\hat{S}_z|\uparrow\rangle = \frac{\hbar}{2}|\uparrow\rangle \qquad \hat{S}_z|\downarrow\rangle = -\frac{\hbar}{2}|\downarrow\rangle \qquad \Rightarrow \qquad \hat{S}_z = \frac{\hbar}{2}\left[|\uparrow\rangle\langle\uparrow| - |\downarrow\rangle\langle\downarrow|\right].$$

In the matrix formalism, the eigenstates for the spin-½ system are defined to be,

$$|\uparrow\rangle = \begin{bmatrix} 1 \\ 0 \end{bmatrix} \qquad |\downarrow\rangle = \begin{bmatrix} 0 \\ 1 \end{bmatrix},$$

which, when substituted, yield the previously postulated Pauli matrix in the *z*-direction.

For $\hat{S}_x$ and $\hat{S}_y$, construction is simplified if their associated eigenstates are first determined in the established basis. As a matter of symmetry, if the $\hat{S}_x$ or $\hat{S}_y$ acts on an eigenstate, they must yield the same eigenvalues as $\hat{S}_z$. Geometry dictates that the $\hat{S}_x$ and $\hat{S}_y$ eigenstates must lie completely on the *x*- and *y*-axis, which can be achieved by the superposition of the basis states. Thus,

$$|\Psi_x\rangle = \frac{1}{\sqrt{2}}\left[|\uparrow\rangle \pm |\downarrow\rangle\right],$$

are the $\hat{S}_x$ eigenstates. The choice of the plus sign selects the spin state pointed in the positive *x*-direction, and the minus sign, the negative *x*-direction. An in-plane ⅞ rotation turns the $\hat{S}_x$ eigenstates to the *y*-axis, and generates

$$|\Psi_y\rangle = \frac{1}{\sqrt{2}}\left[|\uparrow\rangle \pm i|\downarrow\rangle\right]$$

as the eigenstates for $\hat{S}_y$. The operators, themselves, become,

$$\hat{S}_x = \frac{\hbar}{2}\left[|\uparrow\rangle\langle\downarrow| + |\downarrow\rangle\langle\uparrow|\right] \qquad \hat{S}_y = \frac{i\hbar}{2}\left[|\downarrow\rangle\langle\uparrow| - |\uparrow\rangle\langle\downarrow|\right],$$

which complete the previously stated Pauli matrices. As operators of observables, the spin operators are Hermitian.

The commutation properties of spin operators are

$$\left[\hat{S}_i, \hat{S}_j\right] = \varepsilon_{ijk} \cdot i\hbar\hat{S}_k \qquad \left[\hat{\boldsymbol{S}}^2, \hat{S}_i\right] = 0.$$

In the first expression, the value of ε_{ijk} is unity if the order of the spin operators comply with the indices. A factor of negative one is applied to the right-hand side of the equation each time the order of the operators is exchanged in the equation. The property of cyclic commutation implies that the spin operators constitute a *Lie group*. More concretely, it points to the fact that each component of the spin cannot be known simultaneous. What can be known is indicated by the second commutation relation: the *magnitude* of the spin and any single component of the spin state can be observed with arbitrary precision.

3.2 Isolated-Spin Dynamics

A spin behaves as a quantum mechanical magnetic moment. The nature of its interactions are magnetic—a magnetic field is required to observe it, and when observed it is either aligned with or against a static magnetic field. In fact, a magnetic moment can be defined from spin,

$$\hat{\vec{\mu}} = \gamma\hat{\vec{S}}$$

where γ is the gyromagnetic ratio of the particular spin (a proton has a different gyromagnetic ratio than an electron, for example) and $\hat{S}$ is the spin operator. The associated Hamiltonian is,

$$\hat{H} = -\hat{\vec{\mu}} \cdot \vec{B},$$

the dot product of the moment and the magnetic field. In the case of NMR, the magnetic field in the *z*-direction is a strong and static, while the transverse (those in the *x* and *y*-direction) fields are oscillatory and relatively weak,

$$\vec{B} = \vec{\boldsymbol{x}}B_{1x}\cos(\omega t + \phi) + \vec{\boldsymbol{y}}B_{1y}\sin(\omega t + \phi) + \vec{\boldsymbol{z}}B_0.$$

By convention, the static field is referred to at the B_0 field, and the transverse, rotating fields are called B_1 fields. If only a *z*-directed field exists, then the Hamiltonian reduces to

$$\hat{H} = -\gamma B_0\hat{S}_z,$$

and the time dependence of the wave function, determined through the use of Schrodinger's equation, is

$$\left|\Psi(t)\right\rangle = c_{\downarrow} e^{-i\left(\frac{E_{\downarrow}}{\hbar}t-\theta_{\downarrow}\right)}\left|\downarrow\right\rangle + c_{\uparrow} e^{-i\left(\frac{E_{\uparrow}}{\hbar}t-\theta_{\uparrow}\right)}\left|\uparrow\right\rangle,$$

where $c_{\downarrow}, c_{\uparrow}$ are now real numbers, $\theta_{\downarrow}, \theta_{\uparrow}$ account for the relative phase between eigenstates, and $E_{\downarrow}, E_{\uparrow}$ are the energy eigenvalues generated by the Hamiltonian. The parts are now in place to calculate the expected value of the magnetic moment—what is observed when many measurements are made on the spin. Component by component,

$$\begin{aligned}
\left\langle \mu_x \right\rangle &= \langle \Psi | \hat{\mu}_x | \Psi \rangle = \gamma \langle \Psi | \hat{S}_x | \Psi \rangle \\
\left\langle \mu_y \right\rangle &= \gamma \langle \Psi | \hat{S}_y | \Psi \rangle \\
\left\langle \mu_z \right\rangle &= \gamma \langle \Psi | \hat{S}_z | \Psi \rangle,
\end{aligned}$$

where the total moment is

$$\left\langle \vec{\mu} \right\rangle = \vec{x}\left\langle \mu_x \right\rangle + \vec{y}\left\langle \mu_y \right\rangle + \vec{z}\left\langle \mu_z \right\rangle.$$

Using the general form of the time-dependent wave function and the previously defined spin operators,

$$\begin{aligned}
\left\langle \mu_x \right\rangle &= \hbar\gamma c_{\uparrow} c_{\downarrow} \cos\left(\theta_{\downarrow} - \theta_{\uparrow} + \frac{\Delta E}{\hbar} t\right) \\
\left\langle \mu_y \right\rangle &= \hbar\gamma c_{\uparrow} c_{\downarrow} \sin\left(\theta_{\downarrow} - \theta_{\uparrow} + \frac{\Delta E}{\hbar} t\right) \\
\left\langle \mu_z \right\rangle &= \frac{\hbar\gamma}{2}\left[c_{\uparrow}^2 - c_{\downarrow}^2\right],
\end{aligned}$$

where

$$\Delta E = E_{\uparrow} - E_{\downarrow}$$

is the energy required or released during a transition between the spin energy eigenstates. Experimentally, these levels can be observed through spectra, a recording of the electromagnetic radiation released or absorbed when a spin makes transitions. These photons which are absorbed or emitted have energy quanta related to their wavelength. Associated with each transition is

$$\Delta E = \frac{\hbar c}{\lambda} = \hbar\omega_0.$$

The connection between the energies produces final expressions,

$$\langle \mu_x \rangle = \hbar\gamma c_\uparrow c_\downarrow \cos\left(\theta_\downarrow - \theta_\uparrow + \omega_0 t\right)$$
$$\langle \mu_y \rangle = \hbar\gamma c_\uparrow c_\downarrow \sin\left(\theta_\downarrow - \theta_\uparrow + \omega_0 t\right)$$
$$\langle \mu_z \rangle = \frac{\hbar\gamma}{2}\left[c_\uparrow^2 - c_\downarrow^2\right].$$

The *z*-component of the magnetic moment is a constant of motion, while the *x*- and *y*-components evolve in a rotationally at the *Larmor frequency*,

$$\omega_0 = \gamma B_0 ,$$

a resonant frequency parallel and proportional to the static, bias magnetic field. On average, the spin precesses about the bias field at the Larmor frequency, a result previously calculated using classical models. A quick calculation to predict the time-evolution of the expected value of the moment using the expression,

$$\frac{d\langle \mu_i \rangle}{dt} = \frac{1}{i\hbar}\langle \Psi | \left[\hat{\mu}_i, \hat{H}\right] | \Psi \rangle = \frac{1}{i\hbar}\left\langle \left[\hat{\mu}_i, \hat{H}\right] \right\rangle$$

produces

$$\frac{d\langle \vec{\mu} \rangle}{dt} = \langle \vec{\mu} \rangle \times \gamma \vec{B} ,$$

the torque relation.

With only two effective degrees of freedom, a transformation into a spherical coordinate system produces a useful interpretation for the behavior of the expected behavior of spins—a vector of length ½ $\gamma\hbar$ at a fixed angle from the *z*-axis, which precesses in the *x*-*y* plane, as in Figure 3.1. This is an interesting result, as the Hilbert space for a single spin is a vector from the origin to the surface of a unit sphere.

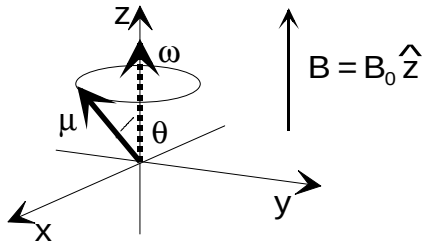

Figure 3.1. The vector model developed by Purcell describes the spin dynamics in terms of the evolution of its expectation value. The *x*-, *y*- and *z*- axes establish the coordinate system. The spin magnetic moment is depicted as the vector μ directed from the origin with a length equal to its magnitude. The axis of precession for the spin moment is represented by the vector ω, and represents the component of spin angular momentum aligned with the bias magnetic field.

With the intuitive picture of spin reconciled with its quantum mechanical origins, the effects of transverse fields can taken into account. The expression for the time-evolution of the spin can be expressed as

$$\frac{d\langle\vec{\mu}\rangle}{dt} = \langle\vec{\mu}\rangle \times \gamma\left[\vec{x}B_{1x}\cos(\omega t + \phi) + \vec{y}B_{1y}\sin(\omega t + \phi) + \vec{z}B_0\right].$$

To account for a static, bias magnetic field and a time-varying excitation field. To remove the time-dependence in the excitation field, a coordinate transformation is made from the laboratory frame to the rotating frame of the spin. If the frame is chosen to rotate with the *z*-component of the excitation frequency, ω_z,

$$\frac{d\langle\vec{\mu}\rangle}{dt} = \langle\vec{\mu}\rangle \times \gamma\vec{B}_{eff}, \qquad \vec{B}_{eff} = \vec{x}B_{1x}\cos(\phi) + \vec{y}B_{1y}\sin(\phi) + \vec{z}B_0 - \frac{\omega}{\gamma}.$$

Analysis of the spin in the rotating frame finds the spin precessing about an effective field—the effect of applying transverse excitation fields is to rotate the spin precession axis in the laboratory frame. The addition of B_1 to the Hamiltonian adds a rotation of the precession axis to the time-evolution of the spin. The amount the spin precession axis is tilted away from the *z*-axis is

$$\theta_{rotate,k}(\tau) = \gamma B_{1k}\tau.$$

The application of the B_1 field for a properly chosen time, τ, can produce arbitrary rotations of the spin precession axis away from the *z*-axis about either the *x*- or *y*-axis. The amplitude of B_1 governs the rate of rotation.

The effect of the B_1 frequency, ω, is evident with the continuous application of the excitation field at constant amplitude. If the B_1 field frequency is swept from DC, the axis about which the spin precesses rotates away from the *z*-axis. The spin, following the precession axis, precesses toward and then away from the *z*-axis. When a magnetic moment is aligned with the bias field, it is in the minimum energy configuration. When it is anti-aligned, the moment assumes its maximum energy configuration. The excursion from alignment with the bias field requires the absorption of magnetic energy from the excitation field to increase magnetic potential. As the spin precesses, it will eventually align itself with the field. The energy previously acquired in the excursion from alignment is then emitted. This is the resonant nature of spin—the absorption and then emission of energy. At resonance, when $\omega = \omega_0$, the effective field is B_1; the spin will precess about an axis perpendicular to the *z*-axis as in Figure 3.2. As the precession progresses, the spin passes through maximal and minimal energy configurations—it aligns and anti-aligns itself with the bias field in each precession period. In spectra, a peak results at the resonant frequency due to the maximal absorption and emission of energy.

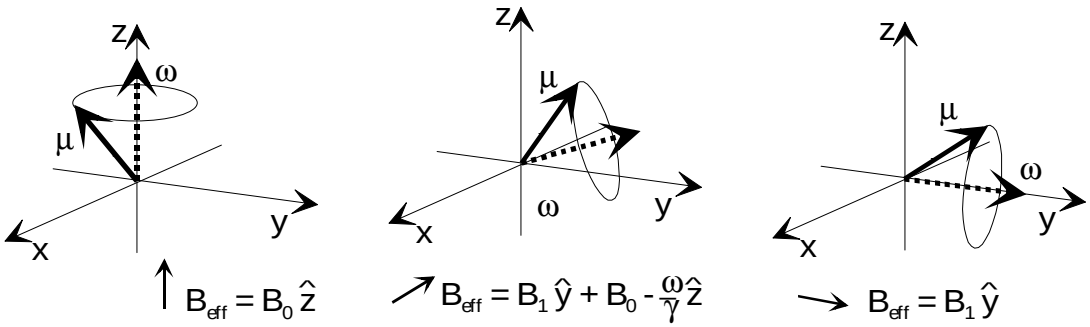

Figure 3.2: This progression illustrates the effect of an excitation field when its frequency is increased from DC to the resonance frequency. In the rotating frame, on-resonance, a spin on perceives a bias field in the direction of excitation.

Quantum mechanically, a similar description follows. The resonant frequency corresponds to the exact quanta of energy needed for a spin in a lower energy state to be excited to the higher energy state. Equivalently, a transition from the higher energy state to the lower energy state is accompanied by the emission of a photon of the same energy. Only excitation fields at the Larmor frequency will supply the correct quanta of energy required for transitions, producing a spectral peak on resonance.

Berry's Phase

An interesting failure of the classical picture is illustrated when an excitation field is applied to cause a 2π rotation. If the spin is rotated about *x*-axis 2π radians, in the classical analogy, the spin returns to the same state it was in prior to the excitation. The fact of the matter is that spins are purely quantum mechanical entities which possess an internal degree of freedom called *Berry's phase*. The 2π rotation performs a *parallel transport*. The variables which describe the external degrees of freedom of the spin have been altered and then returned to their original values. However, a change in the internal degree of freedom was incurred—a *holonomy* was generated. A spin is a *spinor*, a class of entities with certain symmetries which exhibit holonomy. In the case of the 2π rotation, a factor of negative one is incurred to the spin state. To completely return the spin back to its original state, another 2π rotation is required.

3.3 Isolated, Coupled Spin Systems: Molecules

Liquid state NMR considers spins in molecules in an aqueous solution. In these liquids, molecules are free to tumble. These random motions average out inter-molecular interactions[1]. A sample composed of a single molecular species can be considered as an ensemble of non-interacting molecules. Each molecule may have more than one free proton spin. These spins are coupled through their magnetic interactions with each other.

The most rudimentary spin system is a molecule with two hydrogen atoms in electronically different environments. If there were no coupling between the two spins, the Hamiltonian would simply be the sum of the two spin Hamiltonians. However, since a spin is like a magnetic moment, it generates local magnetic field perturbations felt by neighboring spins. These magnetic interactions are the nature of spin-spin coupling, and are embodied in the Hamiltonian as a dipole coupling term,

[1] See "Homogeneous NMR Spectra in Inhomogeneous Fields," Vathyam, S., Lee, S., Warren, W.S., *Science*, vol. 272, April 5, 1996, for an interesting violation of this assumption.

$$\hat{H} = \gamma B_{0A}\hat{S}_{AZ} + \gamma B_{0X}\hat{S}_{XZ} + \frac{2\pi J_{AX}}{\hbar}\hat{S}_{AZ}\cdot\hat{S}_{XZ} \qquad (3.3.1).$$

A and *X* are used to label the two different spin types in a *heteronuclear* spin system and J_{AX} is the spin-spin coupling constant in units of hertz. The spin-spin interaction is relatively small, and its magnitude is independent of the external field strength. The effects of higher-order spin-spin interactions are negligible compared to the dipole interaction. To extend the Hamiltonian to *N* coupled spins requires the sum of each independent spin Hamiltonian and a summation over all possible spin pair interactions.

The quantum mechanical state of a *N*-spin system is denoted as

$$\left|a_1, a_2, \ldots a_{N-1}, a_N\right\rangle,$$

where each a_i represents the binary state of the *i*-th spin. The available states for a two-spin system are

$$\left|A, X\right\rangle = \left\{\left|\uparrow,\uparrow\right\rangle, \left|\downarrow,\uparrow\right\rangle, \left|\uparrow,\downarrow\right\rangle, \left|\downarrow,\downarrow\right\rangle\right\}.$$

Though two of the states appear to be degenerate, the local magnetic environment of each spin maybe different due to the structure of the molecule. The result is that a shielded spin may perceive a weaker bias field than an unshielded spin. The corresponding change in energy-levels is referred to as the *chemical shift*. In practice, measured chemical shifts are used to determine the structure of the molecule.

Due to the spin-spin coupling, the energy levels must include the contributions from spin interactions. Figure 3.3 illustrates the shifts in energy levels due to spin-spin coupling. The effect on spectra is the manifestation of minor energy shifts due to local perturbations in magnetic fields induced by spin orientation.

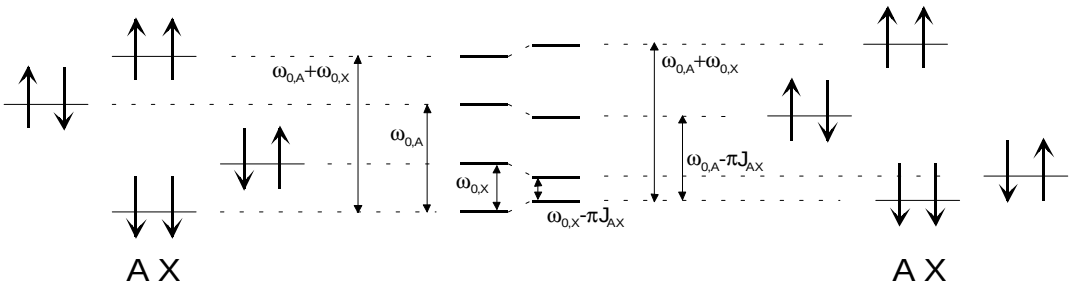

Figure 3.3: To the right is an energy-level diagram for an uncoupled spin system. The transition between energy-levels is set by the quanta of energy to flip the chosen spin. To the left is an energy-level diagram for a coupled spin system. The spin-spin interactions introduces shifts in the energy-levels due to the alterations in local magnetic fields induced by the orientation of neighboring spins. These energy shifts are characterized by the contribution of the coupling constant J_{AX} scaled by the spin orientation in the coupled-spin Hamiltonian as in Equation (3.3.1).

3.4 Thermal Spin Ensembles: Pure & Mixed Ensembles and the Density Matrix

Though understanding the nature of an isolated spin system is useful, isolated spin systems are difficult to access experimentally. More often, they are dealt with as ensembles in bulk materials. If an ensemble of spin systems are identically prepared and act in unison, then they constitute what is termed a *pure ensemble*. Each system can be described by a single state vector; their phase space distribution is a single point. The realization of a pure ensemble is difficult without a means to completely isolate the spins. More often, physical ensembles composed of equivalent individual systems are prepared in different states. These are referred to as *mixed ensembles*. Canonical and generalized ensembles are mixed ensembles. To deal with mixed ensembles, Dirac notation is extended by the *density matrix formalism* to realize *quantum statistical mechanics*. Quantum statistical mechanics is simply the application of statistical mechanics to an ensemble of quantum mechanical systems.

The basis of quantum statistical mechanics is the *density operator* or *density matrix*, the quantum mechanical phase space density function, defined as

$$\hat{\rho} \equiv \sum_i p_i \left|\psi_i\right\rangle\left\langle\psi_i\right| \qquad (3.4.1),$$

where the general states, $\left|\psi_i\right\rangle$, that describe the members of the ensemble are weighted by the probability, p_i. Equation (3.4.1) describes a mixed ensemble. To describe a pure ensemble, Equation (3.4.1) reduces to

$$\hat{\rho}_{pure} = \left|\psi_i\right\rangle\left\langle\psi_i\right|,$$

since each member of the ensemble is described by a common wave function. As a phase space density function, the density operator must be normalized. It must also be Hermitian. To sum through phase space, the *trace* is used. The trace of a matrix is the sum of its diagonal elements. The normalization condition is

$$Tr(\hat{\rho}) = \sum_i \rho_{ii} = 1,$$

where the *ii* indexes through the matrix elements of the density operator. In this case only the diagonal elements are indexed. This operation is equivalent to an integral sum through all of phase space in classical statistical mechanics, and suggests a method to calculate ensemble averages,

$$\left\langle \hat{A} \right\rangle = Tr\left(\hat{A}\hat{\rho}\right).$$

In the case of a pure ensemble the normalization condition means,

$$\hat{\rho}_{pure}^2 = \hat{\rho}_{pure} \quad \Rightarrow \quad Tr\left(\hat{\rho}_{pure}^2\right) = 1,$$

and corresponds to a matrix which has zeroes for all its off-diagonal elements and a single one in one of diagonal elements. For a mixed ensemble, the trace of the squared density operator is always less than one.

As with the classical density function, the density operator evolves under Hamiltonian dynamics according to Liouville's equation, and can be used to make connections between microscopic dynamics and macroscopic observables through the various ensemble formulations. Phase space, however, is quantized into elemental volumes of $N!(\hbar)^{3N}$ to account for quantum mechanical uncertainty and particle indistinguishability.

In NMR, the spins in a material constitute a canonical ensemble. They are at thermal equilibrium with their environment, but do not fluctuate in number. The quantum mechanical canonical probability distribution is,

$$\hat{\rho}(E_i) = \frac{e^{-\beta E_i}}{Z(T,V,N)},$$

where

$$Z(T,V,N) = \sum_j e^{-\beta E_j}$$

is the partition function and E_k are the quantum energy levels. Once the density matrix of operator is constructed, all the techniques of classical statistical mechanics can be applied to analyze aggregate quantum mechanical systems.

To describe an ensemble of two-spin systems solvated in liquid requires a density matrix. The non-interacting nature of the molecules simplifies the construction of the complete density matrix since it can be characterized by the tensor product of the density matrices that represent each spin system. For a sample with N molecules,

$$\hat{\rho}_{ensemble} = \hat{\rho}_1 \otimes \hat{\rho}_2 \otimes ... \hat{\rho}_{N-1} \otimes \hat{\rho}_N .$$

However, there is a simpler approach. Since the sample constitutes a canonical ensemble of two-spin systems, in equilibrium each energy state is populated according to the canonical distribution function. By definition, the complete density matrix is

$$\begin{aligned}\hat{\rho}_{ensemble} &= p_{\uparrow\uparrow}|\uparrow\uparrow\rangle\langle\uparrow\uparrow| + p_{\downarrow\uparrow}|\downarrow\uparrow\rangle\langle\downarrow\uparrow| + p_{\uparrow\downarrow}|\uparrow\downarrow\rangle\langle\uparrow\downarrow| + p_{\downarrow\downarrow}|\downarrow\downarrow\rangle\langle\downarrow\downarrow| \\ &= \begin{bmatrix} p_{\uparrow\uparrow} & 0 & 0 & 0 \\ 0 & p_{\downarrow\uparrow} & 0 & 0 \\ 0 & 0 & p_{\uparrow\downarrow} & 0 \\ 0 & 0 & 0 & p_{\downarrow\downarrow} \end{bmatrix},\end{aligned}$$

where the p_{ij}'s are canonical distribution function for each state divided by the lowest energy state distribution as reference, i.e.,

$$
\begin{aligned}
p_{\uparrow\uparrow} &= 1 \\
p_{\downarrow\uparrow} &= e^{-\beta(E_{\downarrow\uparrow}-E_{\uparrow\uparrow})} \\
p_{\uparrow\downarrow} &= e^{-\beta(E_{\uparrow\downarrow}-E_{\uparrow\uparrow})} \\
p_{\downarrow\downarrow} &= e^{-\beta(E_{\downarrow\downarrow}-E_{\uparrow\uparrow})}.
\end{aligned}
$$

From the density matrix, all physical behavior can be predicted by applying rotation operators to manipulate spins, evolution operators to perform free evolution, or projectors to observe physical properties.

A quick examination of a density matrix provides insight into the ensemble. The diagonal elements are the relative populations of the energy levels. The density matrix is symmetric: the elements below the diagonal are a reflection of the elements above the diagonal—the matrix is Hermitian. The off-diagonal elements indicate *quantum coherences*—couplings between state transitions.

3.5 Mathematical Rotation, Evolution, and Observation

Fundamentally, NMR techniques involve the manipulation, evolution and observation of spins. Physically, transverse radio-frequency (RF) magnetic fields are used to excite or manipulate spins. Excitations consist of an arbitrary angle rotations of spins from the bias field axis. Evolution to uncover spin-spin couplings and other behavior require evolution time to allow those mechanisms to unfold after a spin has been rotated. The spin response can be measured as a changing bulk magnetization. These actions all have corresponding mathematical operators.

In the density matrix formalism, the application of an operator is performed by applying the density matrix to the adjoint of the operator, and then pre-applying the operator, itself, to the density matrix. For an arbitrary rotation of the spins in a two-spin system, the matrix operators are

$$
R_{\theta xA} = \begin{bmatrix} \cos\left(\frac{\theta}{2}\right) & i\sin\left(\frac{\theta}{2}\right) & 0 & 0 \\ i\sin\left(\frac{\theta}{2}\right) & \cos\left(\frac{\theta}{2}\right) & 0 & 0 \\ 0 & 0 & \cos\left(\frac{\theta}{2}\right) & i\sin\left(\frac{\theta}{2}\right) \\ 0 & 0 & i\sin\left(\frac{\theta}{2}\right) & \cos\left(\frac{\theta}{2}\right) \end{bmatrix}, \; R_{\theta yA} = \begin{bmatrix} \cos\left(\frac{\theta}{2}\right) & \sin\left(\frac{\theta}{2}\right) & 0 & 0 \\ -\sin\left(\frac{\theta}{2}\right) & \cos\left(\frac{\theta}{2}\right) & 0 & 0 \\ 0 & 0 & \cos\left(\frac{\theta}{2}\right) & \sin\left(\frac{\theta}{2}\right) \\ 0 & 0 & -\sin\left(\frac{\theta}{2}\right) & \cos\left(\frac{\theta}{2}\right) \end{bmatrix}
$$

$$
R_{\theta xX} = \begin{bmatrix} 0 & 0 & \cos\left(\frac{\theta}{2}\right) & i\sin\left(\frac{\theta}{2}\right) \\ 0 & 0 & i\sin\left(\frac{\theta}{2}\right) & \cos\left(\frac{\theta}{2}\right) \\ \cos\left(\frac{\theta}{2}\right) & i\sin\left(\frac{\theta}{2}\right) & 0 & 0 \\ i\sin\left(\frac{\theta}{2}\right) & \cos\left(\frac{\theta}{2}\right) & 0 & 0 \end{bmatrix}, R_{\theta xX} = \begin{bmatrix} 0 & 0 & \cos\left(\frac{\theta}{2}\right) & \sin\left(\frac{\theta}{2}\right) \\ 0 & 0 & -\sin\left(\frac{\theta}{2}\right) & \cos\left(\frac{\theta}{2}\right) \\ \cos\left(\frac{\theta}{2}\right) & \sin\left(\frac{\theta}{2}\right) & 0 & 0 \\ -\sin\left(\frac{\theta}{2}\right) & \cos\left(\frac{\theta}{2}\right) & 0 & 0 \end{bmatrix}
$$

The rotation matrices generate arbitrary rotations of spin *A* and *X* about the *x*- and *y*-axis. The non-zero quadrant of each matrix constitutes a rotation operator for a single spin. Rotation operators for a *N*-spin systems can be constructed by taking tensor products of the spin rotation operators.

The free evolution of a density operator is performed by applying the density operator to the adjoint of unitary evolution operator and then pre-applying the unitary evolution operator to the density matrix. The time of evolution is chosen as a scale factor of the Hamiltonian in the exponent of the unitary evolution operator.

The bulk magnetization is the observed quantity of interest in NMR. It is the vector sum of the spin defined magnetic moments,

$$\left\langle \vec{M} \right\rangle = \sum_i \left\langle \vec{\mu}_i \right\rangle .$$

The calculation can be performed using the density matrix, but a more intuitive argument exists. Since proton spins are binary in nature, at thermal equilibrium they are either aligned or anti-aligned with the magnetic bias field. The bulk magnetization is due to the small population difference between spin in the two states. The population difference, again, is set by the Boltzmann distribution.

$$\begin{aligned}
\left\langle \vec{M} \right\rangle_0 &= N_\uparrow \vec{\mu}_\uparrow + N_\downarrow \vec{\mu}_\downarrow \\
&= \left(N_\uparrow - N_\downarrow \right) \vec{\mu} \\
&= \left(\tanh\left(\beta \left(E_\downarrow - E_\uparrow \right) \right) \right) N \gamma \hat{S}_z \\
&= \left(\tanh\left(\beta \Delta E \right) \right) N \gamma \hat{S}_z \\
\left\langle \vec{M} \right\rangle_0 &\approx \frac{N \hbar^2 \gamma^2 B_{z0}}{4 k_B T} \equiv M_0 .
\end{aligned}$$

M_0 is the equilibrium magnetization for a spin-½ system, oriented in the direction of the applied bias field. The bulk magnetization is an intrinsic property of the material. The chemical structure of different molecules shield proton spins differently. Since proton spins are *paramagnetic* by nature, they want to align themselves with the bias field. The material characteristic of *magnetic susceptibility* is defined as,

$$\chi_0 \equiv \frac{M}{H} = \frac{N \hbar^2 \gamma^2 \mu_0}{4 k_B T},$$

where M is the observed magnetization and H is the applied field strength (B is the magnetic field flux).

3.6 Spin-Lattice Relaxation, Spin-Spin Relaxation, Saturation and the Bloch Equations

The analysis of single spin systems was performed under the assumption of thermal isolation. If a spin was excited, there is no mechanism for the system to return to a ground state. In the case of a spin ensemble in contact with a thermal reservoir, spins can exchange energy with the

reservoir to return to a lower energy state. Any excitation introduced will eventually decay due to heat transfer between the spin and its environment.

The are two mechanisms by which the bulk magnetization can relax. The first, spin-lattice (or longitudinal) relaxation, is a true thermodynamic relaxation mechanism, which effects the *z*-component (or longitudinal component) of magnetization. After a spin ensemble comes to equilibrium with a bias magnetic field, a macroscopic bulk magnetization appears due to population difference in the two energy states. This population difference is

$$n(t) \equiv N_{\uparrow}(t) - N_{\downarrow}(t) .$$

The total number of spins,

$$N \equiv N_{\uparrow} + N_{\downarrow},$$

is constant in a canonical ensemble (i.e., a closed system). The members of the ensemble can exchange energy with the environment (or lattice) or with an external energy source, such as an applied B_1 field. The absorption and emission necessitate energy-state populations to re-organize with certain transition probabilities. The change in populations of each energy state can be given by the two-state *master equation*,

$$\frac{dN_{\uparrow}}{dt} = N_{\downarrow}\left(W_{\downarrow-\uparrow} + w_{\downarrow-\uparrow}\right) - N_{\uparrow}\left(W_{\uparrow-\downarrow} + w_{\uparrow-\downarrow}\right) \qquad (3.6.1a)$$

$$\frac{dN_{\downarrow}}{dt} = N_{\uparrow}\left(W_{\uparrow-\downarrow} + w_{\uparrow-\downarrow}\right) - N_{\downarrow}\left(W_{\downarrow-\uparrow} + w_{\downarrow-\uparrow}\right), \qquad (3.6.1b)$$

where $W_{m\text{-}n}$ denotes the probability for transition per second from state *m* to state *n* due to interactions with the lattice and $w_{m\text{-}n}$ is the transition probability due to an external injection of excitation energy. In general, the master equation describes the time evolution of the occupation of a certain state by summing the difference between the in-flux and out-flux of members from a given state over all other possible states.

The transition probabilities due to energy exchanges with an external source depend on the frequency of the excitation since the system is resonant. The $w_{m\text{-}n}$'s are also symmetric. The calculation of the transition probabilities from quantum mechanics yields the wave function,

$$w_{m-n} \propto \langle m|\hat{H}|n\rangle\langle m|\hat{H}|n\rangle^* .$$

Since the Hamiltonian is Hermitian, the quantity on the right-hand side is real and remains the same regardless of the direction of the transition, i.e.,

$$\langle m|\hat{H}|n\rangle = \langle n|\hat{H}|m\rangle^* .$$

So,

$$w_{m-n} = w_{n-m} = w(\omega) .$$

The transition probabilities for interactions with the lattice, however, are not symmetric. Since the lattice is considered a body of infinite heat capacity, it is assumed to always be in a state of internal equilibrium. The master equation for the lattice, then, has no time dependence, and the transition probabilities, in the absence of external excitation, are related by the ratio of relative populations in the two states given by the Boltzmann distribution,

$$\frac{W_{\uparrow-\downarrow}}{W_{\downarrow-\uparrow}} = \frac{N_{\downarrow}}{N_{\uparrow}} = e^{\beta\hbar\omega_0}.$$

The same transition probabilities hold for the spin ensemble since the lattice and the spin ensemble form an isolated system. Since energy must be conserved within an isolated system, the spin ensemble can only interact with the lattice at a rate set by the transition probabilities of the lattice.

To calculate the time evolution of the population difference, *n*, expressions for $N_{\uparrow}$ and $N_{\downarrow}$ are derived from expressions for *N* and *n* and substituted into either Equation (3.6.1a) or Equation (3.6.1b). The result is

$$\frac{dn}{dt} = \left(W_{\uparrow-\downarrow} + W_{\downarrow-\uparrow}\right)\left[N\frac{W_{\downarrow-\uparrow} - W_{\uparrow-\downarrow}}{W_{\uparrow-\downarrow} + W_{\downarrow-\uparrow}} - n\right] - 2wn, \qquad (3.6.2)$$

which is suggestive of first-order decay. Intuitively, the term on the right-hand side from which the population difference is subtracted is the equilibrium population difference. Confirmation comes through the realization that in equilibrium the left-hand side of the master equation is zero. A gentle massage of the equilibrium master equations proves intuition to be truth. And, the convenient chose of

$$\frac{1}{T_1} \equiv W_{\uparrow-\downarrow} + W_{\downarrow-\uparrow},$$

where T_1 is the characteristic decay time of any deviation from equilibrium, yields a solution to Equation (3.6.2) of

$$n(t) = n_0\left(1 - e^{\frac{-t}{T_1}}\right),$$

in the absence of a external excitation. The natural tendency of the ensemble is to remain in equilibrium.

In the presence of external excitation on resonance, the interactions with the lattice become comparatively small, and

$$n(t) = n_0 e^{-2wt}.$$

In the presence of prolonged external on-resonance excitation, the population difference will eventually decay away in a process called *saturation*. A spin ensemble has a finite heat capacity—it can only absorb a finite amount of energy. As the "spin temperature" goes to infinity, the spin ensemble must assume an increasing state of disorder, characterized by an equal occupation of energy-states. Since the transition probability of the spins are equal in both directions, the net flux of transitions between states is zero, and the population difference remains zero for the duration of the applied excitation. After the excitation is stopped, spin interactions with the lattice will restore equilibrium occupations of the spin energy-levels.

The connection between these population differences to physical observables is natural. Since the *z*-component of the bulk magnetization of a spin ensemble is the population difference scaled by the magnitude of a single spin magnetic moment, then the bulk magnetization in the *z*-direction possesses the same tendency to return to an equilibrium state,

$$\frac{dM_z}{dt} = \frac{M_0 - M_z}{T_1}.$$

The second relaxation mechanism effects the transverse component of magnetization. This so-called *spin-spin relaxation*, does not involve heat exchange with an external heat reservoir and is reversible. The nature of spin-spin relaxation is related to the manner in which bulk magnetization is observed. Bulk magnetization is a vector sum of individual spin magnetic moments. For equal numbers of spin moments pointed opposite each other, the net magnetization is zero. Spin-spin relaxation is due to the effect of vector cancellation of magnetization.

If a magnetic field rotates an ensemble of spins into the transverse plane and is then removed, the spins will precess in the transverse plane for the characteristic time T_1 until the ensemble returns to equilibrium. The net transverse magnetization, however, will degrade much faster. Since the spins precess about the bias magnetic field with a precession frequency proportional to their perceived bias field strength, even minute inhomogeneities in bias fields will produce varying precession frequencies. Similarly, spin interactions within a spin system will slightly alter perceived magnetic environments. After the initial tip, the spins are in-phase: they begin by being rotated into the transverse plane together. As they begin to precess, these minor deviations in perceived magnetic fields cause some spins to precess faster than others. The spins lose *phase coherence*. Eventually, the spins completely fan out, so although the spin moments still precess in the transverse plane, the bulk magnetization observed as a vector sum of those individual spin moments is zero.

The relations for the decay of the transverse components of bulk magnetization are

$$\frac{dM_x}{dt} = -\frac{M_x}{T_2}$$
$$\frac{dM_y}{dt} = -\frac{M_y}{T_2}.$$

The characteristic decay time is denoted as T_2. Since the mechanism for spin-spin relaxation is loss of phase coherence, the characteristic time for decay is generally much shorter than T_1. The

symmetry of the problem demands that T_2 is same decay constant for both the *x*- and *y*-components of magnetization.

With the effects of relaxation, the equations of motion for bulk magnetization due to spins are

$$\frac{d\vec{M}}{dt} = \vec{M} \times \gamma\vec{B} - \vec{T}^{-1}\left(\vec{M} - \vec{M}_0\right),$$

where

$$\vec{T} = \begin{bmatrix} T_2 & 0 & 0 \\ 0 & T_2 & 0 \\ 0 & 0 & T_1 \end{bmatrix}.$$

These equations of motion for quantum mechanical spins in bulk were first introduced by Felix Bloch in 1947. They are referred to as the *Bloch equations*. They are the same as the equations derived in the opening from classical considerations of spin.

The sinusoidal decay signal measured due to spin-spin relaxation modulated by spin precession is called a free induction decay (FID). It is simply the sinusoidal decay of a resonant structure and is depicted in Figure 3.4. This decay is reversible.

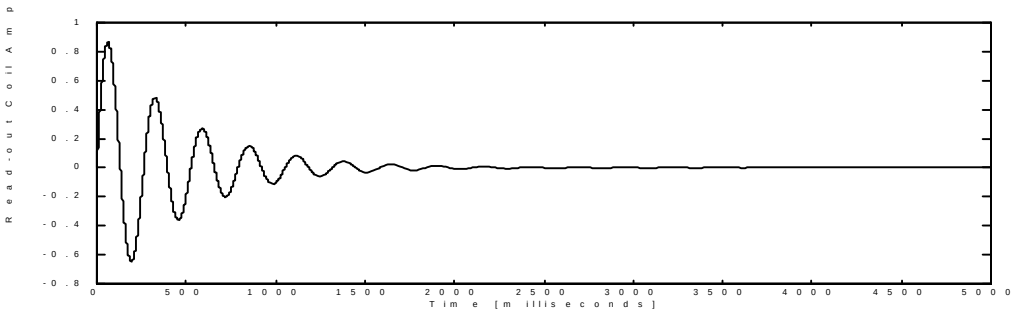

Figure 3.4: The FID oscillates at the Larmor frequency and decays with a characteristic time-constant T_2. The decay is due to loss of phase coherence among the spins in the sample.

The reversal of spin-spin relaxation observed in a FID requires a second injection of energy to restore phase coherence to the spins. Erwin Hahn first developed a technique to observe the reversal of spin-spin relaxation. After the application of a $\pi/2$-rotation pulse about either the *x*- or *y*-axis to rotate the bulk magnetization into the transverse plane, he waited a time, τ, and applied a second $\pi/2$-pulse. What he observed was the reappearance of the FID—a "spin echo." A more illustrative example was later developed by Carr based on the vector model proposed by Purcell. The technique is called *refocusing*. Rather than applying a second $\pi/2$-pulse, Carr applied a π-pulse. The application of a π-pulse after the $\pi/2$-pulse effectively reversed the time-evolution of the spins. The wait time, τ, after the first pulse allows the spins to lose phase coherence. The application of a π-pulse flips them in the transverse plane—they mirror their original positions across the axis of excitation. Now, the spins with the slower precession

frequencies are ahead of the spins with faster precession frequencies. As the spins with the faster precession frequencies catch up, all the spins eventual re-align. They re-establish phase coherence, and result in a maximum transverse magnetization before losing phase coherence again.

Excitations to manipulate spins are referred to as *pulse sequences*. In the case of the spin echo experiments, the pulse sequence consisted of two pulses, both at the resonant frequency, differing in duration. More complex pulse sequences have been designed to extract even more information from spins regarding their environment. The length of a pulse sequence is ultimately constrained by the T_1 coherence time of the spins.

4 NMR QUANTUM COMPUTATION

4.1 Classical Computation

Modern digital computation consists of bits and operations on bits. A *bit* is a binary value—either 1 or 0, positive or negative, present or absent. An arbitrary number can be represented by a sequence of bits. Operations can be performed on a single bit or on many bits. These operations are implemented as *logic gates*. Any function can be generated from a single-bit operation called NOT and a two-bit operation call XOR. Figure 4.1 is schematic drawing of the NOT and XOR operations with their associated truth tables. Algorithms and arithmetic operations such as addition can be implemented from a network of logical gates.

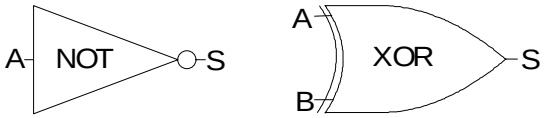

A	S
0	1
1	0

A	B	S
0	0	0
0	1	1
1	0	1
1	1	0

Figure 4.1: The schematic representation and truth tables for the NOT and XOR logical operations

The requirements for general computation are the ability to set arbitrary initial values, a means to operate on those values, a means to preserve state—to retain intermediate answers for consecutive operations, and the ability to measure or read the final result. A practical implementation also requires a mechanism for error correction. With these capabilities, a computer can produce an answer for any computable problem over a finite period of time.

As with all processes, computation must obey physical laws. Computation is information processing, and the representation and manipulation of information has a physical reality. Be it electrical charge coursing through a network of transistors, a bundle of photons traversing an optic fiber, or beads sliding back and forth on a rod, the physical manifestation of a bit must obey the laws of physics. Equivalently, there is also a physical consequence to the act of computation. Energy is required to manipulate the physical bits; there are thermodynamic repercussions to the creation and annihilation of bits. Computation is a physical process which evolves in time in a prescribed manner, by a program. This perspective is binding, yet revealing: computation has physical limits, however traditional computation deals exclusively with classical behaviors and limits. The world is truly quantum mechanical. What if the computations were performed in a manner which took advantage of purely quantum mechanical interactions like entanglement and interference? How could these physical interactions enhance computation?

4.2 Quantum Computation

For decades, the notion of quantum computation has been of great theoretical interest. From the perspective of the physicist, a quantum computer is invaluable as a laboratory in which to study quantum mechanics. For a traditional computer to simulate a quantum system requires exponential time to account for the exponential combination of states in which a quantum mechanical system exist. A quantum computer, however, exists in these superposition of states,

and can thus simulate quantum mechanical systems in linear time. Also, the physical reality of setting initial conditions to prepare for a computation corresponds to placing a quantum mechanical system in a state that maybe probabilistically unlikely. There have been quantum states which have been postulated by never observed. Such a system promises to provide to means to not only observe these states, but to also create them.

The path to a quantum computer parallels that of a classical computer with a couple differences. A quantum computer needs to represent values in a form amenable to information processing—it needs a means to represent bits. These bits must exhibit quantum mechanical behavior; candidate quantum bits, or qubits, are any quantum mechanical two-state systems like spins and photons. Because these bits are quantum mechanical, they must obey Hamiltonian dynamics and evolve unitarily. This is again a departure from classical notions of computation where dissipation prevents reversible computations. For example, if a computation adds four and four, the solution is eight. To perform the reverse computation is impossible. Given an eight, it is not possible to determine whether the addends were four and four, three and five, six and two or one and seven. Information is destroyed and energy dissipated. Since dissipative processes are absent in microscopic, Hamiltonian dynamics, all quantum computations are reversible.

Quantum logic gates must be constructed with the properties of unitarity and reversibility. In analogy to the NOT and XOR gates, any computation can be realized through a network of controlled-not (CNOT) and single-bit operations. A schematic and truth table for a CNOT gate is presented in Figure 4.2. A single-bit operation consists of an operator which performs an arbitrary rotation on a state in Hilbert space. The effect of performing a single-bit operation may be a NOT gate or a ROOT-NOT gate: a single-bit operation can be used to inject an arbitrary phase shift between the basis states available to the system. With these rudiments, as with the NOT and XOR in classical computation, any desired function can be generated.

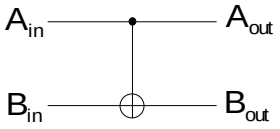

$\|A_{in}B_{in}\rangle$	$\|A_{out}B_{out}\rangle$
$\|00\rangle$	$\|00\rangle$
$\|01\rangle$	$\|01\rangle$
$\|10\rangle$	$\|11\rangle$
$\|11\rangle$	$\|10\rangle$

Figure 4.2: The CNOT is essentially a conditional-not performed with an entangled pair of qubits. B_{in} is inverted if A_{in} is one; if A_{in} is zero, B_{in} is untouched. A_{out} is always the same as A_{in}.

The fragility and power of quantum computation comes from the quantum mechanical behavior of its bits. Quantum computers can explore an exponentially larger computational space than its classical counterpart. A classical *N*-bit register holds a single value. A quantum mechanical *N*-bit register can hold 2^N values simultaneously due to the superposition properties of quantum mechanical systems. If a computation is cast in the form of a finite-state machine (FSM), rather than occupying a single state of the FSM, a quantum computer can occupy *all* states of the FSM *simultaneously*. In this sense, a quantum computer is a massively parallel computation device. However, in order to maintain a coherent superposition of states, a quantum computer cannot be disturbed. That is the paradox: to effect a computation requires the initialization, manipulation, and measurement of a computer's information. These are all actions which disturb the system. In quantum mechanics, the complexity of being in a superposition of states is lost as a system is disturbed and assumes an eigenstate. A quantum computer in thermal contact with its environment is already in jeopardy as thermal exchanges prevent the existence of a pure

ensemble, a possible initialization value. Early attempts to realize quantum computers used atom traps and quantum cavities to isolate and shelter atoms and photons as qubits. These systems were large, super-cooled experiments of greater labor and precision. The achievement of one- and two-bit computations were heroic, but effort required to realize those early successes suggested a dead-end on the road to practical quantum computations.

4.3 Molecules as Computers: NMR Quantum Computation

The breakthrough made by Neil Gershenfeld and Isaac Chuang was that molecules in a conventional liquid state system were perfect candidate quantum computers. This is unusual. NMR samples are thermal, bulk materials. All previous attempts to realize quantum computation were performed on quantum mechanical systems that were isolated, and composed of individual quantum mechanical entities. How could the quantum mechanical constituents of a thermal, bulk material possibly avoid the problem of maintaining a coherent superposition if individual quantum mechanical entities in an isolated, closed system could barely do so?

Buried in the nomenclature and practice of NMR is the answer. Liquid state NMR samples have demonstrated extremely long coherence times. They can remain in a coherent superposition of states for seconds, and, with extreme effort, for minutes. The NMR term for decoherence time is T_1, the spin-lattice relaxation time, the time is takes for spins to relax to thermal equilibrium. This suggests the molecules in a liquid state sample are essentially thermally isolated for a fair period of time. The assumption that rapid tumbling averages out intermolecular interactions further isolates individual molecules from each other.

Spins in NMR samples can also be manipulated without forcing them into eigenstates, i.e., unnecessarily disturbing their coherent superposition of states. The simple spin echo pulse sequence is proof: the spins in the system are twice manipulated with pulses—first a $\pi/2$-pulse and then a π pulse. The state of the spins can be observed during the pulse sequence—an FID appears after the $\pi/2$-pulse, and then a spin echo appears a short time after the application of the π pulse. All the while, the spins maintain a coherent superposition of states; T_1 has not expired. The spins have been manipulated and observed without being unduly disrupted. The reason for this apparent imperviousness is that NMR samples contains roughly 10^{23} identical molecules. Any thermal interactions with the environment or intentional measurements only weakly perturb the system. Only some members of the ensemble, those effected by the decoherence interactions, are lost. This, in part, explains why T_1 is a decay process, and not a sharp defining moment when the entire ensemble loses coherence.

The tools of NMR are the tools of NMR quantum computation (NMRQC). The systems of interest are the spin systems of individual molecules, and the means to manipulate and interrogate—apply algorithms and read-out results—are simply the pulse sequences and observed magnetization of the system. NMR is tailor-made for quantum computation.

Since an NMR sample is in thermal equilibrium, to establish initial condition, manipulations must begin with the density matrix in thermal equilibrium. From the equilibrium density matrix is distilled a pure ensemble, which may serve as an initial state for a quantum computer. In equilibrium,

$$\hat{\rho}_{eq} = \begin{bmatrix} p_{\uparrow\uparrow} & 0 & 0 & 0 \\ 0 & p_{\downarrow\uparrow} & 0 & 0 \\ 0 & 0 & p_{\uparrow\downarrow} & 0 \\ 0 & 0 & 0 & p_{\downarrow\downarrow} \end{bmatrix},$$

for a two-spin system. The density matrix can be separated into an identity matrix and a deviation matrix, which constitutes the portion of the sample that can actually be manipulated and observed,

$$\hat{\rho}_{eq} = \frac{1}{4}\begin{bmatrix} 1 & 0 & 0 & 0 \\ 0 & 1 & 0 & 0 \\ 0 & 0 & 1 & 0 \\ 0 & 0 & 0 & 1 \end{bmatrix} + \frac{1}{4}\begin{bmatrix} \alpha_1 + \alpha_2 & 0 & 0 & 0 \\ 0 & \alpha_1 - \alpha_2 & 0 & 0 \\ 0 & 0 & -\alpha_1 + \alpha_2 & 0 \\ 0 & 0 & 0 & -\alpha_1 - \alpha_2 \end{bmatrix},$$

where α_i is $\hbar\omega_i / 2kT$. The identity matrix portion of the density matrix is unaffected by unitary evolution. Since the identity matrix physically implies that all states of the system are equally populated, any rotation operation simply shifts the spin populations into different states, which are again equally populated, leaving the identity matrix unaltered. Any interesting behavior, then, resides in the deviation density matrix,

$$\hat{\rho}_{\Delta} = \begin{bmatrix} \alpha_1 + \alpha_2 & 0 & 0 & 0 \\ 0 & \alpha_1 - \alpha_2 & 0 & 0 \\ 0 & 0 & -\alpha_1 + \alpha_2 & 0 \\ 0 & 0 & 0 & -\alpha_1 - \alpha_2 \end{bmatrix}.$$

Though there are many competing techniques to manufacture a pure state, the most illustrative is the temporal labeling technique developed by Manny Knill at Los Alamos National Laboratories. Beginning with the deviation density matrix, the initial equilibrium populations are generically designated as *a*, *b*, *c* and *d*,

$$\hat{\rho}_{\Delta} = \begin{bmatrix} a & 0 & 0 & 0 \\ 0 & b & 0 & 0 \\ 0 & 0 & c & 0 \\ 0 & 0 & 0 & d \end{bmatrix}.$$

By applying pulse sequences, the equilibrium populations of the deviation density matrix can be permuted and then the results measured over time,

$$\hat{\rho}_{\Delta} = \begin{bmatrix} a & 0 & 0 & 0 \\ 0 & b & 0 & 0 \\ 0 & 0 & c & 0 \\ 0 & 0 & 0 & d \end{bmatrix} \quad \overset{permutation}{\Rightarrow} \quad \hat{\rho}_{\Delta 1} = \begin{bmatrix} a & 0 & 0 & 0 \\ 0 & c & 0 & 0 \\ 0 & 0 & b & 0 \\ 0 & 0 & 0 & d \end{bmatrix}$$

$$\hat{\rho}_{\Delta} = \begin{bmatrix} a & 0 & 0 & 0 \\ 0 & b & 0 & 0 \\ 0 & 0 & c & 0 \\ 0 & 0 & 0 & d \end{bmatrix} \quad \overset{permutation}{\Rightarrow} \quad \hat{\rho}_{\Delta 2} = \begin{bmatrix} a & 0 & 0 & 0 \\ 0 & d & 0 & 0 \\ 0 & 0 & c & 0 \\ 0 & 0 & 0 & b \end{bmatrix}$$

$$\hat{\rho}_{\Delta} = \begin{bmatrix} a & 0 & 0 & 0 \\ 0 & b & 0 & 0 \\ 0 & 0 & c & 0 \\ 0 & 0 & 0 & d \end{bmatrix} \quad \overset{permutation}{\Rightarrow} \quad \hat{\rho}_{\Delta 3} = \begin{bmatrix} a & 0 & 0 & 0 \\ 0 & b & 0 & 0 \\ 0 & 0 & d & 0 \\ 0 & 0 & 0 & c \end{bmatrix}$$

By summing the permuted density matrices,

$$\hat{\rho}_{\Delta 1} + \hat{\rho}_{\Delta 2} + \hat{\rho}_{\Delta 3} = \begin{bmatrix} 3a & 0 & 0 & 0 \\ 0 & b+c+d & 0 & 0 \\ 0 & 0 & b+c+d & 0 \\ 0 & 0 & 0 & b+c+d \end{bmatrix},$$

which is essentially a pure ensemble since,

$$\hat{\rho}_{\Delta 1} + \hat{\rho}_{\Delta 2} + \hat{\rho}_{\Delta 3} = b+c+d \begin{bmatrix} 1 & 0 & 0 & 0 \\ 0 & 1 & 0 & 0 \\ 0 & 0 & 1 & 0 \\ 0 & 0 & 0 & 1 \end{bmatrix} + 3a-b-c-d \begin{bmatrix} 1 & 0 & 0 & 0 \\ 0 & 0 & 0 & 0 \\ 0 & 0 & 0 & 0 \\ 0 & 0 & 0 & 0 \end{bmatrix}.$$

Again, the identity matrix is not effected by manipulations and is an absent during observation. The second term of the sum is effectively a pure ensemble—it behaves exactly like a pure ensemble when manipulated and observed. Convention required that a pure ensemble be generated prior to the execution of quantum computation. The temporal labeling method not only demonstrates how to create an effective pure ensemble from a thermal ensemble, but also suggests the incorporation of the ensemble purification process into quantum computational algorithms, as opposed to performing the purification explicitly prior to computation. Though the temporal labeling technique is illustrative, an increase in the size of the spin system is accompanied by a linear loss in signal strength. Logical labeling techniques developed by Neil Gershenfeld and Isaac Chuang promise to overcome this decrease in signal strength.

To actually implement quantum computation in NMR systems requires two rudiments, single-bit operations and a CNOT gate, to realize any computable function. A single-bit operation in NMR is simple. Any rotation suffices. To realize a NOT gate, for example, simply requires the

application of a π-pulse to invert the spin. A ROOT-NOT gate is simply a $\pi/2$ rotation. In fact an angle rotation can be implemented to realize any desired phase shift. The more involved task is the creation of a CNOT gate between two coupled bits. The pulse sequence as developed by Gershenfeld and Chuang, given by $R_{yA}(-90)\ R_{zB}(-90)\ R_{zA}(-90)\ R_{zAB}(180)\ R_{yA}(90)$, provides this necessary operations up to an overall phase factor, which is easily removed. The associated rotation matrix, when calculated, yields

$$\hat{C}_{AB} = \sqrt{-i}\begin{bmatrix} 1 & 0 & 0 & 0 \\ 0 & 1 & 0 & 0 \\ 0 & 0 & 0 & 1 \\ 0 & 0 & 1 & 0 \end{bmatrix}.$$

This pulse sequence essential performs a population transfer with corrective pulses to insure phase coherence between the non-zero elements of the matrix.

With the elements of quantum computation in hand, the steps to follow are dual. High-resolution NMR spectrometers already exist. Experiments to demonstrate the validity of these techniques have been performed and the testing of quantum algorithms is underway. The second path is to realize NMR quantum computation in a desktop system, to illustrate the potential for NMR quantum computers to be as pervasive as current day silicon, digital computers. To do this requires the construction of a table-top NMR spectrometer with the sensitivity and resolution specifications required to resolve spin-spin couplings using commercially available technologies.

5 INSTRUMENTATION DESIGN CONSIDERATIONS

5.1 A General NMR Spectrometer

The construction of a desktop quantum computer is the same as that of a high-resolution spectrometer. The task of performing a relatively complex quantum computation and extracting the result is equivalent to probing a protein to determine its structure. The general model for an NMR spectrometer is fairly simple. The fundamental requirements are means by which to excite spin transitions and a means to measure their relaxation to equilibrium. Though the reality of building a system is something short of an evolved art, the staples are basic. Figure 5.1 illustrates such a system in generality. The process of excitation and measurement need to be automated and controlled by a centralized controller. A bias magnetic field source is required to induce a spin population difference and thus a net bulk magnetization. High current amplifiers are required to drive inductive coils to generate B_1 fields for excitation. A low-noise pre-amplification stage is needed to amplify the small induced magnetization in a read-out coil positioned transverse to the bias field. A gain stage follows the low-noise pre-amplification to insure a high-level signal for processing. The high-level signal is filtered to reduce the admission of noise and extraneous interference, and then digitized for analysis.

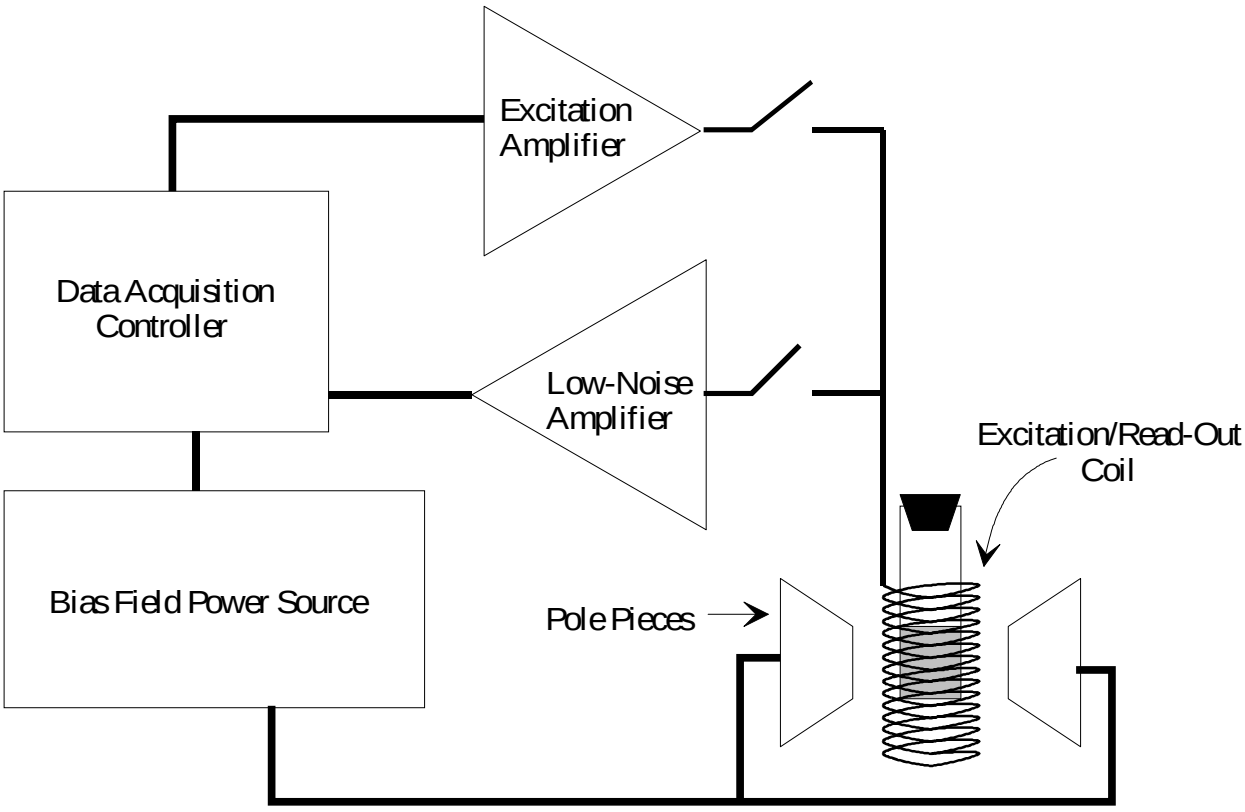

Figure 5.1: The canonical NMR spectrometer consists of a bias field source to generate a macroscopic magnetization, an excitation field source to manipulate spins, and a low-noise amplifier to read-out minute transverse magnetization. The pole piece are generally mu-metal piece used to create a region uniform bias field region for the sample. A single coil can be used for excitation and read-out with switches to multiplex between the two.

A survey of equipment and instrumentation is instructive to understand the which technologies are available for the design of a table-top spectrometer. For reproducible spectra, homogeneous,

stable sources of DC magnetic fields are required. Sensitive magnetometers are also required to measure the response of the spins to applied excitation magnetic fields. Table 5.1 offers a preliminary list of specifications for candidate magnets and magnetometers.

Magnetometer	Resolution	Field Range	Bandwidth	SNR
Solenoid	6nT/sqrt(Hz)	10e-6G->inf	1Hz-1MHz	6nT/sqrt(Hz)
Hall Probe	130mV/T	10e-10G->1000G	DC-1MHz	0.5uT/sqrt(Hz)
Magnetoresistive Bridge	0.1uT/sqrt(Hz)	10e-6G->50G	DC-1GHz	0.8nT/sqrt(Hz)
Flux Gate	0.1-10nT(100pT)	1e-10T->1e-4T	DC-10kHz	3.8pT/sqrt(Hz)
Magnetic Resonance Force Microscopy	50Ang deflection		DC-GHz	5e-3 Ang/sqrt(Hz)
SQUID	200fT->3pT	10e-10G->10e-4G	2MHz	10fT/sqrt(Hz)
NMR (proton precession magnetometer)	1nT	10e-8G->1G		0.5nT/sqrt(Hz)

Field Source	Strength	Homogeneity	Stability
Permanent Magnet	~1T	~30ppm/cm	
Intramagnet	~2e5G	5ppm	5ppm
Earth's Field	~0.5G	10e-8ppm/cm	2.5e-8T/year
Electromagnet	~0.5T	~10ppm/10cmDSV	0.1ppm/3s
Superconducting	~20T	3ppm/50cmDSV	0.1ppm/hr

Ang=Angstrom, G=Gauss, T=Tesla, ppm=part per million, W=weber

Table 5.1: Typical Magnet and Magnetometer specifications

5.2 Measurement of Magnetization

The physical observable of interest in magnetic resonance systems is the bulk magnetization. Macroscopically, the magnetization manifests itself as a property of media in a manner equivalent to magnetic field strength

$$\vec{B} = \mu_o(\vec{H} + \vec{M}) .$$

Thus, the same techniques used to measure magnetic fields can be applied to measure magnetic resonances.

Though many magnetometers exist, and are listed in Table 5.1, the most common technique employed in NMR spectrometers is the use of a simple solenoid or coil. The use of a solenoid to measure a particular magnetic resonance system is a problem in flux linkage. Though a direct measurement of the bulk magnetization due to population differences is possible, the expected

signal is extremely small. The choice to measure the transverse magnetization affords the advantage of increased signal strength due to the precession dynamics of the spin.

Maxwell's equations in differential and integral form are

$$\nabla \cdot \varepsilon \vec{E} = \rho \qquad \varepsilon \oint_S \vec{E} \cdot d\vec{A} = \int_V \rho dV \qquad \text{(Gauss' Law)}$$

$$\nabla \times \vec{E} = -\frac{d\vec{B}}{dt} \qquad \int_C \vec{E} \cdot d\vec{S} = -\frac{d}{dt}\int_S \vec{B} \cdot d\vec{A} \qquad \text{(Faraday's Law)}$$

$$\nabla \cdot \vec{B} = 0 \qquad \oint_S \vec{B} \cdot d\vec{A} = 0$$

$$\nabla \times \vec{H} = \vec{J} + \frac{d\vec{D}}{dt} \qquad \int_C \vec{B} \cdot d\vec{S} = \int_S \vec{J} \cdot d\vec{A} + \frac{d}{dt}\int_S \varepsilon \vec{E} \cdot d\vec{A}\,. \qquad \text{(Ampere's Law)}$$

For the measurement of the macroscopic transverse magnetization, Faraday's Law in integral form is of interest. It states that a difference in electric potential is created and due to the changes in magnetic field strength in the area circumscribed by the path. Faraday's induction law is pictorially represented in Figure 5.2. In the vernacular, Faraday's law says the voltage measured at the terminals of a solenoid equals the change of the magnetic field within the coils.

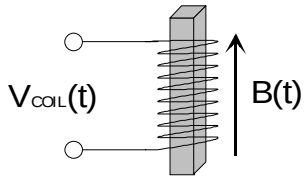

Figure 5.2: Faraday's law states that a changing magnetic field flux will induce a rotating electric field. If the magnetic flux within a winding of coils changes over time, a voltage will develop across the terminal of the coil proportional to the rate of change of the magnetic field flux.

To calculate the maximum signal strength expected from a solenoid measurement on a magnetic resonance system, the expression of magnetic flux in the presence of media is used. The expression derived from quantum mechanics for the bulk magnetization is substituted. The derivation yields

$$\begin{aligned}
\left|\frac{V_{coil}}{N_{coil}}\right| &= \left|-\frac{d}{dt}\int_S \vec{B} \cdot d\vec{A}\right| \\
&= \left|-\frac{d}{dt}\int_S \mu_0 \vec{M} \cdot d\vec{A}\right| \\
&= \left|-\frac{d}{dt}\int_S \mu_0 M_0 \sin(\omega_0 t + \phi) \cdot d\vec{A}\right| \\
&= \left|-\frac{d}{dt}\left[\mu_0 M_0 \sin(\omega_0 t + \phi) \cdot \pi R_{coil}^2\right]\right|
\end{aligned}$$

$$= \left| -\omega_0 \mu_0 M_0 \sin(\omega_0 t + \phi) \cdot \pi R_{coil}^2 \right|$$

$$= \left| \frac{N\hbar^2 \gamma^3 B_{z0}^2}{4k_B T} \mu_0 \pi R_{coil}^2 \right|$$

$$V_{coil} = N_{coil} \left| \frac{N\hbar^2 \gamma^3 B_{z0}^2}{4k_B T} \mu_0 \pi R_{coil}^2 \right|,$$

where N_{coil} is the number of turns in the coil; N is the number of spins in the sample; and R_{coil} is the radius of the coil..

5.3 Noise and Interference

The corruption of desired signals limits instrumentation measurement precision. Unwanted signals stem from two main sources, physical sources and external sources. Physical noise sources comprise of noise signals generated through physical mechanisms like those in resistors and current transport in solid-state circuits. They are inherent to an instrument. Though their contribution can be reduced, their presence is unavoidable. The second source of unwanted signals is generally referred to as interference. Interference is an unwanted signal which electrically or magnetically couples into an instrument from an external source such as a radiating antenna or a turning magnetic motor. Through proper design and thoughtful packaging, interference can be significantly reduced. With great effort, interference can be all together avoided.

5.3.1 Physical Noise Sources

Physical noise sources are intrinsic to the solid-state components used in circuits, and find their origin in fundamental thermodynamic processes. Fluctuation-dissipation processes manifest as Johnson noise in resistors. Equipartition noise contributions are attributed to capacitors and inductors. Current transport across potential barriers are also a source of noise. For monolithic integrated circuits (ICs), such as operational amplifiers, manufacturers specify noise quantities in the form of voltage noise, current noise, and the noise figure. In combination, these noise sources constitute the noise floor of the system—the absolute minimal noise level a system can attain.

Perhaps the most enigmatic physical noise source is 1/f or flicker noise. 1/f noise is ubiquitously found in a divergent range of physical systems, however there is no unifying physical mechanism to describe its presence. The name, 1/f, is due to the spectra of 1/f noise. Figure 5.3 displays a divergence in the noise spectra as frequency goes toward zero.

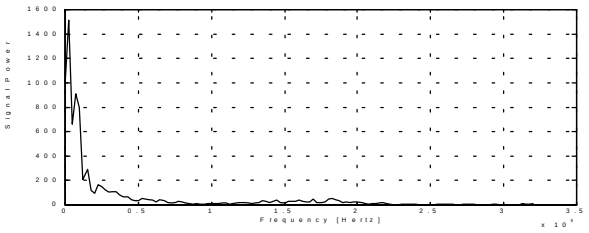

Figure 5.3: The spectral of character of 1/f noise diverges toward DC.

Shot noise is due to the granularity of current. Since current is actually a flow of electrons, there is necessarily a statistical fluctuation in the arrival times of the electrons across a junction. With the assumption that the electrons are independent of each other, the arrival times can described by the *Poisson probability distribution*, and yield a current fluctuation,

$$I_{shot} = \sqrt{2qI_{dc}B},$$

where q is the charge per electron, I_{dc} is the DC current flowing across the junction, and B is the bandwidth of the measurement device. The units for the shot noise current is in amperes-per-root-hertz, $\left[{}^{A}/_{\sqrt{Hz}}\right]$.

Johnson noise belongs to a greater class of physical processes described by the *fluctuation-dissipation theorem*. The fluctuation-dissipation theorem has many manifestations, among them Einstein's relations for Brownian motion in mechanical systems and Nyquist's relations for electronic systems, which leads to Johnson noise. The intuitive explanation for Johnson noise is simple. Electrons in a resistor become excited due to thermal agitation—energy fluctuations. They then move randomly due to Brownian motion induced by heat energy—dissipation of the acquired energy. These electrons, however are charged particles, and the flux due to their random motions constitute a current through the resistor. A current through a resistor generates a voltage across the resistor. This spurious voltage is referred to as the *Johnson noise* of the resistor. Without a complete derivation of Nyquist's theorem from the fluctuation-dissipation theorem, the expression for Johnson noise is

$$V_R = \sqrt{4k_B TRB}.$$

The notation is indicative of the manner in which noise is characterized. V_R is obviously a root-mean squared (rms) measurement. The k_B is the thermodynamic Boltzmann factor, T is the temperature in units of Kelvin, R is the resistance of the resistor, and B is the bandwidth of the measurement device in hertz. The inclusion of the bandwidth factor indicates that this noise voltage is measured in units of voltage-per-root-hertz $\left[{}^{V}/_{\sqrt{Hz}}\right]$.

The rationale for this unit is obvious with the consideration of the nature of noise. Since Johnson noise is the result of a time-invariant, collective random process, in mathematical terms it is stationary, Gaussian, broadband noise. Figure 5.4 elucidates these terms with a time-series, histogram and associated spectrum of Johnson noise. The amount of noise admitted to the system can be considered as the area under the noise spectrum in the frequency band on interest. This area is the power of the noise signal. If the system is very narrowband—it measures a frequency range of only a couple of hertz, for example—then the amount of noise it admits is much less than a wideband device, hence the bandwidth dependence.

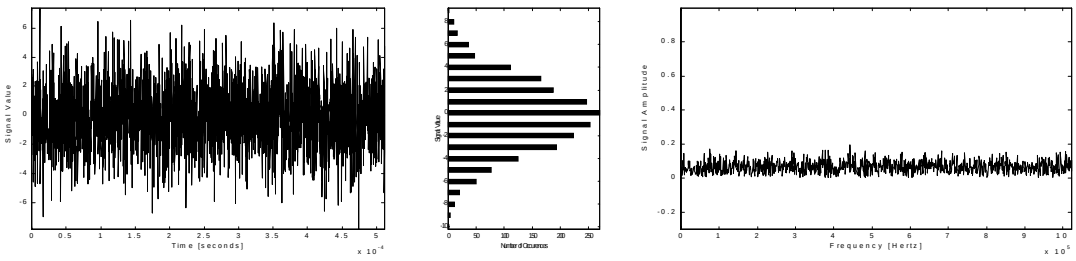

Figure 5.4: A time-series, histogram, and spectrum of gaussian-distibuted, stationary, white noise.

With each capacitor and inductor is associated an equipartition contribution of noise. The inclusion of either passive, energy-storing components adds an extra degree of freedom to the system. As with a volume of ideal gas, associated with each degree of freedom is an equipartition contribution of energy. In the volume of gas, a gas molecule has three degrees of translational freedom. For each degree of freedom, $\frac{1}{2}k_B T$ of internal energy is attributed to the gas, thus the familiar $E=3/2Nk_B T$ expression for internal energy of a N-molecule gas. In the case of an electronic system, this is no different. Each capacitor and inductor contributes another degree of freedom, which is evidenced mathematically by an increasing system order per addition of energy storage element. A mean energy is stored in each component due to an equipartition contribution of energy, which implies the existence of a baseline root-mean squared current or voltage through an inductor or across a capacitor expressed as,

$$I_L = \sqrt{\frac{k_B T}{L}}, \qquad \text{for an inductor,}$$

$$V_C = \sqrt{\frac{k_B T}{C}}, \qquad \text{for a capacitor.}$$

Noise in systems is generally characterized by the *noise figure*. The noise figure of a system is a measure of the noise contributed by the system over the baseline of noise introduced by the source resistance of what is being measured. Mathematically, the noise figure is

$$NF \equiv 10 \cdot \log_{10}\left(\frac{V_{n,sys}^2 + I_{n,sys}^2 R_{sys}^2 + V_{n,source}^2}{V_{n,source}^2}\right),$$

and is measured in decibels (dB). Though values for voltage and current noise accompany operational amplifiers, they are also characterized by a noise figure. A low noise figure is a strong figure of merit for low-noise preamplifiers and other systems which condition very small signals.

5.3.2 Interference Sources and Solutions

Interference from external sources is the predominant source of signal corruption in measurement systems. The three main mechanisms for the introduction of interference into a circuit are electrical (capacitive) coupling, magnetic (inductive) coupling, or irradiation by propagating electromagnetic waves.

Capacitive coupling of electrical signals involve the introduction of unwanted low frequency signals into the system. The model for this mechanism is a parallel plate capacitor, pictured in Figure 5.5. If the voltage on one plate of the parallel plate capacitor is driven, an electric field is created between the two plates. If the electric potential on the second plate is not secured to a voltage source, its voltage will change in accordance with the changes on the first plate to satisfy Maxwell's equations. If the second plate is secured to a voltage source, displacement currents in the second plate will arise as the electric field adjusts to meet the boundary condition set by the second plate.

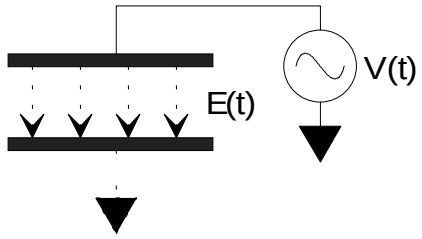

Figure 5.5: An electrode driven by a changing voltage will couple to a floating electrode through an electric field. The signal which develops on the floating electrode is proportional to the change of voltage on the driven plate.

The effect of these electrostatic couplings can be quantified through Maxwell's Equations cast in the form of boundary condition constraints. In practice, the oscillating plate of the parallel plate capacitor is any wire or metallic objects which has an changing voltage. This includes power lines, wires in and around computers or electronic circuits, phone lines, or even wires and pins within the measurement electronics. The second plate is a wire in the measurement device; a resistor, capacitor or inductor lead; a pin on a chip; or anything conductive.

The same mechanism which allows for the measurement of bulk magnetization also admits signal corruption. If a motor suddenly starts, if a computer monitor degausses, if there is any jolt of magnetic field flux, that change in magnetic field could induce a current in and a voltage across the terminals of the coil resident in a measurement circuit. This is the nature of inductive coupling. Figure 5.6 portrays a possible scenario for magnetic coupling.

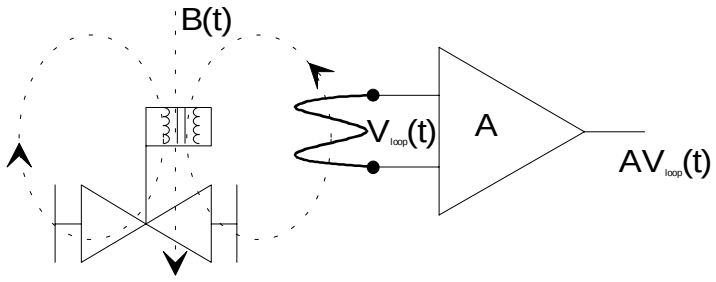

Figure 5.6: The abrupt ignition of a motor induces a magnetic field flux impulse which can couple into a sensitive measurement circuit through a loop of wire.

The final mechanism for the introduction of electromagnetic interference is simply electromagnetic radiation. RADARs, fluorescent lights, cellular phone, wireless local area network links—an antenna of any sort—are all possible sources of propagating electromagnetic radiation which may couple into measurement electronics. Though the mechanism for coupling

into a circuit is the same as either capacitive or inductive coupling—the electric and magnetic fields act quasi-statically locally—the deviousness of radiation is that it propagates and can potentially bathe an entire laboratory in interference.

The defense against interference includes physical and algorithmic solutions. The most obvious solution is to make sensitive measurements far from the electromagnetic pollution of urban development. For applications which require the use of electronics near sources of interference, physical shielding of the electronics will help. For electrostatic interference, conductive materials held at a potential (like ground) surrounding the circuit will swallow stray electric fields. The physical mechanism which enables electrostatic coupling is now used to keep the sensitive electronics from accidentally measuring unwanted signals.

For the case where the interference source is resident with the measurement electronics, proper design steps must be taken. Digital systems and sensitive analog systems should always be physically separated. Extremely sensitive analog systems should be completely shielded. On a printed circuit board a ground plane can be poured to protect individual pins, and small, grounded, metallic box should enclose sensitive electronics to establish a physical barrier between it and the environment.

For magnetically coupled interference, a similar method works. Rather than conductive materials, mu-metal, a material with a high magnetic permeability, must be used to guide magnetic flux away from a circuit. Since electromagnetic radiation must obey the same boundary conditions as static fields, these shielding methods work equivalently well to protect electronics from radiated interference.

Often, large workspaces need to be protected against interference to develop sensitive instrumentation. In order to create an electromagnetic oasis in the middle of civilization, Faraday cages are used. Faraday cages are large (sometimes walk-in sized) boxes completely lined with fine metal mesh, usually copper, which is held at ground potential. The copper mesh keeps the enclosed area free of electrostatic noise external to it. It also prevents electromagnetic radiation with wavelengths longer than the mesh size from entering. Magnetic interference, however, still needs be shielded with mu-metal. Faraday cages are commonly used to shelter entire experiments from interference.

If physical shielding is not possible or impractical, understanding the nature of electromagnetic interference is useful in its elimination. Most sources of electromagnetic interference are man-made, and possess a characteristic spectra. For instance, power lines carry current at 60Hz. Computer monitors often have refresh rates between 50 and 70kHz. If the nature of the interference source is known, then electronic filters can be designed to reject noise outside the frequency bands of the signal of interest.

6 EXPERIMENTAL CONSIDERATIONS

For specific applications, certain measurement techniques can be applied to reduce noise and enhance signal strength. These techniques involve both instrumentation design and the use of physical principles. Ultimately, the sensitivity of a measurement is not determined by absolute signal strength, but rather by the *signal-to-noise ratio* (SNR) of the measured signal. If a signal is too noisy, then the uncertainty in the measurement is large. If there is no noise or uncertainty whatsoever, then measurement is infinitely resolved. The signal-to-noise ratio is measured in units of dB, and is defined in a manner analogous to the noise figure,

$$SNR \equiv 10 \cdot \log_{10}\left(\frac{P_{signal}}{P_{noise}}\right) = 20 \cdot \log_{10}\left(\frac{V_{signal}}{V_{noise}}\right),$$

where P_{signal}, P_{noise} are the power of the signal and noise, and V_{signal}, V_{noise} are the voltages.

In NMR, a good signal to noise ratio is necessary to detect the small transverse magnetization signal against a background of noise. A back of the envelope calculation of the voltage that can be expected across the terminals can be performed using

$$V_{mag} = N_{coil}\left|\frac{N\hbar^2\gamma^3 B_{z0}^2}{4k_B T}\mu_0 \pi R_{solenoid}^2\right|. \qquad (6.1).$$

6.1 NMR Signal Strength Enhancement Methods

The observed magnetization due to spin precession is quite small. Since a figure of merit in such a sensitive measurement is the signal-to-noise ratio, it is imperative to eliminate all sources of interference, reduce the effect of physical noise sources and enhance signal strength as much as is practically possible.

Averaging can be used to limit the effect of unavoidable physical noise sources. Since physical noise sources are generally gaussian-distributed with zero mean, the central limit theorem suggests an average of their processes will yield progressively tighter variance and a very peaked distribution about zero. Figure 6.1 illustrates the effect of averaging more and more samples of a gaussian-distributed noise source with zero mean.

Equivalently effective is the use of a tuned coil. If the read-out coil is tuned to the desired resonant frequency of the spins, noise can also be reduced. Since physical noise sources tend to have a broadband character, the tuned coil acts as a sharp, bandpass filter which only passes the bulk magnetization signal of interest and the small band of noise found at the frequencies of the resonance.

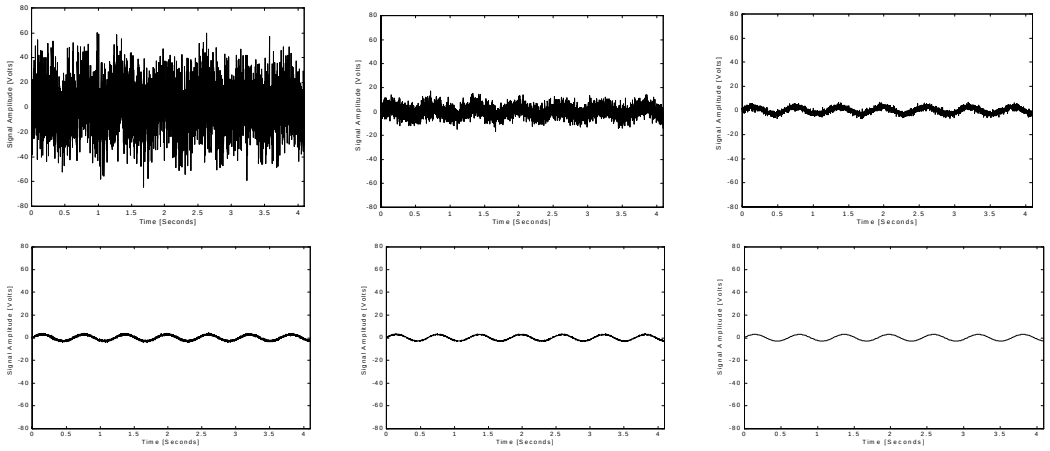

Figure 6.1: Sample averaging reduces the influence of gaussian-distributed, zero-mean, white noise, such as those generated by physical noise sources. The data sets are simulations generated with a three-volt peak-to-peak signal buried in a gaussian, white noise source with zero mean and a standard deviation of 12.75 volts. The panel in the upper left-hand corner is a single-shot. To its left and following from left to right across the second row, the data sets represent averages of ten, one-hundred, one-thousand, ten-thousand. The right-most panel in the second row is the original, uncontaminated sinusoidal signal.

Equation (6.1) suggests the following means of increasing signal strength for a read-out coil NMR spectrometer system.

- Use the strongest bias field available. The square dependence of signal strength on the strength of the bias field plainly illustrates the use of increasingly higher and higher bias fields in high-resolution NMR spectroscopy.

- Add more turns to the read-out coil. This is a simple design implementation. The signal strength has linear dependence on the number of coils used in the read-out coil. The cautionary note to the addition of turns is that an increase in turns incurs an increase in coil resistance and inductance. Coil also have an intrinsic capacitance. Read-out coils can be designed to be self-resonant, rather than the attachment of parallel or series capacitance for tuning. However, if the read-out coil is also used as an excitation coil, undesired increases in resistance and poor intrinsic frequency response due to the coil inductance and capacitance may preclude the use of an extremely large number of turns.

- Use samples with more spins or high spin densities. Obviously, more spins will provide more signal. Intuitively, there exists a linear dependence between signal strength and spin number. The practical limitation of using this technique is more spins require more volume. The generation of a strong, uniform bias magnetic field is difficult across a bathtub-sized sample. Winding an excitation and read-out coil around a large sample is equally daunting. The choice of sample is useful in only certain circumstances as a sample is usually chosen because it has chemical properties of interest.

- Use a wide diameter sample. A linear dependence on the radius of the sample enters in the signal strength expression through the flux linkage calculation.

Again, the exploitation of this means of increasing signal strength is limited for the same reasons which limits the use of a large volume of spin.

- Physically cool the sample. The inverse dependence on temperature is an artifact of a Taylor expansion of the Boltzmann distribution. In a super-cooled (millikelvin) experiment, the equilibrium magnetization itself is enhanced. With the current state of technology portable cryogenic systems are a reality. The limit of physical cooling is that a liquid sample must remain a liquid for the assumption of liquid state NMR to hold. Solid-state NMR is more complicated.

- Optically pump the sample. The use of optical pumping significantly increases the population difference, challenging the thermal constraint imposed by the Boltzmann distribution.

- Choose a different type of spin. The gyromagnetic ratio is a intrinsic property of the type of spin under investigation. An electron spin has a gyromagnetic ratio 1000 times larger than a proton spin. Magnetic resonance investigations on electrons, ESR or EPR, provides a much strong magnetization due to the linear dependence on the gyromagnetic ratio. However, associated with a higher gyromagnetic ratio is higher resonant frequencies, which require more carefully constructed instrumentation.

The use of the electron gyromagnetic ratio to polarize proton populations is also possible. The process is generically referred to as *dynamic nuclear polarization* (DNP), an example of which is the *Overhauser Effect*. It is a form of *polarization transfer*. When a static magnetic field is applied to a spin system, it becomes polarized in the sense that the two available energy states are populated differently, inducing a bulk magnetization pointed or polarized in the direction of the bias field. The process of polarization transfer is simply swaps of the energy state populations between two different spin types as in Figure 6.2.

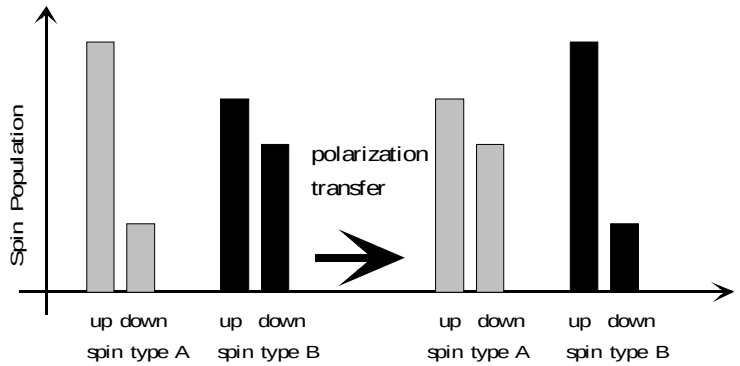

Figure 6.2: A polarization transfer simply swaps the energy-level spin population of two non-equivalent spins types.

The mechanism underlying polarization transfer is symmetry. The argument follows that given by Reif in his explanation of the Overhauser effect, a polarization transfer between a proton and electron spins. Axial symmetry is established by the bias magnetic field. The component of magnetization along the direction of the bias field is a constant of motion, the implication being that the *z*-component of angular moment is conserved. As such, if a paired electron and proton

spin are aligned in the same direction, an unmediated transition to flip both spins in the opposite direction is forbidden, since spin angular momentum would not be conserved. The only transition of interest is the case where an electron spin is align in one direction and the proton spin is aligned in the opposite direction. The conservation of momentum requires that if one spin is flipped, the other must flip as well. The equilibrium master equation for the allowed transitions is

$$N_{e\downarrow}N_{p\uparrow}W\left(\downarrow\uparrow\Rightarrow\uparrow\downarrow\right)=N_{e\uparrow}N_{p\downarrow}W\left(\uparrow\downarrow\Rightarrow\downarrow\uparrow\right),$$

where N_{ij} are the populations of the *i*th spin type in the *j*th orientation and W is, again the transition probability per second. In thermal equilibrium, the populations of each spin type can be re-expressed in a ratio,

$$\frac{N_{e\downarrow}N_{p\uparrow}}{N_{e\uparrow}N_{p\downarrow}}=\frac{e^{\beta\mu_e B}e^{-\beta\mu_p B}}{e^{-\beta\mu_e B}e^{\beta\mu_p B}}=e^{2\beta\left(\mu_e-\mu_p\right)B}.$$

If an excitation field is introduced to saturate the electrons spins so that,

$$\frac{N_{e\downarrow}}{N_{e\uparrow}}\approx 1,$$

the population expression becomes,

$$\frac{N_{p\uparrow}}{N_{p\downarrow}}\approx e^{2\beta\left(\mu_e-\mu_p\right)B}.$$

However, the gyromagnetic ratio of an electronic is a 1000 times that of a proton. So,

$$\frac{N_{p\uparrow}}{N_{p\downarrow}}\approx e^{2\beta\mu_e B}$$

to a good approximation. The result is that the proton spins are now polarized with the gyromagnetic ratio of electron spins. The population difference, and magnetization, have been appreciably increased through polarization transfer.

6.2 Spectral Resolution

Equally important is the frequency resolution of the spectra. The effect of a short T_2 is a broadening of spectral peaks. Line broadening smears the spectral peaks associated with a spin resonance. The reduced frequency resolution can prevent the identification of different spins due to chemical shifts and the observation of interesting spectral structure due to spin-spin interactions. Spin-spin relaxation is an inherent artifact of the spin systems, so T_2 cannot be completely eliminated. However, spectral line broadening can also be attributed to imhomogeneities in the bias magnetic field, since

$$\delta\omega_0 = \gamma \cdot \delta B_0 \qquad \Rightarrow \qquad \frac{\delta\omega_0}{\omega_0} = \frac{\delta B_0}{B_0},$$

Variations in the bias field are reflected in variations (or a spread) in the resonant frequency. The effect on T_2 can be quantified by

$$\frac{1}{T_2^*} = \frac{1}{T_2} + \frac{2\pi}{\gamma \cdot \delta B_0}.$$

The intrinsic T_2 due to spin-spin interactions is augmented by the bias field inhomogeneities to produce an observed spin-spin relaxation time, T_2*. Sources of line broadening related to bias field uniformity can be reduced, but not completely eliminated due to thermodynamic fluctuations.

6.3 Bias Field Inhomogeneity and Shimming

The most obvious source of field inhomogeneity is the design limit of the bias magnet. In state-of-the-art NMR spectrometers, bias fields produced by superconducting electromagnets are stronger than 12T with a uniformity of a part-per-ten-billion. Such uniform fields are achieved through the use of a secondary set of coils, called *shim* coils, which adjust the magnetic field generated by a primary electromagnet. The process of enhancing bias field uniformity is called *shimming*. State-of-the art spectrometer further enhance frequency resolution in spectra by taking a field profile of the bias field and performing software adjustments to the acquired data. Since such highly uniform fields are required for high-resolution spectra, the very presence of ferrous materials can alter a strong bias field. The magnetic permeability of iron is significant enough to introduce a nano-Tesla perturbation in a magnetic field from ten meters away.

An NMR quantum computer requires a bias field uniformity sufficient to resolve multiplet structure, which reveals spin-spin interactions. A test to insure a bias magnetic field is sufficiently uniform for NMRQC is to resolve the septuplet splitting of a hydrogen resonance due to chlorine in chloroform ($CHCl_3$). The coupling constant, *J*, for the hydrogen-chlorine interaction is roughly 215Hz. This implies a T_2* of roughly 4.7 milliseconds. Assuming the T_2* decay is due completely to bias field inhomogeneities, the upper limit on bias field variations is roughly 10^{-3} gauss. The achievement of such small magnetic field variations seems to be an Herculean task. However, bias magnetic fields in a state-of-the-art NMR spectrometers have produced observed T_2*'s of over a second, and suggests that shimming fields to these necessary specifications is realistic in desktop apparatus.

In state-of-the-art spectrometers, shimming is a built-in feature; for homemade systems, shimming remains an art which requires careful electromagnet and shim coil design, permanent magnet and iron placement, and ingenuity. Though the steps toward building an active shim system for a NMR quantum computer which can dynamically adjust the bias field to compensate for diurnal variations is still a topic of research, the theoretical problem is basic, and is one that has been addressed in a systematic fashion by Chmurny and Hoult.

The essence of their method requires the modal expansion of the bias magnetic field into spherical harmonics. The general expression for the B_0 field in terms of a modal expansion in spherical harmonics in spherical coordinates is

$$B_0 = \sum_{n=0}^{\infty} \sum_{m=0}^{n} C_{nm} \left(\frac{r}{a} \right)^n P_{nm}(\cos\theta) \cos\left[m\left(\phi - \phi_{nm} \right) \right],$$

where *n* refers to the *order* of the harmonic and *m* refers to the *degree* of the harmonic. The C_{nm} is the weight of the term in the expansion, the functions $P_{nm}(\cos\theta)$ are the *associated Legendre polynomials* of order *n* and degree *m*, and ϕ_{nm} is an arbitrary phase term. The use of spherical harmonics is due to the axial symmetry of the problem. Harmonics with degree zero, i.e., $m=0$, are termed *zonal harmonics*, and do not vary rotationally about the *z*-axis since the ϕ dependence disappears. The remaining harmonics where *m* is not zero are called *tesseral harmonics*. The division is important in light of spinning techniques which mechanically spin the sample about the *z*-axis as a means of averaging away inhomogeneities due to field variations in ϕ.

The advantage of describing the field in terms of a modal expansion is that the terms of a modal expansion (the terms in the summation) are orthogonal to each other. Conceptually, the model for the design of shim coils required an active feedback system in which the bias field is constantly monitored. The shim coil system is comprised of a set of coils, each of which generate a single harmonic. As inconsistencies in the field are measured, each shim coil can be adjusted to either add or subtract its harmonic from the field to restore uniformity. Since the shim fields are orthogonal, there is no concern regarding the interaction of shim fields; shimming is reduced to toggling terms in an expansion. In practice, the design and construction of shim coils is not so easy. Even turning the knobs to properly shim fields in a state-of-the art NMR spectrometer is still regarded as a skill. For an NMRQC, the issues of sample geometry, power constraints, and required field homogeneity for complex computations, all of which play a role in the determination of the geometry and design of a shim coil system, need be to addressed.

7 INSTRUMENTATION CONSTRUCTION AND EXPERIMENTAL METHODS

The primary thrust of this body of work is to demonstrate the feasibility of desktop NMR quantum computation. The realization of this goal requires the construction of a desktop NMR spectrometer capable of performing the tasks required to effect quantum computations, which include the application of arbitrary pulse sequences to effect computations and the necessary signal resolution to determine the calculated results. The path to a practical desktop NMR quantum computer requires the use of bias magnetic fields far weaker than those used in high-end spectrometers, and relies on the creative use of current technologies and developments in electronics and algorithms to compensate for the corresponding decrease in signal strength and spectral resolution.

7.1 Earth's Field Range NMR, Pre-polarization Techniques.

The first attempt to build a desktop NMR spectrometer involved the use of bias magnetic field strength in the Earth's field range, about 0.5 G. To overcome the severe reduction in signal strength associated with weak magnetic fields, the entire experiment was performed in a Faraday cage to reduce the interference which may overwhelm the signal, and pre-polarization techniques were employed.

Pre-polarization techniques are useful in circumstances where a strong, uniform bias magnetic field is unavailable or impractical, but the resources to generate a strong inhomogeneous bias field for a short duration are. The use of pre-polarization is illustrated in Figure 7.1. A weak magnetic field, perhaps the Earth's magnetic field, acts as the bias field. A strong DC magnetic field is applied to the spins in the direction orthogonal to the bias field for the duration of a couple T_1's. The spins align themselves with the vector sum of the magnetic fields. If the strong DC field is much stronger than the weak bias field, to a good approximation the spins are aligned with the strong DC field. After a couple T_1's, the strong DC field is quenched. If the quench is non-adiabatic (faster than the Larmor frequency) then the spins, aligned orthogonally to the weak bias, precess about the bias field. If the quench is perform adiabatically, the spins slowly follow the decrease applied field and eventually align with the weak bias field.

The virtue of this technique is the dramatic increase in magnetization that it provides. The measured signal has a squared dependence on the bias field strength. A more descriptive expression of the equation is

$$V_{mag} = N_{coil}\left|\frac{N\hbar^2\gamma^3 B_{bias}B_{polarization}}{4k_B T}\mu_0\pi R_{solenoid}^2\right|.$$

Indeed, the first magnetic field term is attributed to the magnetic field which generates an equilibrium bulk magnetization; it is the magnetic field which polarizes the spins. The second instance of a magnetic field term comes from the Hamiltonian evolution of the spins as they precess. Since the measured transverse magnetization is a function of the *change* in magnetization, the bias magnetic field enters through the Larmor frequency. In the case of conventional NMR, the bias field polarizes the spins and sets the Larmor frequency. If only a low bias field is available, a severe reduction in sensitivity is incurred. If pre-polarization is employed a signal boost can be acquired through the use of a strong polarization field, and only a partial reduction is incurred due to the slow precession frequency.

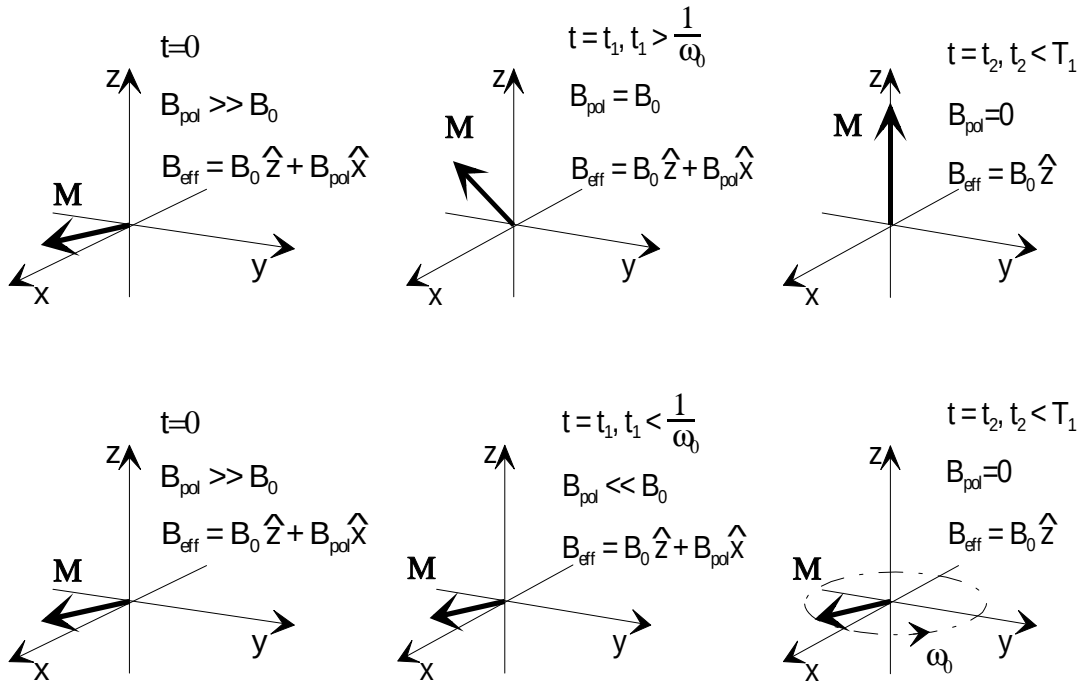

Figure 7.1: The top sequence illustrates the progression of the magnetization in an adiabatic pre-polarization. The lower sequence is an non-adiabatic pre-polarization.

For the Earth's field range experiments, three solenoids were constructed. One to generate a low-bias field, one to generate a strong pre-polarization field and excitation field, and one to act as a read-out coil. The bias field and pre-polarization coils were designed with the expression,

$$B = \frac{\mu_0 NI}{l},$$

in mind. B is the magnetic flux generated by the solenoid of length l with N turns and a current I running through the wire. This is the approximation for a long solenoid, in the limit that the length of the solenoid is much longer than the diameter of the solenoid. The amount of current through the coil is set by the resistance of the wire and the voltage placed across the wire. A coil with many turns is no longer inductive, but rather resistive, placing a constraint on the strength of the magnetic field it can generate. The coil also has a frequency response. The more turns in a coil, the tighter a low-pass filter it becomes. This becomes an issue for excitation coil. If too many turns are used in the excitation coil, it may not be able to deliver the necessary field strengths at the frequency of interest. Coils also possess their own resonant frequency due to their intrinsic inductance and capacitance.

The bias field coil was constructed from 18 gauge wire and wrapped around a water-cooler bottle. It was twelve centimeters long, with a diameter of 24 centimeters. Driven with an HP 6623A system DC power supply, it generated a 20G magnetic field at 1.74A.

The excitation coil, used for pre-polarization and excitation, consisted of 1000 turns of 22 gauge copper-enameled wire. It had an inductance of 33.4mH and a resistance of 10.11ohms. The excitation coil was driven by a power-amplifier consisting of a push-pull output stage built with

Motorola TIP31 and TIP32 power transistors and an AD712 operational amplifier. Cross-coupled diodes were placed on the output for directional coupling. The power source for the power-amplifier was an HP E3631 triple supply, which could deliver 1A at 50 volts peak-to-peak. The 120kHz sinusoidal excitation was generated by an HP 33126A waveform generator and fed into the SmartFish. The SmartFish gated the excitation signal and controlled the sequences for pre-polarization, excitation and data acquisition.

The read-out coil is 400 turns of 30 gauge copper enameled wire was wrapped around a Pyrex flask. It was self-resonant a roughly 119kHz. The end-wires of the coil were twisted together to prevent pick-up of extraneous fields. The terminals of the read-out coil were fed into a Stanford Research SR560 low-noise pre-amplifier, who output was connected to the SmartFish.

The SmartFish is a DSP-based data acquisition system capable of digitizing data at rates up to 10MSPS and generating arbitrary waveforms with an on-board digital-to-analog converter (DAC). The SmartFish communicates with a personal computer through an RS-232 protocol, and can be remotely programmed and controlled through this link. The schematics, printed circuit board artwork, bill of materials, and final microprocessor code for the SmartFish can be found in the Appendix. A front-end software application was written to control the SmartFish and to log and analyze data.

For the actual experiment, 5,000 shots were taken in an attempt to overcome the poor signal-to-noise ratio expected in a low-field experiment. Adiabatic pre-polarization was used. A sample of 100mL of water was placed in the read-out coil, and then the entire apparatus was placed in a Faraday cage. The SmartFish executed the following sequence 5000 times: pre-polarize the sample for $5T_1$, wait for five decay constants of the excitation coil, perform a $\pi/2$ pulse, and acquire data. Two-thousand forty-six points of data were acquired at 300kSPS for a Larmor frequency of roughly 120kHz.

7.2 Mid-Field NMR

Though a desktop system would ideally operate in an Earth's field regime, the poor signal sensitivity requires an unwieldy number of trials to see the most rudimentary effect, an FID. The mid-field regime is relative with the progress of technology, but roughly spans the kilogauss range with an upper limit of a couple Tesla. A system operating in the mid-field regime enjoys a significant increase in signal strength while allowing for a significant decrease is sample size. A compact physical design can be further developed with the use of permanent magnets which can generate magnetic field strengths of up to 2.2T with reasonable uniformity and acceptable dimensions.

A move to a magnetic field strength three-orders of magnitude stronger than the Earth's magnetic field takes the operating frequency from audio frequencies to RF. The instrumentation lexicon must be extended from simple operational amplifiers and wires to power-splitters, double-balanced mixers, RF amplifiers and transmission lines. Notions of impedance matching and reflections effect the operation of seemingly simple circuits. Maxwell's equations can no longer be used in the quasi-static regime. Luckily, the design of RF systems have been greatly simplified with the commercialization of monolithic RF parts. Proper considerations, however, should still be made when working in the RF regime.

The NMR apparatus used for the mid-field experiments was that of the MIT Physics Department Experimental Physics (Junior) Laboratory, courtesy of Prof. Jordan Kirsch. The pulse sequence

generation and data acquisition was again performed with the SmartFish under software control from a laptop computer.

The system is based about an operation frequency of 5MHz. The bias field is generated by a water-cooled electromagnet, with a field of roughly 1kG. The probe circuit, pictured in Figure 7.2, is a simple resonant LC tank circuit tuned to the Larmor frequency. The inductive element is the read-out/excitation coil. A capacitive divider is used. The capacitance in parallel with the coil is adjusted to tune the circuit to the Larmor frequency. The series capacitance is then tuned such that the probe is impedance matched at 50 ohms. The number of coil windings is small, and the length of the coil need only encompass the sample to the extent that the excitation fields are uniform across the sample. The probe is then potted to secure prevent mechanical vibrations and enclosed in an aluminum box to shield it from electromagnetic interference.

Figure 7.2: Two possible configurations for a probe circuit. The one on the left uses a capacitor in series with a capacitor in parallel with the coil. The one on the right uses a capacitor in parallel with a capacitor connected in series with the coil. The two configurations are equivalent.

The instrumentation to manipulate spins and measure spin properties are basic. The SmartFish, again served as a means of coordinating excitation and data acquisition, and was programmed through a software interface on a laptop computer. A schematic representation of the system is pictured in Figure 7.3.

A 5MHz oscillator generated the waveform used to excite the spins and served as a local oscillator to mixed-down the incoming magnetization to audio frequencies. The 5MHz signal is fed into a power-splitter which, in turn, feeds an RF switch and double-balanced mixer. At RF frequencies, impedance matching is critical to prevent the signal from reflecting back to the source. If there is an impedance mismatch, reflections prevent the signal from delivering its full power to its destination. The power-splitter simply insures impedance matching: if a 50 ohm cable were fed two 50 ohm cables, it would see an equivalent 25 ohm resistance due to the parallel impedance of the two cables—an impedance mismatch. The power-splitter insures that the feed and receive cables sees a 50 ohm load. The SmartFish provides a TTL-level (0 to 5 volt) control signal to the RF switch to gate the excitation signal. The output of the RF switch is fed to a power amplifier which drives the coil. Between the coil and the power amplifier is a pair of cross-coupled diodes. In a single-coil apparatus, these cross-coupled diodes are essential to decouple the drive circuitry from the coil and sensitive detection electronics when its not in use. When the coil is driven, the cross-coupled diodes pass the signal. When the coil is not being driven, the diodes act as an open circuit, separating the drive electronics from the probe.

The detection electronics consist of a second pair of cross-coupled diodes and a high-gain, low-noise preamplifier. The cross-couple diodes sit between the input of the preamplifier and ground. This prevents the drive circuitry from destroying the preamplifier during excitation. When the signal is larger than a diode drop, the diodes conduct to ground, channeling current away from the preamplifier input to ground. When signals, like the magnetization signal, are less than a diode drop, the diodes act as an open-circuit.

The amplified magnetization signal is fed into the double-balanced mixer, which is used for phase detection. Mixed-down with the signal from local oscillator, the output of the phase detector is the magnetization signal at the *beat frequency*, the difference between the local oscillator and Larmor frequency. The output of the phase detector is fed into the SmartFish which logs the time-series waveform for presentation and analysis.

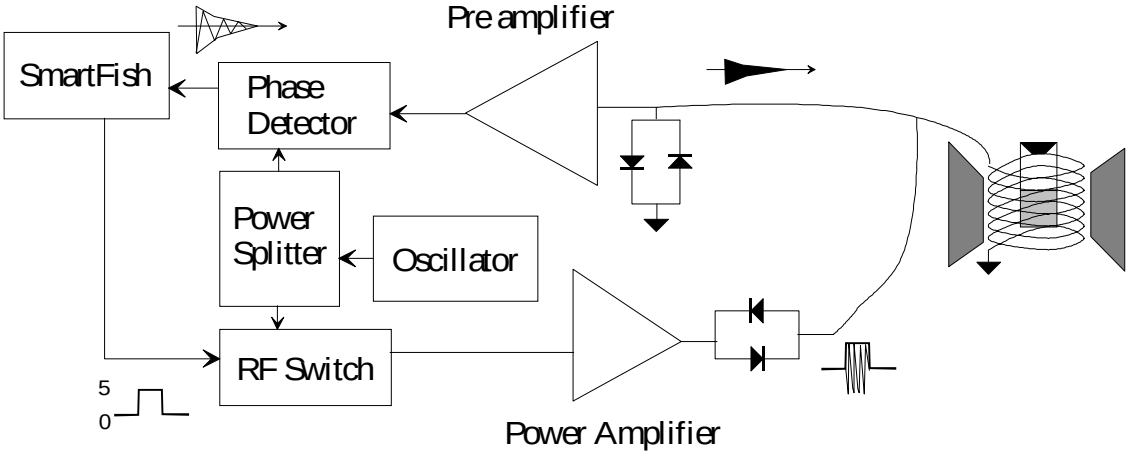

Figure 7.3: An outline of the mid-field NMR apparatus used to observe spin precession.

Initial experiments used a thumb-sized sample of glycerin; glycerin was chosen for its strong resonance signal. Two experiments were performed to characterized the system and insure the complete functionality of the system. To measure the proper $\pi/2$-pulse duration, the spins were tipped with excitation pulses. Beginning with a 1μs pulse, the pulse duration lengthen by 1μs increments for 300 shots. After each pulse, the FID which result was acquired. A plot of the FID signal strength versus pulse duration was made. The pulse length which generated the maximum signal strength indicates the correct $\pi/2$-pulse duration. A spin echo experiment was then performed to verify the empirically derived $\pi/2$-pulse width, and to gain a qualitative feel for T_2* of the bias magnetic field before undertaking further work which requires fine spectral resolution.

8 RESULTS

The spectra taken from both the low-field and mid-field apparatus were limited. The greatest obstacle encountered in both experiments was the limited bias field homogeneity. The large T_2* produced extremely broad spectra and quickly decaying FID's.

The low-field experiments yielded no signals and generated no results. The large bias field gradient suggested the appearance of a broad swell in the spectra as in indication of the poor homogeneity. Unfortunately, the spin resonance energy was divided so divergently among the different frequencies that external interference easily overwhelmed the signal of interest. Rather than measuring spin resonance, the apparatus measured spectral components related to various other projects in the lab and artifacts of power systems.

The mid-field experiments boasted slightly more promising results, but were nonetheless disappointing. Due to the phase detection method of measurement, the RF pulses were slightly off-resonance. Calibration experiments were performed to find an optimal $\pi/2$-pulse width. The trials were slightly flawed as a sufficient relaxation time was not permitted between pulses for the spins to return to equilibrium. Rather than a sinusoid, the plot of resonance signal strength versus pulse length displays a decay, pictured in Figure 7.4. Drift in the bias magnetic field also produced corresponding deviations in the Larmor frequency, and resulted in error as the data collection process proceeded. The salient feature of the plot, the periodicity, however remained intact, and from it, $\pi/2$-pulse and π-pulse periods were inferred to be 39μs and 78μs respectively.

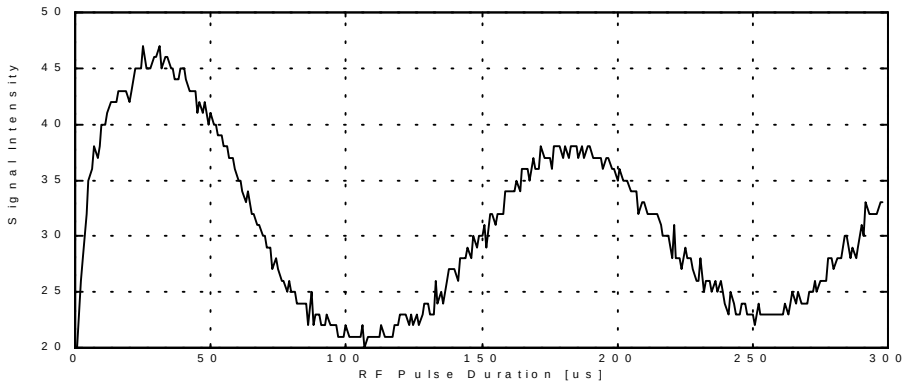

Figure7.4: A plot of pulse length versus time used to determine the optimal $\pi/2$-pulse duration.

With the value determined for an optimal $\pi/2$-pulse width, spin echo experiments were performed to enhance the observable magnetization and to gain a qualitative feel for T_2*. Initial plans were to quantify the value of T_2* through a series of spin echo experiments, but preliminary results suggested that the magnetic field in the electromagnet bore were sufficiently non-uniform to preclude the necessity of proceeding with those experiments. The results of those spin echo experiments are presented in Figure 7.5. Though the signal-to-noise ratio of the measured signal is excellent, the frequency resolution indicated by the broad spectral peaks prevent the appearance of spectral structure indicative of spin-spin interactions—the physical interactions of interest in NMR quantum computation.

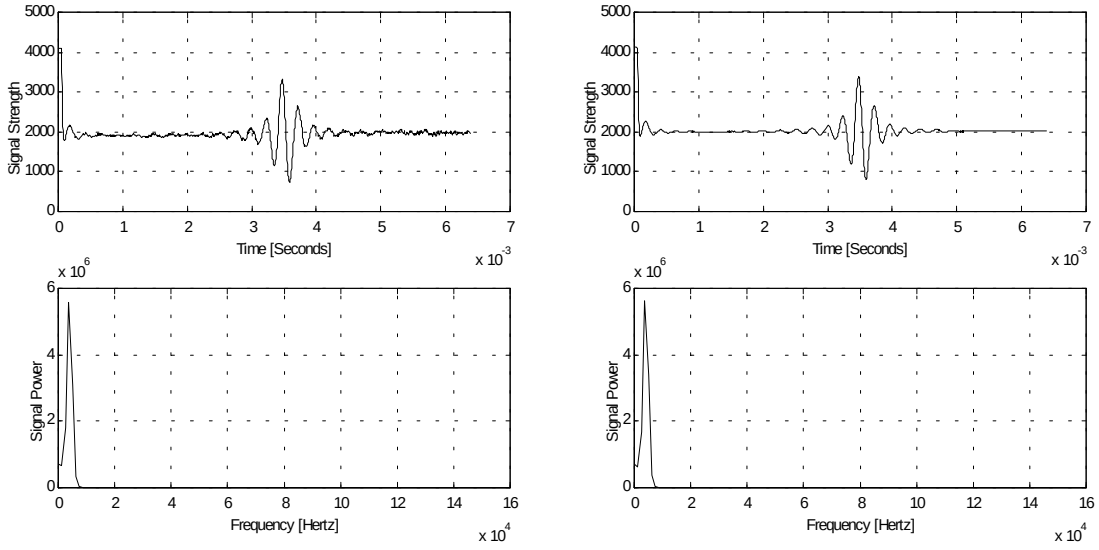

Figure 7.5: Time-series and spectra of glycerin spin-echoes taken in a ~1kG magnetic field. The signal strength has been quantized into 12-bits across and analog range of five volts.. A 90-180 pulse sequence was applied to the glycerin sample. The initial plateau in the time-series is the pre-amplifier recovering from the 180 pulse. What follows is the spin-echo, as the transverse magnetization regains phase coherence and loses it again in a characteristic time scale T2. The resonant frequency is not properly represented as a phase detection scheme was used to measure the magnetization. The observed frequency is actually the beat frequency between the resonance and a local oscillator. The data set to the left is a one-shot. The data set to the right was averaged over 100 shots.

9 REFLECTIONS

This thesis has been written, not in closure, but in preparation. It is a marker for trials past, and a prescription to guide research for the future. In performing the task leading to the construction of a desktop quantum computer many pitfalls were encountered and many lessons learned. The most important lesson is the necessity of extremely uniform bias magnetic fields. Without them, interesting spectral structure attributed to spin-spin interactions—interactions required for quantum computation—are unobservable.

Though the original concern in constructing a desktop NMR spectrometer was with regard to boosting the signal-to-noise ratio, the experimental results clearly show that the limitations are that of frequency resolution. Current electromagnet and permanent magnet systems are compact and amenable for commercial use. They generate field strengths necessary to observe magnetic resonance easily. These magnet systems, however, seldom produce fields with the uniformity required to generate highly resolved spectra. The focus of future research must address this shortcoming of field uniformity with either active shim systems; better bias magnet geometry; or experimental techniques, such as sample spinning, which allow for the variations in magnetic field to be averaged away.

In closing, a potential geometry for an NMR quantum computer is proposed. Though it is true that an NMR quantum computer is essentially an NMR spectrometer, a NMR quantum computer need not possess the generality and flexibility which are available in a high-resolution spectrometers. For example, an NMR spectrometer allows for the switching of samples. An NMR quantum computer operates on only one sample, which need not be changed. NMRQC needs are simple: uniform and stable magnetic fields and consistent excitation fields. To generate consistent excitation fields is simply a matter of constructing sound, matched, low-drift drive electronics. The creation of uniform bias fields provides an avenue for creativity.

The proposed NMR quantum computer consists of a flux-ball electromagnet within which resides a flux-ball excitation/read-out coil and a spherical sample. The sample itself perturbs the bias field. Using a spherical sample geometry is a means of reducing those perturbations. A flux-ball electromagnet geometry is a structure which produces uniform magnetic field within a sphere, as illustrated in Figure 9.1. As opposed to a solenoid, which only generates an uniform magnetic field in the ideal case of being infinite, a properly wound spherical coil will always generate a uniform field.

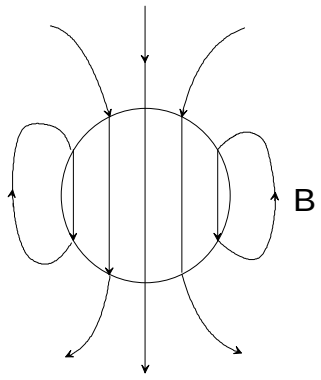

Figure 9.1: Flux-ball electromagnet is built by winding coils around a sphere. The current in the coils constitute a surface current which gives rise to a magnetic field. The field is dipole in nature; the magnetic field within the sphere is uniform.

Similarly, the non-ideality of a solenoid affects the performance of the excitation coils. For the application of a tipping pulse, the rate of tipping is determined by the excitation field strength. If a sample sits unevenly in an excitation coil, part of the sample sees a weaker excitation field than other parts of the sample. The results is that the application of a $\pi/2$-pulse turns some spins into the transverse plane, and leaves other spins rotated at an angle less than $\pi/2$ from the bias field axis. This error adds as the number of pulses in the pulse sequence increases, and presents a significant problem in the accuracy of the quantum computation. With a flux-ball excitation coil, the uniformity of the fields prevents errors due to uneven excitation of spins. Though the signal strength may suffer with the read-out coil being of spherical geometry, it is painfully obvious that a slight loss in signal strength for a tremendous gain in frequency resolution is a good trade-off.

The journey down the road to realizing practical quantum computation for the general population has just begun. The recent innovation of using NMR to perform quantum computation has represented a huge step forward toward this goal. Though this effort may terminate with results short of a quantum coprocessor in the motherboard of a desktop computer, the effort toward that end is rich with opportunity and discoveries which will benefit the practice of NMR, the study of quantum mechanics, and the design of electromagnet systems and magnetometers. As with all ambitious endeavors, the means to a personal quantum computer is every bit as important as the end.

10 APPENDIX

SmartFish Data Acquisition System

Schematics
Board Fabrication Artwork
Firmware

11 BIBLIOGRAPHY

Quantum Computation

Chuang, I.L, Gershenfeld, N. A., Kubinec, M. G., Leung, D. W., "Bulk Quantum Computation with Nuclear Magnetic Resonance: Theory and Experiment." Preprint.

Chuang, I. L., "Quantum Computing 101: Fundamental Concepts." Lecture notes.

Gershenfeld, N. A., and Chuang, I. L., "Bulk Spin-Resonance Quantum Computation." *Science*, Vol. 275, pp. 350, 1997.

Ekert, A., and Josza, R., "Quantum computation and Shor's factoring algorithm." *Reviews of Modern Physics*, Vol. 68, No. 3, July 1996.

Magnetic Resonance Theory and Practice

Abragam, A., *The Principles of Nuclear Magnetism*. Oxford: Clarendon Press, 1961.

Battocletti, J. H., Kamal, H. A., Myers, T, J., and Knox, T. A., "Systematic Passive Shimming of a Permanent Magnet for P-31 NMR Spectroscopy of Bone Mineral." *IEEE Transactions on Magnetics*, Vol. 29, No. 3, July 1993.

Bene, G. J., "Nuclear Magnetism of Liquid Systems in the Earth Field Range." *Physics Reports*, Vol. 58, No. 4, pp. 213-267, 1980.

Bloch, F., "Nuclear Induction." *Physical Review*, Vol. 70, Nos. 7 and 8, October 1946.

Chmurny, G. N., and Hoult, D. I., "The Ancient and Honourable Art of Shimming." *Concepts in Magnetic Resonance*. Vol. 2, pp. 131-149, 1990.

Conolly, S., Brosnan, T. and Macovski, A., "A Pulsing Circuit for Prepolarized MRI." *Proceedings of the Society of Magnetic Resonance*, 1995.

Fukushima, E., and Roeder, S. B. W., *Experimental Pulse NMR : a Nuts and Bolts Approach.* Reading, Massachusetts: Addison-Wesley Publishing Company, 1981.

Kernevez, N., Duret, D., Moussavi, M., and Leger, J., "Weak Field NMR and ESR Spectrometers and Magnetometers." *IEEE Transactions on Magnetics*. Vol. 28, No. 5, September 1992.

Kirsch, J, and Newman, R., "A Pulse NMR experiment for an undergraduate physics laboratory." Submitted to the *American Journal of Physics*.

Klein, W., "Nuclear magnetic resonance: Free-induction decay and spin-echoes in a 0.05T magnetic field." *American Journal of Physics*. Vol. 58, No. 2, February 1990.

Mateescu, G. D., and Valeriu, A. *2D NMR : Density Matrix and Product Operator Treatment.* Englewood Cliffs, New Jersey: Prentice Hall, 1993.

Moreland, John. NIST. Personal communication.

Olson, D. L., Peck, T. L., Webb, A. G., Magin, R. L., and Sweedler, J. V., "High-Resolution Microcoil ^{1}H-NMR for Mass-Limited, Nanoliter-Volume Samples." *Science*, 1995.

Peck, T. L., Magin, R. L., Lauterbur, P. C., "Design and Analysis of Microcoils for NMR Microscopy." *Journal of Magnetic Resonance, Series B*, Vol. 108, pp. 114-124, 1995.

Powles, J. G., and Cutler, D., "Audio-frequency Nuclear-resonance Echoes." *Nature*, Vol. 180, pp. 1344-5, December 14, 1957.

Rugar, D., Yannoni, C. S., Sidles, J. A., "Mechanical detection of magentic resonance." *Nature*, Vol. 360, December 10, 1992.

Sanders, J. K. M., and Hunter, B. K., *Modern NMR Spectroscopy : a Guide for Chemists.* New York: Oxford University Press, 1987.

Slichter, C. P., *Principles of Magnetic Resonance.* Berlin, New York: Springer-Verlag, 1978.

Stepisnik, J., Erzen, V., and Kos, M., "NMR Imaging in the Earth's Magnetic Field." *Magnetic Resonance in Medicine*, Vol. 15, pp. 386-391, 1990.

TonThat, D. M., Augustine, M. P., Pines, A., Clarke, J., "Low magnetic field dynamic polarization using a single-coil two-channel probe." *Review of Scientific Instruments*, Vol 68, No. 3, March 1997.

Vathyam, S., Lee, S., Warren, W. S., "Homogeneous NMR Spectra in Inhomogeneous Fields." *Science*, Vol. 272, April 5, 1996.

Waters, G. S., and Francis, P. D., "A nuclear magnetometer." *Journal of Scientific Instruments*, Vol. 35, pp.88-93, March 1958.

Webb, A. G., and Grant, S. C., "Signal-to-Noise and Magnetic Susceptibility Trade-offs in Solenoidal Microcoils for NMR." *Journal of Magnetic Resonance, Series B*, Vol. 113, pp. 83-87, 1996.

Classical Mechanics

Goldstein, H., *Classical Mechanics*. Reading, Massachusetts: Addison-Wesley Publishing Company, 1980.

Symon, K. R., *Mechanics*. Reading, Massachusetts: Addison-Wesley Publishing Company, 1960.

Haus, H. A., and Melcher, J. R., *Electromagnetic Fields and Energy*. Englewood Cliffs, New Jersey: Prentice Hall, 1989.

Quantum Mechanics
Dirac, P. A. M.. *The Principles of Quantum Mechanics*. Oxford: The Clarendon Press, 1935.

French, A. P. and Taylor, E., *An Introduction to Quantum Physics*. New York: Norton, 1978.

Landau, L. D. and Lifshitz, E.M., *Quantum mechanics : Non-relativistic Theory*. New York : Pergamon Press, 1977.

Morrison, M. A., Estle, T. L., and Lane, N. F., *Understanding More Quantum Physics: Quantum States of Atoms*. Englewood Cliffs, New Jersey: Prentice Hall, 1991.

Peres, A., *Quantum theory: Concepts and Methods*. Boston: Kluwer Academic, 1993.

Sakurai, J. J., *Modern Quantum Mechanics*. Reading, Massachusetts: Addison-Wesley Publishing Company, 1994.

Statistical Mechanics
Huang, K., *Statistical Mechanics*. New York: John Wiley & Sons, Inc., 1987.

Kubo, R., *Statistical mechanics, An Advanced Course with Problems and Solutions*. New York: North-Holland Publishing Company, 1965.

Pathria, R. K., Statistical Mechanics. Boston: Butterworth-Heinemann, Ltd., 1972.

Reichl, L. E., *A Modern Course in Statistical Physics*. Austin: University of Texas Press, 1980.

Reif, F., *Fundamentals of Statistical and Thermal Physics*. New York: McGraw-Hill, Inc., 1965.

Instrumentation Design and Measurement Methods
Bader, S. D., "Thin Film Magnetism." *Proceedings of the IEEE*, Vol. 78, No. 6, June 1990.

Heremans, J., "Solid state magnetic field sensors and applications." *Journal of Physics D: Applied Physics*, Vol. 26, 1993.

Horowitz, P., and Hill, W., *The Art of Electronics*. Cambridge: Cambridge University Press, 1989.

Lenz, J.E., "A Review of Magnetic Sensors." *Proceedings of the IEEE*, Vol. 78, No. 6, pp. 973-989, 1990.

Osiander, R., Ecelberger, S. A., Givens, R. B., Wickenden, D. K., Murphy, J. C., and Kistenmacher, T. J., "A microelectromechanical-based magnetostrictive magnetometer." *Applied Physics Letters*, Vol 69. No. 4, November 4, 1996.

Popovic, R. S., Flanagan, J. A., Besse, P. A., "The future of magnetic sensors." *Sensors and Actuators A*, Vol. 56, pp. 39-55, 1996.

Primdahl, F., "The fluxgate magnetometer." *Journal of Physics E: Scientific Instrumentation*, Vol. 12, 1979.

Ripka, P., "Magnetic sensors for industrial and field applications." *Sensors and Actuators A*, Vol. 41-42, 1994.

Ripka, P., "Review of fluxgate sensors." *Sensors and Actuators A*, Vol. 33, pp. 129-141, 1992.

Smith, L. and Sheingold, D. H., "Noise and Operational Amplifier Circuits." *Analog Dialogue*. Vol. 3, No. 1, March 1969.

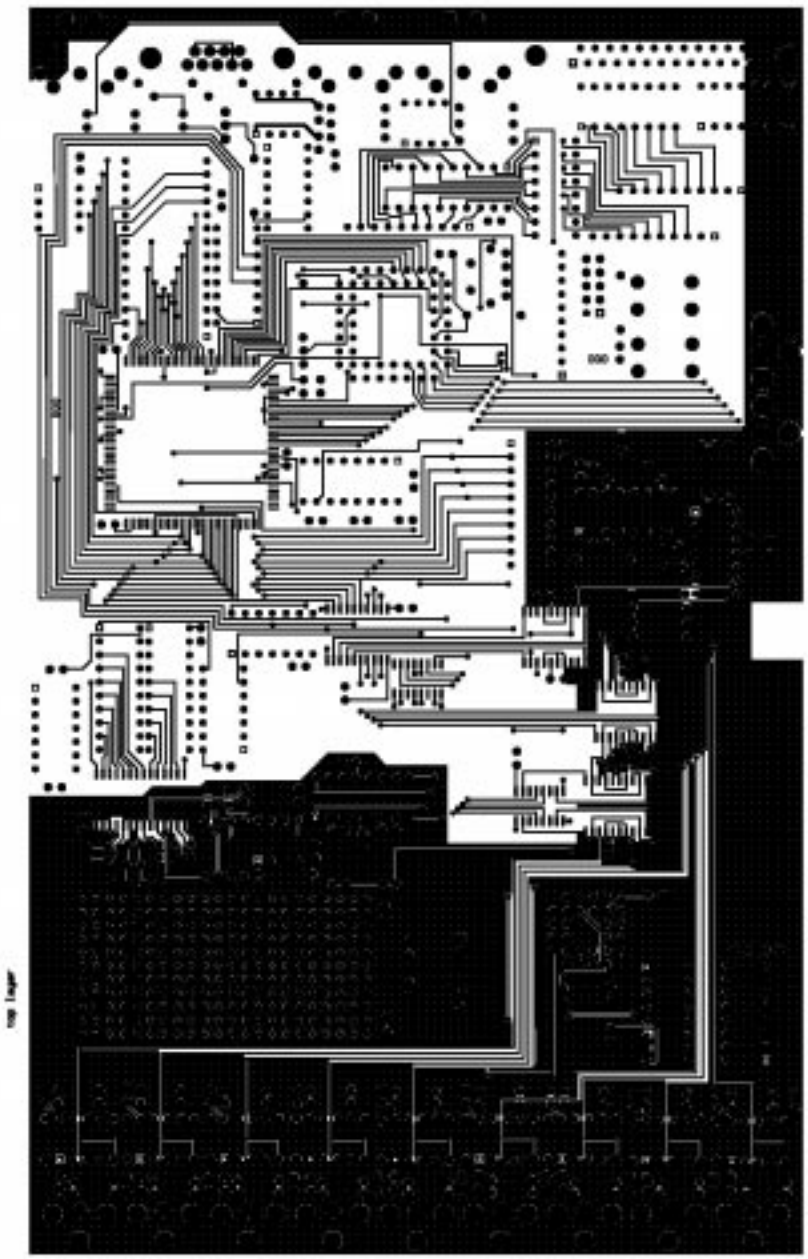
top layer

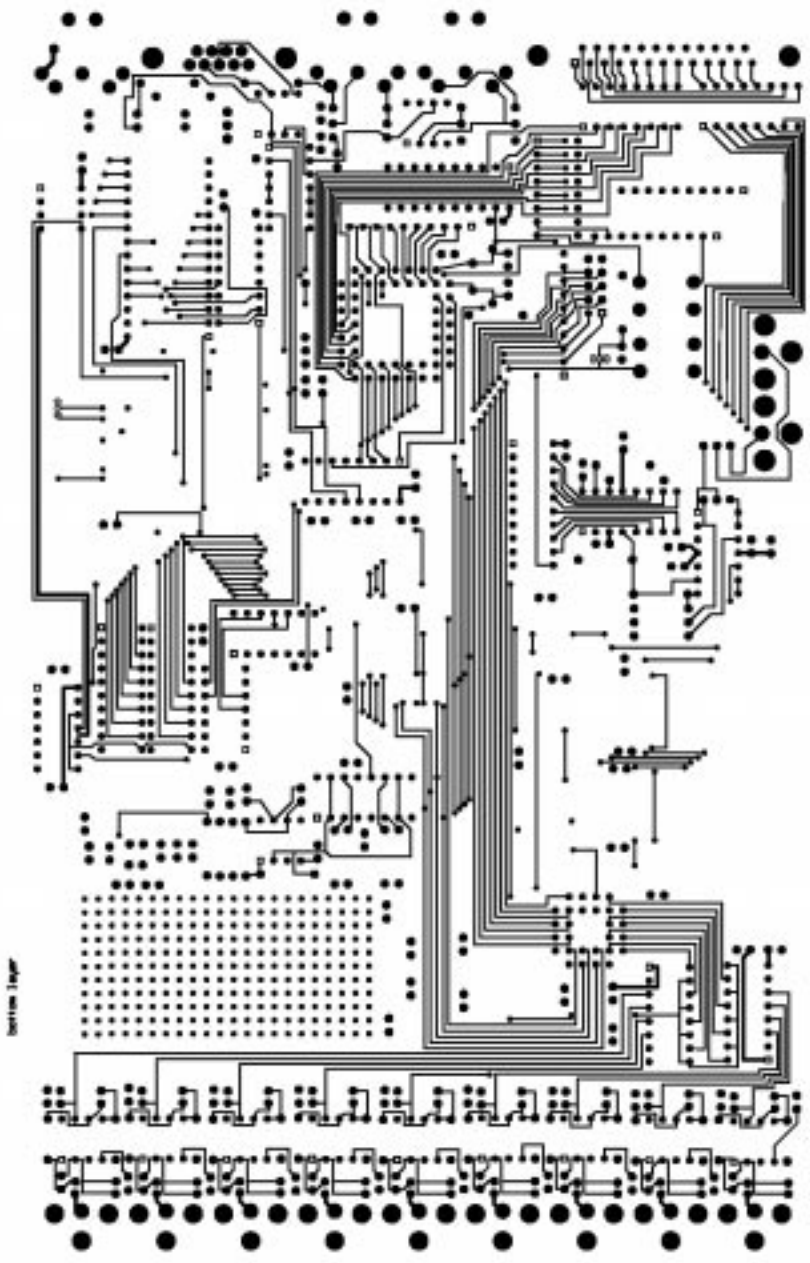
bottom layer

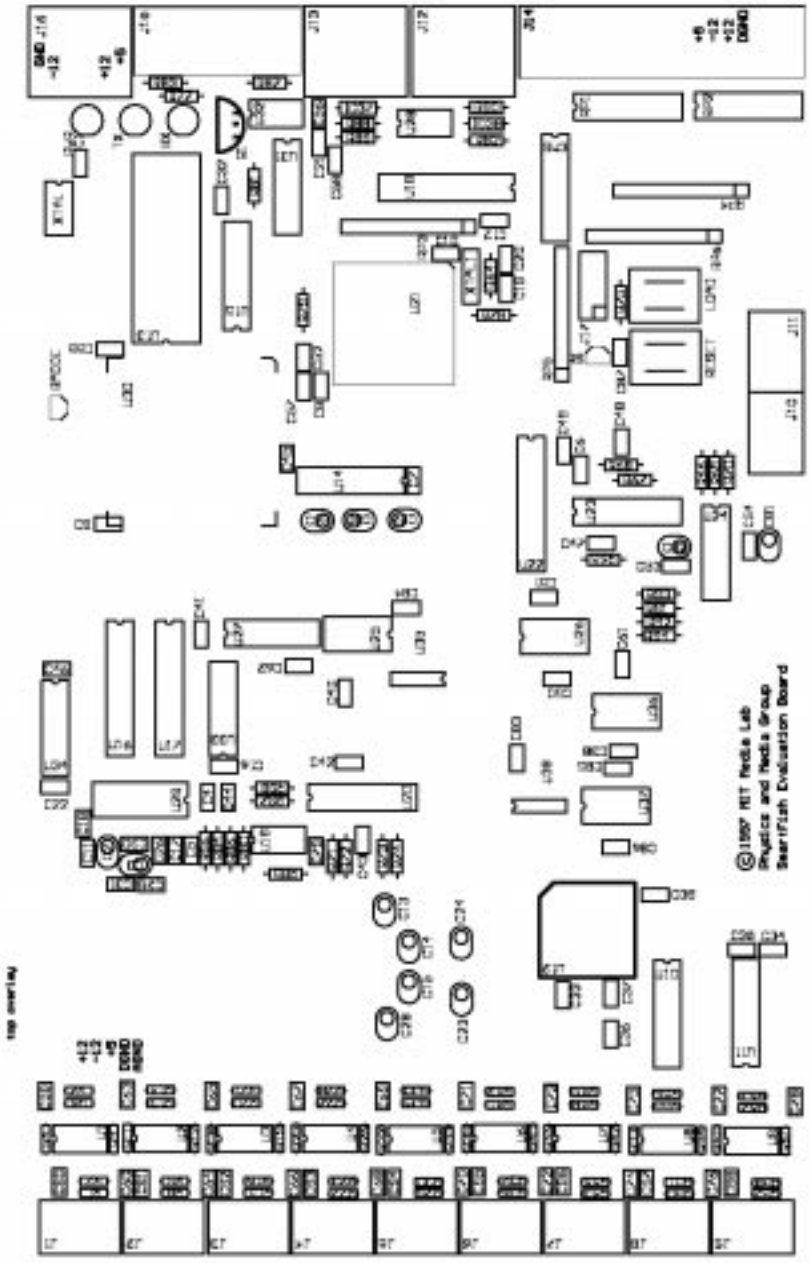
©1997 MIT Media Lab
Physics and Media Group
Swerfish Evaluation Board

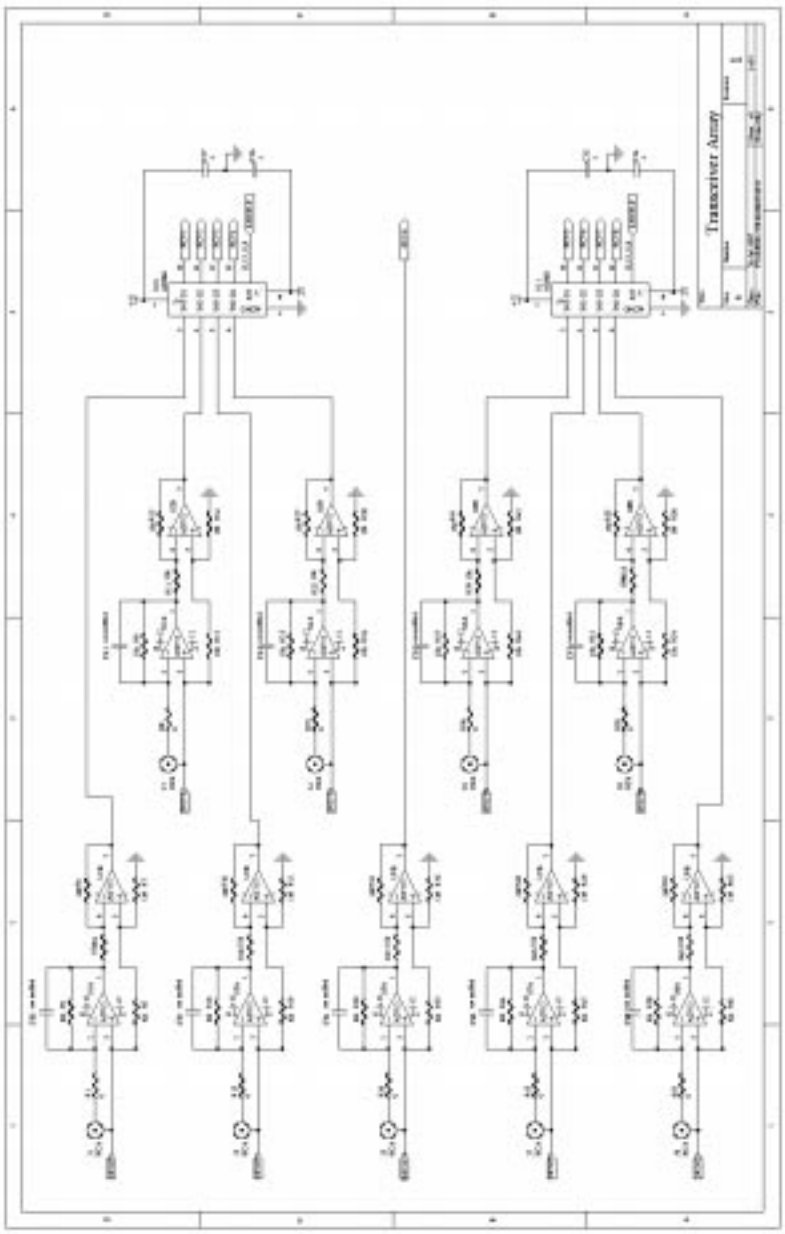
Transceiver Array

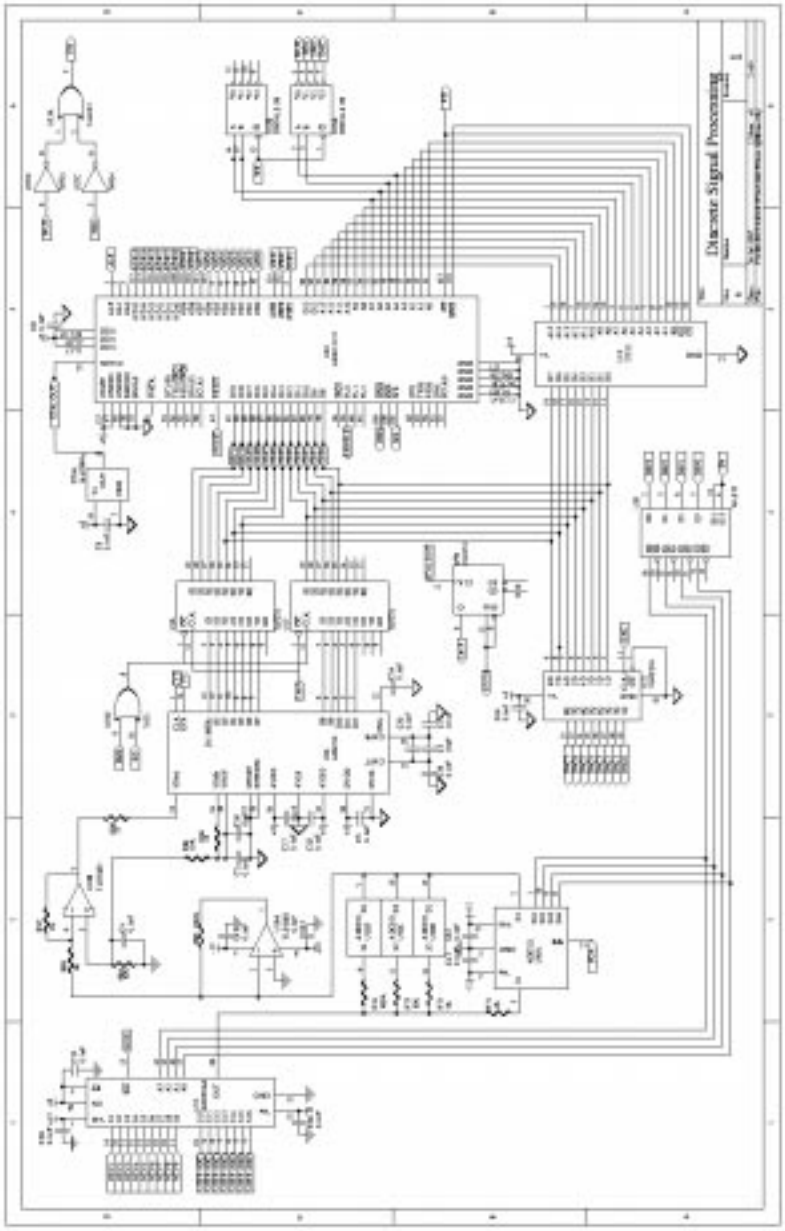
Discrete Signal Processing

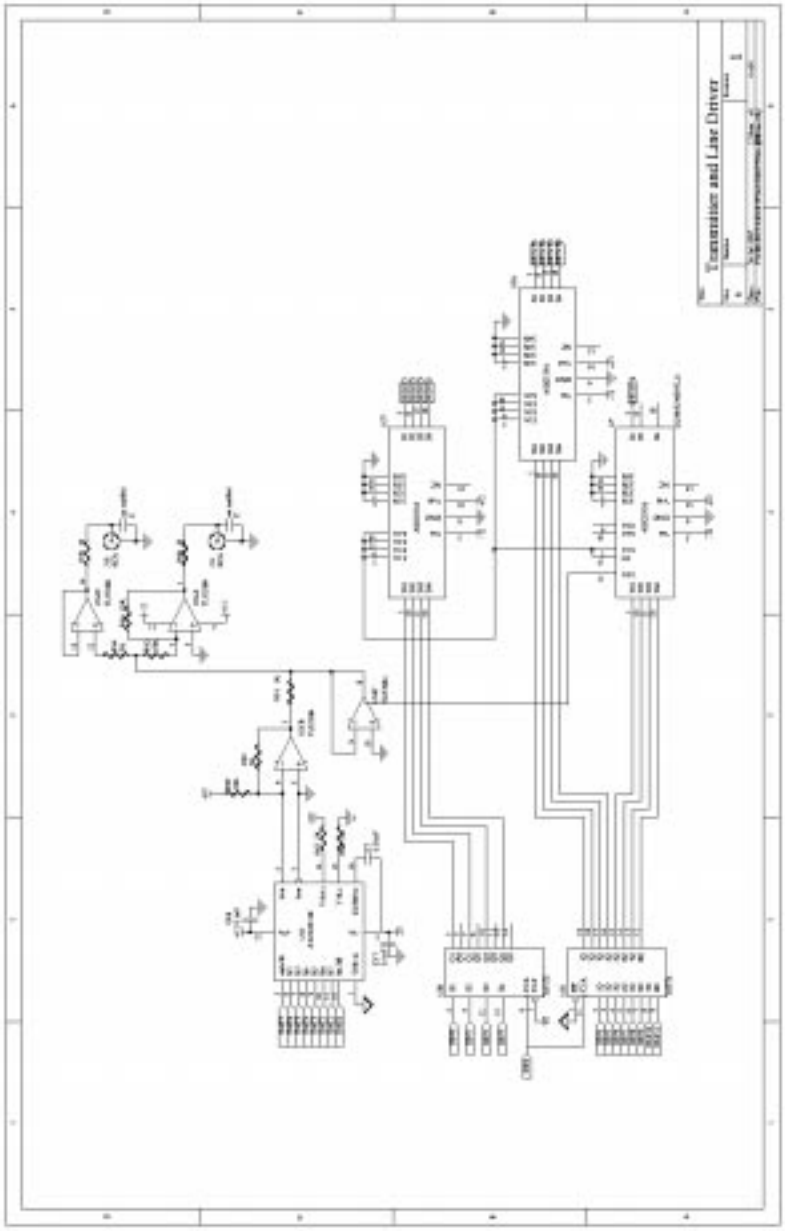
Transmitter and Line Driver

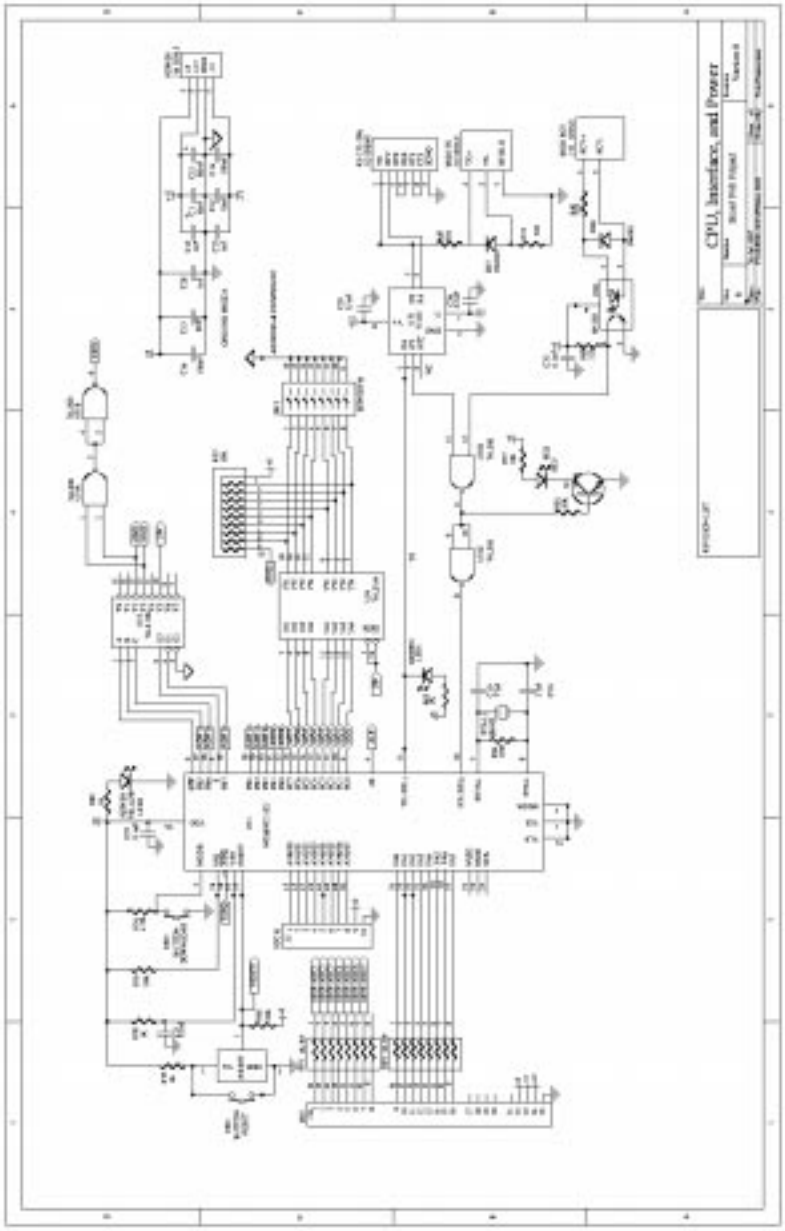
CPU, Interface, and Power

```
{ Smart-Fish ADSP-2171 Code.  Version zero: Crawling.

      Jlab715.dsp nmr controller code for junior
                  lab apparatus.  Spin echo display.
}


.MODULE/RAM/BOOT=0/ABS=0 SMISH;                 {Beginning of SMISH.DSP}

{-----define ports for peripheral access-------}
.PORT bus;

{-----define constants for HIP locations------}
.CONST hsr0=0x3FE0, hsr1=0x3FE1, hsr2=0x3FE2, hsr3=0x3FE3, hsr4=0x3FE4;
.CONST hsr5=0x3FE5, hsr6=0x3FE6, hsr7=0x3FE7;

{----linear buffers----}
.VAR/DM/RAM/ABS=0x3000  command;
.VAR/DM/RAM/ABS=0x3001  halfpi;
.VAR/DM/RAM/ABS=0x3002  fullpi;
.VAR/DM/RAM/ABS=0x3003  wait;
.VAR/DM/RAM/ABS=0x3004  writereg;

{---------Interrupt Vectors----------}

            JUMP start; RTI; RTI; RTI;    {RESET IRQ}
            RTI; NOP; NOP; NOP;           {IRQ2 unused}
            JUMP iread; NOP; NOP; NOP;    {HIP Write IRQ}
            JUMP iwrite; NOP; NOP; NOP;   {HIP Read IRQ}
            RTI; NOP; NOP; NOP;           {SPORT0 TX IRQ}
            RTI; NOP; NOP; NOP;           {SPORT0 RX IRQ}
            RTI; NOP; NOP; NOP;           {Software IRQ1}
            RTI; NOP; NOP; NOP;           {Software IRQ2}
            RTI; NOP; NOP; NOP;           {SPORT1 TX IRQ}
            RTI; NOP; NOP; NOP;           {SPORT1 RX IRQ}
            RTI; NOP; NOP; NOP;           {TIMER IRQ}
            RTI; NOP; NOP; NOP;           {Powerdown IRQ}



{------Start Up Configurations---------}

start:           AX0=0x0018;
            DM(0x3FFF)=AX0;               {System Control Register}

            AX0=0x0142;
            DM(0x3FFE)=AX0;               {DM wait states}

            AX0=0;                        {Timer Registers}
            DM(0x3FFD)=AX0;
            DM(0x3FFC)=AX0;
            AX0=31;                       {prescale for uS}
            DM(0x3FFB)=AX0;

            AX0=0x0020;
            DM(0x3FE8)=AX0;               {HMASK IRQ register}

            M0=0; M4=0;                   {do not increment}
            M1=1; M5=1;                   {increment by ONE}

{----parameter initialization----}

            RESET FL0;                    {no pulse}
```

```
            AX0=0;
            DM(writereg)=AX0;             {initialize writereg}

            AX0=62;
            DM(halfpi)=AX0;
            AX0=66;
            DM(fullpi)=AX0;
            AX0=3500;
            DM(wait)=AX0;


{-------waitloop for console instructions------}

talk:       MSTAT=0x0010;
            IMASK=0x180;
            IDLE;                         {waiting for HOST WRITE}

            JUMP echo;

respond:    CNTR=1;                       {banks to return}
            DO converse UNTIL CE;
            IDLE;
converse:   NOP;

            JUMP talk;

{-----IRQ service routines-----}

{---HOST WRITE IRQ---}
iread:      SR0=DM(hsr0);                 {read registers}
            SR=LSHIFT SR0 by 8 (LO);
            AY0=DM(hsr1);
            AR=SR0 OR AY0;
            DM(halfpi)=AR;

            SR0=DM(hsr2);
            SR=LSHIFT SR0 by 8 (LO);
            AY0=DM(hsr3);
            AR=SR0 OR AY0;
            DM(fullpi)=AR;

            SR0=DM(hsr4);
            SR=LSHIFT SR0 by 8 (LO);
            AY0=DM(hsr5);
            AR=SR0 OR AY0;
            DM(wait)=AR;

            RTI;

{---HOST READ IRQ---}

iwrite:     AX0=DM(writereg);
            AY0=1;                        {no. banks HC11 should read}
            AR=AX0-AY0;
            IF EQ JUMP wrap;

            AR=DM(I0,M1);
            DM(hsr0)=AR;
            SR=LSHIFT AR BY -8 (LO);
            DM(hsr1)=SR0;

            AR=DM(I0,M1);                 {read value}
            DM(hsr2)=AR;
            SR=LSHIFT AR BY -8 (LO);
            DM(hsr3)=SR0;
```

```
            AR=DM(I0,M1);                   {sanity checker}
            DM(hsr4)=AR;
            SR=LSHIFT AR BY -8 (LO);
            DM(hsr5)=SR0;

            AX0=DM(writereg);               {written}
            AR=AX0+1;
            DM(writereg)=AR;

            RTI;

wrap:       AR=0;
            DM(writereg)=AR;
            AR=0x020;
            DM(0x3FE8)=AR;                  {disable HIP read IRQ}
            DM(hsr0)=AR;
            DM(hsr1)=AR;
            DM(hsr2)=AR;
            DM(hsr3)=AR;
            DM(hsr4)=AR;
            DM(hsr5)=AR;

            RTI;


{-----spin echo subroutine-----}

echo:       IMASK=0x0000;
            MSTAT=0x0000;

tip:        AX0=DM(halfpi);
            DM(0x3FFD)=AX0;
            DM(0x3FFC)=AX0;

            IMASK=0x0001;
            SET FL0;
            MSTAT=0x0030;
            IDLE;

evolve:           RESET FL0;
            MSTAT=0x0000;
            IMASK=0x0000;

            AX0=DM(wait);
            DM(0x3FFD)=AX0;
            DM(0x3FFC)=AX0;

            IMASK=0x0001;
            MSTAT=0x0020;

            AX0=DM(fullpi);
            IDLE;

invert:           SET FL0;
            MSTAT=0x0000;
            IMASK=0x0001;

            DM(0x3FFC)=AX0;
            DM(0x3FFD)=AX0;

            IMASK=0x0001;
            MSTAT=0x020;
```

```
            IDLE;

acquire:    RESET FL0;
            MSTAT=0x0000;
            IMASK=0x0000;

            AX0=0xFFFF;
            DM(0x3FFD)=AX0;
            DM(0x3FFC)=AX0;

            IMASK=0x0001;
            MSTAT=0x0020;

            IDLE;

            MSTAT=0x0000;
            IMASK=0x0180;

            AR=166{DM(I0,M1)};
            DM(hsr0)=AR;
            SR=LSHIFT AR BY -8 (LO);
            DM(hsr1)=SR0;

            AR=200{DM(I0,M1)};                  {read value}
            DM(hsr2)=AR;
            SR=LSHIFT AR BY -8 (LO);
            DM(hsr3)=SR0;

            AR=400{DM(I0,M1)};                  {sanity checker}
            DM(hsr4)=AR;
            SR=LSHIFT AR BY -8 (LO);
            DM(hsr5)=SR0;

            AR=1;
            DM(writereg)=AR;

            AX0=0x2000;
            DM(0x3FE8)=AX0;                     {enable HIP read IRQ}

            JUMP respond;


.ENDMOD;
```

```
{ Smart-Fish ADSP-2171 Code.  Version zero: Crawling.

      Jlab716.dsp nmr controller code for junior
                  lab apparatus.  Spin echo acquisition.
}


.MODULE/RAM/BOOT=0/ABS=0 SMISH;                 {Beginning of SMISH.DSP}

{-----define ports for peripheral access-------}
.PORT bus;

{-----define constants for HIP locations------}
.CONST hsr0=0x3FE0, hsr1=0x3FE1, hsr2=0x3FE2, hsr3=0x3FE3, hsr4=0x3FE4;
.CONST hsr5=0x3FE5, hsr6=0x3FE6, hsr7=0x3FE7;

{----linear buffers----}
.VAR/DM/RAM/ABS=0x3000  halfpi;
.VAR/DM/RAM/ABS=0x3001  fullpi;
.VAR/DM/RAM/ABS=0x3002  wait;
.VAR/DM/RAM/ABS=0x3003  writereg;
.VAR/DM                 data[2043];

{---------Interrupt Vectors----------}

            JUMP start; RTI; RTI; RTI;    {RESET IRQ}
            RTI; NOP; NOP; NOP;           {IRQ2 unused}
            JUMP iread; NOP; NOP; NOP;    {HIP Write IRQ}
            JUMP iwrite; NOP; NOP; NOP;   {HIP Read IRQ}
            RTI; NOP; NOP; NOP;           {SPORT0 TX IRQ}
            RTI; NOP; NOP; NOP;           {SPORT0 RX IRQ}
            RTI; NOP; NOP; NOP;           {Software IRQ1}
            RTI; NOP; NOP; NOP;           {Software IRQ2}
            RTI; NOP; NOP; NOP;           {SPORT1 TX IRQ}
            RTI; NOP; NOP; NOP;           {SPORT1 RX IRQ}
            RTI; NOP; NOP; NOP;           {TIMER IRQ}
            RTI; NOP; NOP; NOP;           {Powerdown IRQ}


{------Start Up Configurations---------}

start:      AX0=0x0018;
            DM(0x3FFF)=AX0;               {System Control Register}

            AX0=0x0142;
            DM(0x3FFE)=AX0;               {DM wait states}

            AX0=0;                        {Timer Registers}
            DM(0x3FFD)=AX0;
            DM(0x3FFC)=AX0;
            AX0=31;                       {prescale for uS}
            DM(0x3FFB)=AX0;

            AX0=0x0020;
            DM(0x3FE8)=AX0;               {HMASK IRQ register}

            AX0=DM(hsr0);                 {make sure HWR clear}
            AX0=DM(hsr1);
            AX0=DM(hsr2);
            AX0=DM(hsr3);
            AX0=DM(hsr4);
            AX0=DM(hsr5);

            M0=0; M4=0;                   {do not increment}
```

```
            M1=1; M5=1;                     {increment by ONE}

{----parameter initialization----}

            RESET FL0;                      {no pulse}
            RESET FL1;

            AX0=0;
            DM(writereg)=AX0;               {initialize writereg}

            AX0=62;
            DM(halfpi)=AX0;
            AX0=66;
            DM(fullpi)=AX0;
            AX0=3500;
            DM(wait)=AX0;

            I0=^data;
            L0=0;
            CNTR=%data;
            DO prepare UNTIL CE;
prepare:    DM(I0,M1)=AX0;


{-------waitloop for console instructions------}

talk:       MSTAT=0x0010;
            IMASK=0x180;
            IDLE;                           {waiting for HOST WRITE}

            SET FL1;
            JUMP echo;

respond:    CNTR=681;                       {banks to return}
            DO converse UNTIL CE;
            IDLE;
converse:   NOP;

            JUMP talk;

{-----IRQ service routines-----}

{---HOST WRITE IRQ---}
iread:      SR0=DM(hsr0);                   {read registers}
            SR=LSHIFT SR0 by 8 (LO);
            AY0=DM(hsr1);
            AR=SR0 OR AY0;
            DM(halfpi)=AR;

            SR0=DM(hsr2);
            SR=LSHIFT SR0 by 8 (LO);
            AY0=DM(hsr3);
            AR=SR0 OR AY0;
            DM(fullpi)=AR;

            SR0=DM(hsr4);
            SR=LSHIFT SR0 by 8 (LO);
            AY0=DM(hsr5);
            AR=SR0 OR AY0;
            DM(wait)=AR;

            RTI;

{---HOST READ IRQ---}
```

```
iwrite:     AX0=DM(writereg);
            AY0=681;                        {no. banks HC11 should read}
            AR=AX0-AY0;
            IF EQ JUMP wrap;

            AR=DM(I0,M1);                   {smoothed value}
            DM(hsr0)=AR;                    {filters -- 16bit}
            SR=LSHIFT AR BY -8 (LO);
            DM(hsr1)=SR0;

            AR=DM(I0,M1);                   {read value}
            DM(hsr2)=AR;
            SR=LSHIFT AR BY -8 (LO);
            DM(hsr3)=SR0;

            AR=DM(I0,M1);                   {sanity checker}
            DM(hsr4)=AR;
            SR=LSHIFT AR BY -8 (LO);
            DM(hsr5)=SR0;

            AX0=DM(writereg);               {written}
            AR=AX0+1;
            DM(writereg)=AR;

            RTI;

wrap:       AR=0;
            DM(writereg)=AR;
            AR=0x020;
            DM(0x3FE8)=AR;                  {disable HIP read IRQ}
            DM(hsr0)=AR;
            DM(hsr1)=AR;
            DM(hsr2)=AR;
            DM(hsr3)=AR;
            DM(hsr4)=AR;
            DM(hsr5)=AR;

            RTI;


{-----spin echo subroutine-----}

echo:       IMASK=0x0000;
            MSTAT=0x0000;

tip:        AX0=DM(halfpi);
            DM(0x3FFD)=AX0;
            DM(0x3FFC)=AX0;

            IMASK=0x0001;
            SET FL0;
            MSTAT=0x0030;
            IDLE;

evolve:     RESET FL0;
            MSTAT=0x0000;
            IMASK=0x0000;

            AX0=DM(wait);
            DM(0x3FFD)=AX0;
            DM(0x3FFC)=AX0;

            IMASK=0x0001;
            MSTAT=0x0020;
```

```
            AX0=DM(fullpi);
            IDLE;

invert:     SET FL0;
            MSTAT=0x0000;
            IMASK=0x0001;

            DM(0x3FFC)=AX0;
            DM(0x3FFD)=AX0;

            IMASK=0x0001;
            MSTAT=0x020;

            IDLE;

acquire:    RESET FL0;
            MSTAT=0x0000;
            IMASK=0x0000;

            AX0=100;
            DM(0x3FFD)=AX0;
            DM(0x3FFC)=AX0;
            AX0=0;
            DM(0x3FFB)=AX0;

            I0=^data;
            L0=0;
            CNTR=%data;
            AY0=0xFFF;

            IMASK=0x0001;
            MSTAT=0x0020;

            DO record UNTIL CE;
            IDLE;
            AX0=DM(bus);
            AR=AX0 AND AY0;
record:     DM(I0,M1)=AR;

            AX0=31;
            DM(0x3FFB)=AX0;

            MSTAT=0x0000;
            IMASK=0x0180;

            I0=^data;
            L0=0;

            AR=DM(I0,M1);
            DM(hsr0)=AR;
            SR=LSHIFT AR BY -8 (LO);
            DM(hsr1)=SR0;

            AR=DM(I0,M1);                   {read value}
            DM(hsr2)=AR;
            SR=LSHIFT AR BY -8 (LO);
            DM(hsr3)=SR0;

            AR=DM(I0,M1);
            DM(hsr4)=AR;
            SR=LSHIFT AR BY -8 (LO);
            DM(hsr5)=SR0;

            AR=1;
```

```
            DM(writereg)=AR;

            AX0=0x2000;
            DM(0x3FE8)=AX0;               {enable HIP read IRQ}

            JUMP respond;

.ENDMOD;
```

```
{ Smart-Fish ADSP-2171 Code.  Version zero: Crawling.

      jlab.dsp    nmr controller code for junior
                  lab apparatus

      version 7.17.97   FID for pi/2 pulse maximization.
}


.MODULE/RAM/BOOT=0/ABS=0 SMISH;                 {Beginning of SMISH.DSP}

{-----define ports for peripheral access-------}
.PORT bus;

{-----define constants for HIP locations------}
.CONST hsr0=0x3FE0, hsr1=0x3FE1, hsr2=0x3FE2, hsr3=0x3FE3, hsr4=0x3FE4;
.CONST hsr5=0x3FE5, hsr6=0x3FE6, hsr7=0x3FE7;

{----linear buffers----}
.VAR/DM/RAM/ABS=0x3000  halfpi;
.VAR/DM/RAM/ABS=0x3001  writereg;
.VAR/DM                 data[2046];

{---------Interrupt Vectors----------}

            JUMP start; RTI; RTI; RTI;    {RESET IRQ}
            RTI; NOP; NOP; NOP;           {IRQ2 unused}
            JUMP iread; NOP; NOP; NOP;    {HIP Write IRQ}
            JUMP iwrite; NOP; NOP; NOP;   {HIP Read IRQ}
            RTI; NOP; NOP; NOP;           {SPORT0 TX IRQ}
            RTI; NOP; NOP; NOP;           {SPORT0 RX IRQ}
            RTI; NOP; NOP; NOP;           {Software IRQ1}
            RTI; NOP; NOP; NOP;           {Software IRQ2}
            RTI; NOP; NOP; NOP;           {SPORT1 TX IRQ}
            RTI; NOP; NOP; NOP;           {SPORT1 RX IRQ}
            RTI; NOP; NOP; NOP;           {TIMER IRQ}
            RTI; NOP; NOP; NOP;           {Powerdown IRQ}



{------Start Up Configurations---------}

start:      AX0=0x0018;
            DM(0x3FFF)=AX0;               {System Control Register}

            AX0=0x0142;
            DM(0x3FFE)=AX0;               {DM wait states}

            AX0=0;                        {Timer Registers}
            DM(0x3FFD)=AX0;
            DM(0x3FFC)=AX0;
            AX0=31;                       {prescale for uS}
            DM(0x3FFB)=AX0;

            AX0=0x0020;
            DM(0x3FE8)=AX0;               {HMASK IRQ register}

            AX0=DM(hsr0);                 {make sure HWR clear}
            AX0=DM(hsr1);
            AX0=DM(hsr2);
            AX0=DM(hsr3);
            AX0=DM(hsr4);
            AX0=DM(hsr5);
```

```
            M0=0; M4=0;                     {do not increment}
            M1=1; M5=1;                     {increment by ONE}

{----parameter initialization----}

            RESET FL0;                      {no pulse}
            RESET FL1;

            AX0=0;
            DM(writereg)=AX0;               {initialize writereg}

            AX0=62;
            DM(halfpi)=AX0;

            I0=^data;
            L0=0;
            CNTR=%data;
            DO prepare UNTIL CE;
prepare:    DM(I0,M1)=AX0;


{-------waitloop for console instructions------}

talk:       MSTAT=0x0010;
            IMASK=0x180;
            IDLE;                           {waiting for HOST WRITE}

            SET FL1;
            JUMP echo;

respond:    CNTR=682;                       {banks to return}
            DO converse UNTIL CE;
            IDLE;
converse:   NOP;

            JUMP talk;

{-----IRQ service routines-----}

{---HOST WRITE IRQ---}
iread:      SR0=DM(hsr0);                   {read registers}
            SR=LSHIFT SR0 by 8 (LO);
            AY0=DM(hsr1);
            AR=SR0 OR AY0;
            DM(halfpi)=AR;

            SR0=DM(hsr2);
            SR=LSHIFT SR0 by 8 (LO);
            AY0=DM(hsr3);
            AR=SR0 OR AY0;
            {DM(fullpi)=AR;}

            SR0=DM(hsr4);
            SR=LSHIFT SR0 by 8 (LO);
            AY0=DM(hsr5);
            AR=SR0 OR AY0;
            {DM(wait)=AR;}

            RTI;

{---HOST READ IRQ---}

iwrite:     AX0=DM(writereg);
            AY0=682;                        {no. banks HC11 should read}
            AR=AX0-AY0;
```

```
                IF EQ JUMP wrap;

                AR=DM(I0,M1);
                DM(hsr0)=AR;
                SR=LSHIFT AR BY -8 (LO);
                DM(hsr1)=SR0;

                AR=DM(I0,M1);
                DM(hsr2)=AR;
                SR=LSHIFT AR BY -8 (LO);
                DM(hsr3)=SR0;

                AR=DM(I0,M1);                   {sanity checker}
                DM(hsr4)=AR;
                SR=LSHIFT AR BY -8 (LO);
                DM(hsr5)=SR0;

                AX0=DM(writereg);               {written}
                AR=AX0+1;
                DM(writereg)=AR;

                RTI;

wrap:           AR=0;
                DM(writereg)=AR;
                AR=0x020;
                DM(0x3FE8)=AR;                  {disable HIP read IRQ}
                DM(hsr0)=AR;
                DM(hsr1)=AR;
                DM(hsr2)=AR;
                DM(hsr3)=AR;
                DM(hsr4)=AR;
                DM(hsr5)=AR;

                RTI;


{-----spin echo subroutine-----}

echo:           IMASK=0x0000;
                MSTAT=0x0000;

tip:            AX0=DM(halfpi);
                DM(0x3FFD)=AX0;
                DM(0x3FFC)=AX0;

                IMASK=0x0001;
                SET FL0;
                MSTAT=0x0030;
                IDLE;

acquire:        RESET FL0;
                MSTAT=0x0000;
                IMASK=0x0000;

                AX0=50;
                DM(0x3FFD)=AX0;
                DM(0x3FFC)=AX0;
                AX0=0;
                DM(0x3FFB)=AX0;

                I0=^data;
                L0=0;
                CNTR=%data;
```

```
            AY0=0xFFF;

            IMASK=0x0001;
            MSTAT=0x0020;

            DO record UNTIL CE;
            IDLE;
            AX0=DM(bus);
            AR=AX0 AND AY0;
record:     DM(I0,M1)=AR;

            AX0=31;
            DM(0x3FFB)=AX0;

            MSTAT=0x0000;
            IMASK=0x0180;

            I0=^data;
            L0=0;

            AR=DM(I0,M1);                   {smoothed value}
            DM(hsr0)=AR;                    {filters -- 16bit}
            SR=LSHIFT AR BY -8 (LO);
            DM(hsr1)=SR0;

            AR=DM(I0,M1);                   {read value}
            DM(hsr2)=AR;
            SR=LSHIFT AR BY -8 (LO);
            DM(hsr3)=SR0;

            AR=DM(I0,M1);                   {sanity checker}
            DM(hsr4)=AR;
            SR=LSHIFT AR BY -8 (LO);
            DM(hsr5)=SR0;

            AR=1;
            DM(writereg)=AR;

            AX0=0x2000;
            DM(0x3FE8)=AX0;                 {enable HIP read IRQ}

            JUMP respond;

.ENDMOD;
```

```
* bin2fsh.asm
* modified smartp3.asm to handle all channels
* now allows on-the-fly programming of DSP, 3.2.97
* now allows on-the-fly changing of transmit and receive banks size
* fix handshake byte misalignment, 5.28.97

* RAM VALUES, 256 BYTES INCLUDING STACK

        ORG     $0000

TXHEAD  RMB     2T
TXTAIL  RMB     2T
TXBUF   RMB     140T            ; values to PC
BUFWNM  RMB     2T
RXHEAD  RMB     2T
RXTAIL  RMB     2T
RCVBF   RMB     61T             ; sixty-one values from PC
NMOREN  RMB     1
PROGCNT RMB     1               ; counter for HIP loading
BANKCNT RMB     1               ; counter for BANK adjustment
CHARIN  RMB     1               ; number of characters from PC
BANKOUT RMB     2               ; number of banks from DSP to PC
REMAIN  RMB     1
STATREG RMB     1
TMPVAL  RMB     1

        ORG     $103F           ; Config byte
        FCB     $FF
        ORG     $F800

REGBAS  EQU     $1000           ; Base addr of register block
PORTA   EQU     REGBAS+$00
PORTB   EQU     REGBAS+$04
PORTC   EQU     REGBAS+$03
BAUD    EQU     REGBAS+$2B
SCCR1   EQU     REGBAS+$2C
SCCR2   EQU     REGBAS+$2D
SCSR    EQU     REGBAS+$2E
SCDR    EQU     REGBAS+$2F
OPTION  EQU     REGBAS+$39
COPRST  EQU     REGBAS+$3A
HPRIO   EQU     REGBAS+$3C
CONFIG  EQU     REGBAS+$3F

DSPBAS  EQU     $2000           ; Base addr of DSP registers
HIP0    EQU     DSPBAS+$00
HIP1    EQU     DSPBAS+$01
HIP2    EQU     DSPBAS+$02
HIP3    EQU     DSPBAS+$03
HIP4    EQU     DSPBAS+$04
HIP5    EQU     DSPBAS+$05
HOSTWSR EQU     DSPBAS+$06      ; Host write status register
DSPWSR  EQU     DSPBAS+$07      ; DSP write status register
DIPSW   EQU     $4000           ; DIP switch address

EEORG   EQU     $F800
RESET   EQU     $FFFE

* SYSTEM CONFIGURATION

        SEI             ; DISABLE INTERRUPTS DURING INIT

INIT    LDS     #$00FF  ; Init stack

        LDAA    #$30    ; Init SCI
```

```
        STAA    BAUD    ; 1,8,1,n,9600
        LDAA    #$00    ; RS-232 communcations
        STAA    SCCR1
        LDAA    #$2C
        STAA    SCCR2

* CIRCULAR TRANSMIT (TO PC) BUFFER

        LDX     #TXBUF  ; get address of first location
        STX     TXHEAD  ; initialize head and tail pointers
        STX     TXTAIL

* CIRCULAR RECEIVE (FROM PC) BUFFER

        LDX     #RCVBF  ; get address of first location
        STX     RXHEAD  ; initialize head and tail pointers
        STX     RXTAIL

* INITIALIZE WRAPPING POINTER TO HIP REGISTERS

        LDX     #HIP0   ; get first HIP location
        STX     BUFWNM  ; store pointer

* INITIALIZE COUNTERS and STATUS REGISTER

        CLR     NMOREN  ; number of characters from PC
        CLR     PROGCNT ; number of time DSP load requested
        CLR     BANKCNT ; number of time change bank requested
        CLR     STATREG ; indicate loading or normal mode
        CLR     TMPVAL  ; temporary register

        LDAA    #$06    ; initial number of characters from PC
        STAA    CHARIN  ; number of characters to read in
        LDX     #$01    ; initial number of banks to read
        STX     BANKOUT ; number of banks to read out

        CLI             ; ENABLE INTERRUPTS FOR PROGRAM

* MAIN LOOP

GTIFLP  LDAA    NMOREN  ; load number of characters received
        CMPA    CHARIN  ; compare to the number desired
        BLO     GTIFLP  ; wait if all characters are not received

        LDX     #$0006  ; load denominator with 6
        CLRA
        LDAB    CHARIN  ; load numerator with number characters read
        IDIV            ; number of banks to stuff in IX
        XGDX            ; now in ADDD
        XGDY            ; now in IY, # of banks to stuff into DSP

WTOSTF  LDAA    HOSTWSR ; read status of DSP (if it has read registers)
        LDAA    HOSTWSR ; twice to clear DSP's flag
        ANDA    #$3F    ; mask for pertinent status bits
        CMPA    #$00    ; check if DSP has read last set of values
        BNE     WTOSTF  ; wait if DSP is not ready

STUFF   JSR     GTFRBF  ; go get values from receive buffer
        LDX     BUFWNM  ; load pointer to HIP registers in IX
        STAA    0,X     ; store receive buffer value pointed location
        INX             ; increment HIP address
        CPX     #HIP5   ; check to see if a wraparound it required
        BHI     LOOKAG  ; if yes, go do it
        STX     BUFWNM  ; if no, store address
        JMP     STUFF   ; and stuff until a complete bank is filled
```

```
LOOKAG  LDX     #HIP0   ; one bank is filled
        STX     BUFWNM  ; wraparound
        DEY             ; now, 1-# of DSP banks to stuff
        BNE     WTOSTF  ; wait for DSP to finish reading last bank


MMNLP   LDY     BANKOUT ; # of banks to read from DSP
MAINLP  LDAA    DSPWSR  ; check to see that DSP has written back
        LDAA    DSPWSR  ; twice to clear flag
        ANDA    #$3F    ; mask for pertinent bits
        CMPA    #$3F    ; check status
        BNE     MAINLP  ; wait if not ready

        LDAA     DIPSW  ; binary or ascii communications
        CMPA     #$80
        BHS      BIN

        LDAB    HIP0    ; read LSB
        LDAA    HIP1    ; read MSB
        JSR     BTOD    ; binary to ASCII-decimal conversion
        LDAB    HIP2
        LDAA    HIP3
        JSR     BTOD
        LDAB    HIP4
        LDAA    HIP5
        JSR     BTOD
        JMP     COMP

BIN     LDAB    HIP0    ; read LSB
        JSR     STITXBF
        LDAB    HIP1    ; read MSB
        JSR     STITXBF ; binary send to PC
        LDAB    HIP2
        JSR     STITXBF
        LDAB    HIP3
        JSR     STITXBF
        LDAB    HIP4
        JSR     STITXBF
        LDAB    HIP5
        JSR     STITXBF

COMP    DEY             ; 1-# of banks to read from DSP
        BNE     MAINLP  ; read next bank

        LDAA    HIP0    ; trash handshaking bytes: 0x020
        LDAA    HIP1    ;
        LDAA    HIP2
        LDAA    HIP3
        LDAA    HIP4
        LDAA    HIP5

* TEST FOR DIP SWITCH REQUEST

        CLR     TMPVAL  ; clear that temporary register
        LDAA    PROGCNT ; only DSP load if it has been
        CMPA    #2T     ; on for three consecutive loops (N-1)
        BLO     NOHIP   ; no loader request
        INC     TMPVAL  ; increment if time to load
NOHIP   LDAA    TMPVAL  ; check if either
        CMPA    #$00    ; if TMPVAL unaltered
        BEQ     CHECK   ; not yet three loops, check again
        LDAA    STATREG ; check status register
        CMPA    #$01    ; has not been reset yet
        BEQ     CHECK   ; no false triggering of DSP HIP load
```

```
        LDAB    #$0D    ; complete last transaction
        JSR     STITXBF ; and announce LOAD
        JSR     LOAD    ; announce LOAD to PC
        JMP     LOADER  ; go to LOADER for DSP programming

* DIP SWITCH CHECK ROUTINE

CHECK   LDAB    #$0D
        JSR     STITXBF

        LDAA    DIPSW   ; check dip switch: rewrite
        CMPA    #$55    ; if DIP switch is in 0x55 state
        BEQ     PUPCNT  ; increment PROGCNT
        CLR     PROGCNT ; clear count if not 0x55--maybe fluke
        CLR     STATREG ; schmitt trigger state
        JMP     GTIFLP  ; remain in normal operation

PUPCNT  INC     PROGCNT ; increment counter
        JMP     GTIFLP


* LOADER Routine

LOADER  LDAA    #$01    ; HC11 in DSP HIP loading mode
        STAA    STATREG

GTCODE  LDAA    NMOREN  ; load counter of PC characters received
        CMPA    #$3D    ; want 61 characters: 1 length, 60 code
        BLO     GTCODE  ; wait if all characters are not received

        JSR     GTFRBF  ; get length value
        STAA    TMPVAL  ; store temporarily, must extract byte number
        INCA            ; increment
        LDAB    #$18    ; multiply by 24
        MUL
        LDX     #$3C    ; divide number of 20 instruction chunks
        IDIV            ; no. of chunks in IX, rem. bytes in ACCD
        STAB    REMAIN  ; store remainder, use IY to countdown
        XGDX            ; chunks: IX -> ACCD
        XGDY            ; chunks: ACCD -> IY

        LDAA    DSPWSR  ; load contents of DSPWSR
        ORAA    #$40    ; set reset bit for DSP
        STAA    DSPWSR  ; request software reset

        LDAA    TMPVAL  ; get length value back
        STAA    HIP3    ; place in HSR3

BULK    LDAB    #$14    ; counter is 20 instructions
        JSR     PUTCODE ; place 20 instructions

        DEY             ; decrement number of chunks
        BEQ     ENDGAME ; if no more chunks place remainder

        JSR     OKAY    ; otherwise, ask for more from PC

MOCODE  LDAA    NMOREN  ; load counter
        CMPA    #$3C    ; get 60 bytes (20 instructions)
        BLO     MOCODE  ; wait until all 20 are received

        JMP     BULK    ; go place 'em

ENDGAME CLRA            ; for the remainder, after chunks
        LDAB    REMAIN  ; remainder of byte
        LDX     #$03    ; divided by 3
```

```
        IDIV            ; is the number of instructions
        XGDX            ; save the number of instructions
        STAB    TMPVAL  ;

        JSR     OKAY    ; ask for remainder of bytes

ENDCODE LDAA    NMOREN
        CMPA    REMAIN
        BLO     ENDCODE

        LDAB    TMPVAL
        JSR     PUTCODE ; place 'em

        JSR     DONE    ; signify loading done-age to PC

GTBANK  LDAA    NMOREN  ; load counter of PC characters received
        CMPA    #$03    ; want 2 characters: 1 CHARIN, 2 BANKOUT
        BLO     GTBANK  ; wait if all characters are not received

        JSR     GTFRBF  ; get first value
        STAA    CHARIN  ; the new number of characters in
        JSR     GTFRBF  ; get the next value (LSB of bankout)
        STAA    TMPVAL  ; store temporarily
        JSR     GTFRBF  ; get the last value (MSB of bankout)
        LDAB    TMPVAL  ; now MSB:LSB in ADDD
        XGDY            ; now in IY
        STY     BANKOUT ; the new number of banks to read from DSP

        JSR     DONE    ; signify bank done-age, YO!

        JMP     GTIFLP  ; go back to normal routine


* PUT CODE (in DSP) SUBROUTINE : countdown in ACCB

PUTCODE JSR     GTFRBF
        STAA    HIP0
        JSR     GTFRBF
        STAA    HIP1
        JSR     GTFRBF
        STAA    HIP2

        DECB
        BNE     PUTCODE

        RTS


* LOAD NOTIFICATION SUBROUTINE

LOAD    LDAA    NMOREN  ; load number of characters received
        CMPA    #$06    ; compare to the number desired
        BLO     LOAD    ; wait if all characters are not received

        JSR     GTFRBF  ; trash handshake values
        JSR     GTFRBF
        JSR     GTFRBF
        JSR     GTFRBF
        JSR     GTFRBF
        JSR     GTFRBF

        LDY     #$03
ANLOAD  LDAB    #$4C    ; ASCII "L"
        JSR     STITXBF
        LDAB    #$4F    ; ASCII "O"
```

```
        JSR     STITXBF
        LDAB    #$41    ; ASCII "A"
        JSR     STITXBF
        LDAB    #$44    ; ASCII "D"
        JSR     STITXBF
        LDAB    #$20    ; ASCII space
        JSR     STITXBF
        LDAB    #$20    ; ASCII space
        JSR     STITXBF

        DEY
        BNE     ANLOAD
        LDAB    #$0D    ; ASCII carriage return
        JSR     STITXBF

        RTS


* OKAY NOTIFICATION SUBROUTINE to prompt next 20 instruction chunk

OKAY    LDAB    #$4F    ; ASCII "O"
        JSR     STITXBF
        LDAB    #$4B    ; ASCII "K"
        JSR     STITXBF
        LDAB    #$41    ; ASCII "A"
        JSR     STITXBF
        LDAB    #$59    ; ASCII "Y"
        JSR     STITXBF
        LDAB    #$0D    ; ASCII carriage return
        JSR     STITXBF

        RTS

* DONE NOTIFICATION SUBROUTINE to conclude RS-232 transfers

DONE    LDAB    #$44    ; ASCII "D"
        JSR     STITXBF
        LDAB    #$4F    ; ASCII "O"
        JSR     STITXBF
        LDAB    #$4E    ; ASCII "N"
        JSR     STITXBF
        LDAB    #$45    ; ASCII "E"
        JSR     STITXBF
        LDAB    #$0D    ; ASCII carriage return
        JSR     STITXBF

        RTS

* STUFF IN TRANSMIT BUFFER ROUTINE : VALUE IN ACCB

STITXBF LDX     TXTAIL  ; load address of end of transmit buffer
        STAB    0,X     ; store value in buffer
        INX             ; increment address
        CPX     #BUFWNM ; compare to end of buffer allocation
        BNE     NOWRAP
        LDX     #TXBUF  ; wraparound if at end
NOWRAP  CPX     TXHEAD  ; compare to head pointer
        BEQ     NOWRAP  ; if same, wait until buffer empties
        STX     TXTAIL  ; then, store new pointer address
        LDAB    SCCR2   ; load SCI control register
        ORAB    #$C0    ; turn on TX interrupt
        STAB    SCCR2   ; store SCI control register value
        RTS
```

```
* SCI INTERRUPT ROUTINE

SCIINT  LDAA    SCSR    ; (actually SCSR2) load SCI status register
        BITA    #$20    ; check that a full character is received
        BNE     HDLRCV  ; if so, stuff in receive buffer
        LDX     TXHEAD  ; otherwise load TX buffer head pointer
        CPX     TXTAIL  ; compare to TX buffer tail pointer
        BEQ     GTOUT   ; if so, get out (done with values for PC)
        JMP     GOBB    ; otherwise, empty transmit buffer to PC
GTOUT   LDAA    SCCR2   ; load SCI control register
        ANDA    #$3F    ; turn off SCI transmit interrupt
        STAA    SCCR2   ; store control register
        RTI             ; return from interrupt
GOBB    LDX     TXHEAD  ; load head pointer of transmit buffer
        LDAA    0,X     ; get value from buffer
        STAA    SCDR    ; send out SCI
        INX             ; increment address
        CPX     #BUFWNM ; compare to end of allocated memory
        BEQ     WRHD    ; wrap pointer if at end
        STX     TXHEAD  ; store next address of transmit pointer
        RTI             ; return from interrupt
WRHD    LDX     #TXBUF  ; wrapping pointer
        STX     TXHEAD  ; to beginning of allocated memory
        RTI             ; return from interrupt
HDLRCV  LDAB    SCDR    ; read SCI received character
        JSR     STINRCV ; store in receive buffer
        RTI             ; return from interrupt


* BINARY TO ASCII CONVERSION TO RS-232

BTOD    LDX     #10000T ; 1000 *DECIMAL*
        IDIV
        PSHB            ; push remainder ( 0 <= r < 10000 )
        PSHA
        PSHX            ; push quotient
        PULA            ; throw away MSB of quotient (q < 5 for 12 bit)
        PULB            ; output LSB of quotient
        ADDB    #$30
        JSR     STITXBF ; place ASCII-decimal in transmit buffer

        PULA            ; Pull remainder ( 0 <= r < 1000)
        PULB
        LDX     #1000T   ; 100   decimal
        IDIV
        PSHB            ; push remainder
        PSHA
        PSHX            ; push quotient
        PULA            ; throw away MSB of quotient
        PULB            ; output LSB of quotient
        ADDB    #$30
        JSR     STITXBF ; place ASCII-decimal in transmit buffer

        PULA
        PULB
        LDX     #100T   ; 100   decimal
        IDIV
        PSHB            ; push remainder
        PSHX            ; push quotient
        PULA            ; throw away MSB of quotient
        PULB            ; output LSB of quotient
        ADDB    #$30
        JSR     STITXBF ; place ASCII-decimal in transmit buffer

        CLRA
```

```
        PULB
        LDX     #10T
        IDIV
        PSHB            ; push remainder
        PSHX            ; push quotient
        PULA            ; throw away MSB of quotient
        PULB            ; output LSB of quotient
        ADDB    #$30
        JSR     STITXBF
        PULB            ; restore remainder
        ADDB    #$30
        JSR     STITXBF ; OUTPUT REMANINDER
        LDAB    #$20
        JSR     STITXBF
        RTS


* GET FROM RECEIVE BUFFER ROUTINE : VALUE RETURNED IN ACCA

GTFRBF  LDX     RXHEAD  ; get head of receive buffer address
        LDAA    0,X     ; read value at that address
        DEC     NMOREN  ; decrement number of values read from PC
        INX             ; increment value of address
        CPX     #NMOREN ; compare to end of allocated memory
        BEQ     WRRHD   ; wrap pointer is needed
        STX     RXHEAD  ; store new address
        RTS             ; return from subroutine
WRRHD   LDX     #RCVBF  ; wrap pointer by setting new address
        STX     RXHEAD  ; to beginning of allocated memory
        RTS             ; return from subroutine


* STUFF IN RECEIVE ROUTINE

STINRCV LDX     RXTAIL  ; load end of receive buffer address
        STAB    0,X     ; store value at end of buffer
        INC     NMOREN  ; increment the number of values from PC
        INX             ; increment address of end of receive buffer
        CPX     #NMOREN ; compare to end of allocated memory
        BNE     NORWRAP ; check to see if wraparound need
        LDX     #RCVBF  ; if so, use beginning of allocated memory
NORWRAP STX     RXTAIL  ; store new pointer address
        RTS             ; return from subroutine


* STARTUP VECTOR

        ORG     $FFFE
        FDB     $F800

* INTERRUPT VECTOR

        ORG     $FFD6
        FDB     SCIINT
```